Theory-Based Mechanistic Insight as Stepping Stone for Catalyst Development in Olefin Polymerization

Wouter Heyndrickx

Dissertation for the degree of philosophiae doctor (PhD)

Department of Chemistry
University of Bergen, Norway

Department of Inorganic and Physical Chemistry
Ghent University, Belgium

2011

“La pensée ne doit jamais se soumettre,
ni à un dogme,
ni à un parti,
ni à une passion,
ni à un intérêt,
ni à une idée préconçue,
ni à quoi que ce soit,
si ce n'est aux faits eux-mêmes,
parce que, pour elle,
se soumettre, ce serait cesser d'être.”

“Thinking must never submit itself,
neither to a dogma,
nor to a party,
nor to a passion,
nor to an interest,
nor to a preconceived idea,
nor to whatever it may be,
if not to facts themselves,
because, for it,
to submit would be to cease to be.”

Henri Poincaré, Œuvres

Preface

When I first set foot onto Norwegian soil at Flesland after a stunning descent, it was met by moist snow. Little did it know at that time about fashionable rain boots, cross-country skiing, engineered outdoor jackets or brown cheese. I arrived with a considerable amount of enthusiasm for the project, which concerned *in silico* catalyst development for olefin polymerization, and I am happy to notice that now, after three years of withstanding harsh weather elements all over Norway, Iceland and even Svalbard, my enthusiasm for the project and this field of research in general has anything but diminished. My enthusiasm is fed by the notion that computational chemistry can offer insight in full energy profiles including intermediates and transition states which are difficult to identify experimentally, hereby describing the thermodynamics and kinetics of the reaction. Such understanding can then be exploited for developing improved catalysts. The current accuracy and speed of the calculations makes such an approach both sensible and feasible. With supercomputing facilities becoming more and more commonplace both in industry and academia, I expect computational chemistry to become increasingly prominent in organometallic chemistry in the future paired with an increase in *in silico* developed organometallic catalysts. By such rational catalyst development the element of chance in catalyst discovery is reduced, allowing scarce resources spent more efficiently.

Acknowledgements

In this opening section I would like to thank some people without whom my thesis wouldn't have been possible. First, there are my supervisor Prof. Dr. Ir. Vidar R. Jensen and my co-supervisor Dr. Giovanni Occhipinti from the University of Bergen (UiB), who have guided me during the course of my PhD and from whom I have learnt a great deal about science and the art of presenting the results. Their office doors seemed always open to me no matter how crowded their schedules were. I also had the pleasure of spending a period at Ghent University under the able supervision of my co-supervisor Prof. Dr. Patrick Bultinck, and I would like to thank Prof. Dr. Ir. Vidar R. Jensen and Prof. Dr. Patrick Bultinck for this opportunity. I am also indebted to Prof. Dr. Ir. Vidar R. Jensen for giving me the chance to present this work at several national and international conferences, with the Gordon Conference on Organometallic Chemistry in Newport, Rhode Island, USA as absolute highlight. They have given me perspective in this research field and allowed for interaction with some of the foremost and most inspirational people in the field. In addition I consider myself lucky to have collaborated with Dr. Yunhan Chu and Prof. Dr. Ir. Bjørn Kåre Alsberg from the Norwegian University of Science and Technology (NTNU) in Trondheim. I would like to thank them for their hospitality on my visits there, next to their relentless efforts during the collaboration. Furthermore special thanks goes out to my office mates Yury Minenkov and Dr. Elaine Olsson for the many interesting talks on a wide array of subjects. The former is also acknowledged for some truly memorable fishing and nightly hiking excursions. Dr. Nicolas Merle is thanked for very solid scientific discussions and for offering his advice on this work, as well as many drinks all across town. I am also very grateful towards Mathias Winkler for helping me discover the beautiful Norwegian 'villmark' on splendid weekend trips. I would like to thank all people at the UiB chemistry department for creating a social atmosphere and stimulating environment including Jarle Harnes, Marta Lill Sele, Ingvild Follesø, Fredrik Rosberg Hansen, Alf Holme, Nils Jordheim, Maria Gundersen Zahl, Åsmund Singstad, Prof. Dr. Knut Børve, Prof. Dr. Pascal Dietzel, Prof. Dr. Leif J. Sæthre and Prof. Dr. Erwan Le Roux. The same social atmosphere and stimulating environment applies to Ghent University with thanks to my S3 colleagues Dr. Sofie Van Damme, Helen van Aggelen, Dr. Stijn Fias and Jonas Feys.

In addition I'd like to thank my great flat mates Teresa, Christopher, Pablo, Annette and Cindy for too much to state here. It was a privilege sharing a home with you! Warm thoughts also go out to Fantoft and its inhabitants, especially Laila, Francesco, Igor, Ida and Diederik. I also really appreciate the many visits from my parents, family and friends from Belgium bringing needed

supplies and showing sincere interest in my PhD research. And finally, there is my girlfriend Anneleen whose patience and support in addition to many visits were indispensible. Her positive attitude throughout my PhD period as well as her reading of this work and subsequent advice and technical assistance were very much appreciated.

Table of Contents

Preface ii
Acknowledgements iii
Table of Contents v
List of Papers vi
Chapter 1: Brief History of Coordination-Insertion Polymerization of non-Polar Olefins and Copolymerization with Polar Olefins 1-1
1.1 Initial Ziegler-Natta Catalysts 1-1
1.2 Homogeneous Ziegler-Natta Catalysts 1-1
1.2.1 Metallocenes 1-1
1.2.2 Post-Metallocenes 1-3
Chapter 2: Computational Methods 2-9
2.1 Principles of Quantum Chemistry 2-9
2.2 The Hartree-Fock Method 2-12
2.3 Density Functional Theory 2-14
2.4 Semiempirical Methods 2-19
2.5 Molecular Mechanics 2-21
2.6 Thermodynamic Corrections 2-23
2.7 Effective Core Potential 2-24
2.8 Solvent calculations 2-25
2.9 Regression 2-27
Chapter 3: Modeling Coordination-Insertion Polymerization Catalysts 3-29
3.1 Chain Lengths 3-29
3.2 Counterion 3-29
Chapter 4: Mechanistic Aspects of Coordination-Insertion Ethylene Polymerization with Late Transition Metals 4-31
4.1 Ruthenium Olefin Coordination-Insertion Polymerization Catalysts 4-31
4.2 Neutral Ni Ethylene Oligo- and Polymerization Catalysts 4-35
4.2.1 Termination Pathways from Alkyl Phosphine Complexes 4-35
4.2.2 Termination Pathways from Alkyl Agostic Complexes 4-41
Chapter 5: Challenges in the Random Copolymerization of Polar and Non-Polar Olefins with Late Transition Metals 5-48
5.1 Strong σ-Coordination of the Polar Olefin 5-48
5.2 Weak π-Coordination of the Polar Olefin 5-49
5.3 Stable Chelate Formation 5-49
5.4 Enolate Formation 5-50
5.5 Reduced Migratory Insertion Reactivity 5-50
5.6 ß-Polar Functional Group Elimination 5-51
5.7 Radical Formation 5-51
5.8 Catalyst Decomposition Involving Reductive Elimination 5-51
Chapter 6: The Polar Functional Group Tolerance of Transition Metal Catalysts for Olefin Polymerization 6-54
Chapter 7: *In silico* Catalyst Development 7-58
Chapter 8: Concluding Remarks 8-62
Chapter 9: Suggestions for Future Work 9-64
List of Abbreviations 66
References 67

List of Papers

This thesis is based on the following five scientific papers:

Paper I
On the Nature of the Active Site in Ruthenium Olefin Coordination-Insertion Polymerization Catalysts.
W. Heyndrickx, G. Occhipinti, Y. Minenkov and V. R. Jensen
J. Mol. Catal. A: Chem. **2010**, *324*, 64-74.

Paper II
Neutral Nickel Oligo- and Polymerization Catalysts: The Importance of Alkyl Phosphine Intermediates in Chain Termination.
W. Heyndrickx, G. Occhipinti, Y. Minenkov and V. R. Jensen
Chem.-Eur. J. **2011**. Accepted.

Paper III
Neutral Nickel Oligo- and Polymerization Catalysts: Towards Computational Catalyst Prediction and Design.
W. Heyndrickx, G. Occhipinti and V. R. Jensen
To be submitted.

Paper IV
Striking a Compromise: Polar Functional Group Tolerance Versus Insertion Barrier Height for Olefin Polymerization Catalysts.
W. Heyndrickx, G. Occhipinti, P. Bultinck and V. R. Jensen
To be submitted.

Paper V
De Novo Optimization of Functional Coordination Compounds using a Fragment-Based Evolutionary Algorithm.
Y. Chu, W. Heyndrickx, G. Occhipinti, V. R. Jensen and B. K. Alsberg
To be submitted.

During the course of the PhD also the following paper, although not part of the thesis, was completed:

Performance of 3D-Space-Based Atoms-in-Molecules Methods for Electronic Delocalization Aromaticity Indices.
W. Heyndrickx, P. Salvador, P. Bultinck, M. Solá and E. Matito
J. Comp. Chem. **2011**, *32*, 386-395.

Chapter 1: Brief History of Coordination-Insertion Polymerization of non-Polar Olefins and Copolymerization with Polar Olefins

1.1 Initial Ziegler-Natta Catalysts

In 1953 the first example of coordination-insertion ethylene polymerization was provided by Karl Ziegler who showed that high density polyethylene (PE) could be produced under mild conditions (25 °C and 1 atm) by titanium chloride salts in the presence of organoaluminium species (generally $R_nAlCl_{(n-3)}$) such as diethylaluminiumchloride, Et_2AlCl.[1-3] Before this finding, ethylene could only be polymerized by free radical polymerization, under high temperature (200 °C) and high pressure (2000 atm) conditions. The rather high temperature necessary due to the low reactivity of ethylene in a radical polymerization process facilitates chain transfer, which leads to branches in the polymer structure and ultimately to low density polyethylene. Shortly after, Guilio Natta showed that the polymerization of propene with a similar catalytic system could yield predominantly isotactic polypropylene.[4-6] For their discoveries having huge scientific, technological and commercial impact, Ziegler and Natta received the Nobel Prize in 1963, and have lend their name to the so-called Ziegler-Natta catalysts, which can be broadly defined as olefin polymerization catalysts consisting of a metal alkyl (or hydride) and a transition metal salt.[7] The relevance of Ziegler-Natta catalysts can be illustrated by noting the annual worldwide production of polyethylene which is approximately 80 million metric tonnes,[8] 35 million metric tonnes of which is high density polyethylene. Industrially, high density polyethylene is commonly produced by titanium-based Ziegler-Natta catalysts supported on a heterogeneous support such as $MgCl_2$.[9] Also widely used are the chromium-based, SiO_2-supported Phillips and Union Carbide catalysts.[10]

1.2 Homogeneous Ziegler-Natta Catalysts

1.2.1 Metallocenes

Soon after the discovery of the original heterogeneous Ziegler-Natta catalysts, homogeneous variants were pursued. An early system was Cp_2TiCl_2 combined with Et_2AlCl, with Cp being the η^5-cyclopentadienyl ligand, capable of polymerizing ethylene under mild conditions.[11-13]

The activity of this system was however significantly lower than that of the preceding heterogeneous systems. A spectacular breakthrough was realized many years later when, instead of the alkyl aluminium compounds, methylaluminoxane (MAO), was applied to similar Cp_2ZrCl_2 catalysts resulting in an activity increase by a factor 10000 and also allowing α-olefin polymerization.[14-16] MAO is a oligomeric solid with the general structure formula $(AlMeO)_n$ capable of activating transition metals by methylation and dehalogenation.[17, 18] MAO has a rather poorly understood structure, probably involving numerous equilibria between various structures dependent on the conditions.[19] Adding to the complexity, AlR_3 compounds such as $AlMe_3$ are typically present in MAO, either in free or associated form.[19] This ill-defined structure of MAO is somewhat unfortunate, because homogeneous metallocene polymerization catalysts are otherwise quite well understood thanks to their well-defined reaction sites and better accessibility towards mechanistic and kinetic studies compared to their heterogeneous counterparts.[20-22] An often hailed characteristic of metallocenes and homogeneous polymerization catalysts at large is the precise control that is possible on the polymer microstructure. A good illustration of this is the range of tacticities possible of polypropylene by varying the ligand for ansa-zirconocenes (where the two Cp-ligands are connected by a bridging group).[23] Whereas isotactic polypropylene can be obtained with e.g. the C_2-symmetric (C_2H_4)bisindenyl$ZrCl_2$/MAO catalyst (**I** in Chart 1), syndiotactic polypropylene, which was previously unknown, can be produced by the C_s-symmetric (C_2H_4)Cp(9-fluorenyl)$ZrCl_2$/MAO catalyst (**II** in Chart 1).[24, 25] The polymer tacticity is not determined by the stereochemistry of the last incorporated propene, but rather by enantiomorphic site control.[26, 27]

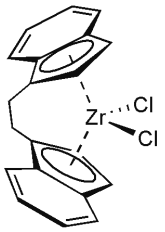

I

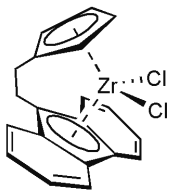

II

Chart 1. Structure formulas for the C_2-symmetric (C_2H_4)bisindenyl$ZrCl_2$ precatalyst **I**, and the C_s-symmetric (C_2H_4)Cp(9-fluorenyl)$ZrCl_2$ precatalyst **II**.

1.2.2 Post-Metallocenes

1.2.2.1 Early Transition Metals

Replacement of one or two Cp ligands in the metallocene catalysts has given birth to a new, broad family of catalysts with the generic name of post-metallocenes.[28] A rather prominent subclass of these contains the constrained geometry complexes (CGCs), in which one Cp ligand of an ansa-metallocene (*vide supra*) is replaced by an amido function (cf. **III** in Chart 2). These monocyclopentadienyl CGCs generally perform superior to the metallocenes in the copolymerization of ethylene and α-olefins and also allow for operation at higher temperatures.[29] As with the metallocenes, group 4 transition metals with oxidation state IV have yielded most successful applications,[30, 31] although ethylene polymerization and high activities for ethylene trimerization have been demonstrated for Cr^{III} CGC precatalysts including a donor amino group instead of an amido group (**IV** in Chart 2).[32] Precatalysts based on group 5 transition metals in oxidation state V such as V^{V} can be stabilized by replacing the amido function in CGCs by an imido function (cf. **V** in Chart 2).[33, 34] Also noteworthy is the generation of active ethylene polymerization catalysts by Ta^{III},[35, 36] Nb^{III}[36-38] and Mo^{III}[39-41] precatalysts ligated by Cp* and a (substituted) butadiene ligand with MAO as cocatalyst (**VI** in Chart 2).

The departure from the Cp ligands for the group 4 transition metals Ti^{IV} and Zr^{IV} has resulted in ethylene polymerization catalysts with exceptionally high activities. A (bis(phenoxy-imine))$Zr^{IV}Cl_2$/MAO catalyst, member of the 'FI catalyst' family (cf. **VII** in Chart 2), is currently the most active ethylene polymerization catalyst known with an activity of 6552 kg PE/(mmol catalyst×h)$^{-1}$ and quite impressively likely the most active catalyst known to mankind.[42, 43] Furthermore, the possibilities for structural variation of the ligand allows for plenty of control on the polymer microstructure, e.g. living polymerization and very high molecular weight PE ($M_v = 5\times10^6$) can be achieved by varying them accordingly.[42, 43]

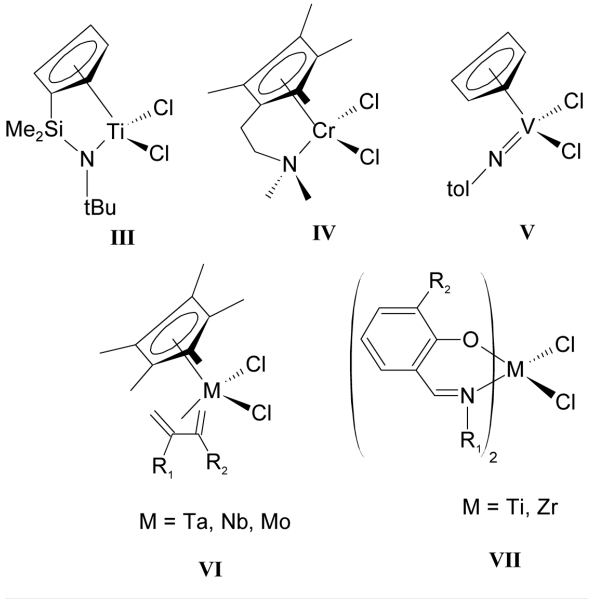

Chart 2. Structure formulas of prominent early transition metal post-metallocenes such as a typical representative of the constrained geometry complexes (CGCs) **III**, a Cr CGC **IV**, a V post-metallocene precatalyst **V**, Cp* butadiene precatalysts **VI** and the bis(phenoxy-imine) or FI precatalysts **VII**.

1.2.2.2 Late Transition Metals

Already in the 1970s, the potential of neutral Ni phosphine complexes for the oligomerization of ethylene was realized in the industrial Shell Higher Olefin Process (SHOP). The single component homogeneous oligomerization catalyst involved is a neutral Ni PPh_3 complex combined with a bidentate (κ^2-P,O) ligand (cf. **VIII** in Chart 3). After oligomerization of ethylene to linear α-olefins, an isomerization catalyst is employed to produce internal olefins, and subsequently a metathesis catalyst to produce more of the desirable C_{10}-C_{14} fraction.[44] Later it was reported that SHOP-type oligomerization catalysts could also be used as ethylene polymerization catalysts, by replacing PPh_3 with a weaker binding ligand or by using a phosphine scavenger such as $Ni(COD)_2$.[45-48] As many late-transition metal-based catalysts, these neutral Ni catalysts are quite polar functional group tolerant, which not only loosens the purity requirements on the media, but also offers perspective for the random copolymerization of polar and non-polar olefins. Indeed, SHOP-type catalysts were found active for the copolymerization of ethylene and polar olefins where the polar functional group is separated by several (>3) atoms from the olefinic function.[47] Two other prominent single component neutral

Ni ethylene polymerization catalysts displaying high activities comparable to early transition metal metallocenes are the salicylaldiminato catalyst due to Grubbs and coworkers (**IX** in Chart 3)[49, 50] and the anilinotropone catalyst due to Brookhart and coworkers (**X** in Chart 3).[51-53] The former also catalyzes the copolymerization of ethylene with functionalized norbornenes where the polar functional group is similarly separated from the olefinic function.[50, 54] Whereas the SHOP-type catalyst oligomerizes ethylene to linear α-olefins, branched olefins can be obtained with a single-component neutral Ni catalyst with a (κ^2-P,N) phosphinosulfonamide ligand (**XI** in Chart 3). It was also shown that the branching in the oligomers was not caused by the reinsertion of linear unsaturated oligomers. These examples illustrate that Ni has played, and still plays, an important role in the oligomerization[55, 56] and polymerization[31, 57] of ethylene. Many Ni catalysts exist, and in the thesis the oligomerization catalyst introduced by Keim and coworkers based on the Ni(1,1,1,5,5,5-hexafluoro-2,4-pentanedionato) or Ni(1,1,1,5,5,5-hexafluoro-2,4-acetylacetonato) fragment[58] (conveniently abbreviated by 'Ni(acac)') (**XII** in Chart 3) was explored in Paper III. This catalyst is representative of many late transition metal complexes that catalyze the insertion of ethylene and produce oligomers provided there is only little steric pressure surrounding the metal center.

Other, early examples of post-metallocene catalysts with late transition metals were provided by $Cp^*Co^{III}P(OMe)_3$[59-61] and $Cp^*Rh^{III}P(OMe)_3$[62, 63] alkyl cations. Rh^{III} centers with κ^3-tertiairy triamines [64, 65] and with κ^4-tetrathioethers or κ^3-trithioethers[66] have also been shown to polymerize ethylene, while the latter ligands also formed active ethylene polymerization catalysts with Pt^{IV} in combination with MAO.[66]

A major breakthrough in the field was realized by Brookhart and coworkers, who illustrated not only ethylene polymerization with their cationic Pd^{II} (κ^2-N,N) α-diimine catalysts (**XIII** in Chart 3),[67] but who also pioneered random coordination-insertion copolymerization of methyl acrylate (MA) and ethylene.[68, 69] This was a hugely desired objective since controlling such copolymerization would lead to polymers with greatly enhanced physical properties, pertaining to adhesion, toughness, surface properties, rheological properties and solvent resistance. The importance of successful random copolymerization of polar and non-polar olefins has been underscored by statements such as 'success in this area would constitute a quantum advance in the polyolefin field',[70] or '… which is regarded as the ultimate goal of coordination-insertion polymerization by some'.[71] The resulting ethylene-MA copolymers by the cationic Pd^{II} (κ^2-N,N) α-diimine catalysts were quite low in %MA incorporation (<25%) and highly branched with the MA units positioned at the chain ends. A later modification of the α-diimine ligand with

cyclophane to produce a cage-like structure around Pd^{II} resulted in an increased MA incorporation.[72, 73] A neutral Pd catalyst with a (κ^2-P,O) phosphine-arylsulfonate ligand, first reported by Drent *et al*. (**XIV** in Chart 3), was shown to produce highly linear polyethylene, in addition to linear copolymers of ethylene with MA.[74] Later these findings were extended and this catalyst was found capable of producing copolymers of a wide range of polar comonomers such as acrylonitrile,[75] vinylacetate,[76] vinylfluoride,[77] and vinylethers.[78] Mecking and coworkers showed that this catalyst with a weaker binding donor ligand L can incorporate more acrylate into the copolymer, and can even catalyze the coordination-insertion homopolymerization of acrylate.[79, 80]

Other cationic Pd ethylene polymerization catalysts, such as those based on (κ^2-P,P) diphosphinidenecyclobutene[81] and (κ^2-P,S) phosphinidine-sulfide ligands,[82] have been reported, but these are not active in the copolymerization of ethylene with polar olefins.

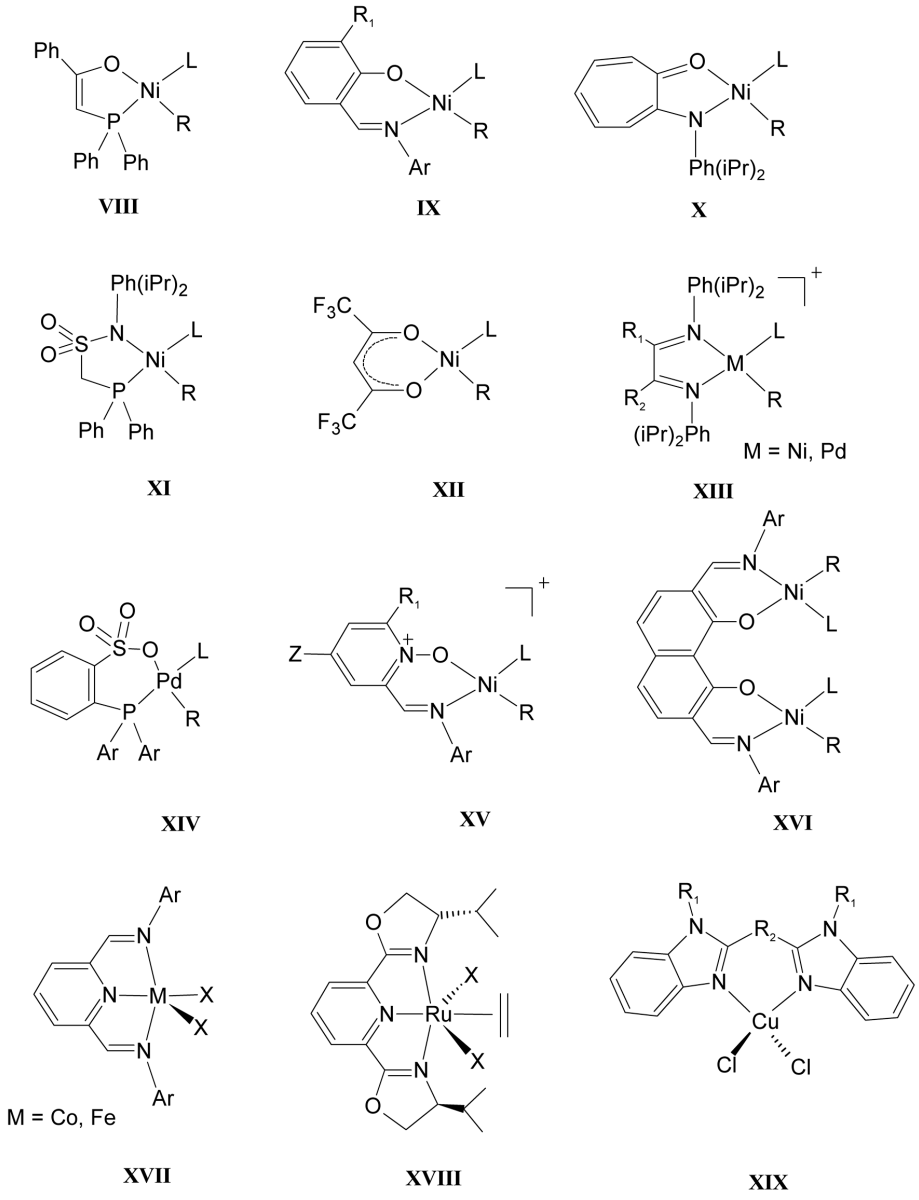

Chart 3. Structure formulas for prominent late transition metal post-metallocene catalysts for olefin polymerization such as the SHOP-type catalyst **VIII**, the Ni salicylaldiminato catalyst **IX**, the Ni anilinotropone catalyst **X**, the Ni phosphinosulfonamide catalyst **XI**, the Ni(acac) catalyst **XII**, the cationic Pd and Ni α-diimine catalyst **XIII**, the Pd phosphine-sulfonate catalyst **XIV**, the Ni PymNox catalyst **XV**, the binickel catalysts due to Marks and coworkers **XVI**, the Co and Fe bis(imino)pyridine catalyst **XVII**, the Ru Pybox catalyst **XVIII** and the Cu bisbenzimidazole catalyst **XIX**. See text for references.

Some examples exist of the copolymerization of acrylates and ethylene with Ni catalysts, although less success has been achieved than with Pd. The cationic Ni α-diimine catalyst due to Brookhart and coworkers[67] is active, but only at higher temperatures and pressure, and incorporating significantly less MA (<1%) than its Pd analogue.[83, 84] Another catalytic system capable of incorportating very small amounts of MA (<2%) is the 2-iminopyridine N-oxide (PymNox)$NiBr_2$/MMAO system (**XV** in Chart 3).[85] The best results with Ni systems however, have been obtained with the single-component neutral (κ^2-N,O) binickel catalysts of Marks and coworkers which combine relatively high activities and MA incorporation (± 10%), attributed to the cooperative effects of the two Ni centers in close proximity (**XVI** in Chart 3).[86]

A particularly successful and highly active family of polymerization catalysts based on relatively cheap transition metals was found simultaneously by the groups of Gibson and Brookhart by stabilizing paramagnetic Fe^{II} and Co^{II} with tridentate bis(imino)pyridine ligands in combination with MAO (**XVII** in Chart 3).[87-89] The only example of a Ru^{II} olefin polymerization catalyst contains a bis(oxazoline)pyridine ('Pybox') ligand structurally similar to the bis(imino)pyridine ligand and requires MAO as cocatalyst to show low polymerization activity (**XVIII** in Chart 3).[90-92]

A number of Cu^{II} precatalysts producing polyethylene in combination with MAO have been reported, among them precatalysts based on (κ^2-N,N) α-diimine,[93] bisbenzimidazole[94], pyrazolylquinoline[95] and pyrazolylpyrimidine[96] ligands in addition to (κ^2-N,O) salicylaldiminato[97] ligands. The Cu^{II} precatalysts with a bisbenzimidazole ligand (**XIX** in Chart 3) also produce a MA-ethylene and MMA-ethylene copolymer, although the copolymer composition (>50% acrylate incorporation) suggests a radical rather than a coordination-insertion polymerization mechanism, since acrylates are more reactive in radical polymerization.[94, 98] Adding to the credibility of a radical mechanism, model catalysts were immediately reduced to diamagnetic Cu^{I} upon addition of MAO.[99]

Clearly great possibilities for structural variation exist in the post-metallocenes, and the above examples only represent some of the most prominent catalytic systems. For comprehensive reviews one can consult several references.[10, 28, 31, 57, 100, 101]

Chapter 2: Computational Methods

In this chapter an overview will be given of the theory underlying the computational methods used in this work. Several textbooks were consulted covering all treated topics,[102] Hartree-Fock theory,[103] density functional theory (DFT),[104, 105] thermodynamic corrections,[106] and regression.[107]

2.1 Principles of Quantum Chemistry

Quantum mechanics, as opposed to classical mechanics, considers the quantization of energy which becomes important at an atomic scale:

$$E = h\nu \tag{2.1}$$

with ν the frequency and h Planck's constant. This quantization arises from the wave-like behaviour of all matter. This is known as the *wave-particle duality* which becomes especially important for particles with small mass m such as electrons and photons as appears in equation (2.2) due to de Broglie with λ the wavelength and momentum p:

$$\lambda = \frac{h}{p} \tag{2.2}$$

which can be derived from (2.1) by using $E = mc^2$ for a photon travelling at the speed of light c.
Due to the wave-particle duality it becomes impossible to simultaneously measure the position and momentum of light particles such as electrons and photons. Instead there exists a linked uncertainty Δ on both quantities:

$$\Delta x \Delta p_x \geq \frac{\hbar}{2} \tag{2.3}$$

with $\hbar = \frac{h}{2\pi}$.
This is known as the *uncertainty principle* and was exemplified by Heisenberg in a slit experiment with electrons where narrowing the slit (decrease in Δx) led to a wider diffraction pattern (increase in Δp_x). The underlying reason is that the quantum mechanical operators for x and p_x do not commute.
Due to these intrinsic uncertainties, quantum mechanics inevitably has a statistical nature. This is expressed in the *wave or state function* $\Psi(\mathbf{x}_1,\ldots,\mathbf{x}_N,t)$, a function of the space and spin coordinates (the product of the position vector $\mathbf{r}_i$ and a spin coordinate s_i) of all N particles and time t, which contains all possible information of the system. The physical meaning of the wave

function lies in the product with its complex conjugate $|\Psi(\mathbf{x}_1, \ldots,\mathbf{x}_N,t)|^2$ which is the probability density or probability amplitude associated with all particles, making $|\Psi(\mathbf{x}_1, \ldots,\mathbf{x}_N,t)|^2 d\mathbf{x}_1 \ldots d\mathbf{x}_N$ the probability for simultaneously finding particle 1 with spin s_1 in the infinitesimal space $d\mathbf{r}_1$, …, particle N with spin s_N in the infinitesimal space $d\mathbf{r}_N$, at time t.

Since the wave function $\Psi(\mathbf{x}_1, \ldots,\mathbf{x}_N,t)$ contains all the information of a system, any physically observable property of interest can be obtained by applying the appropriate linear Hermitian operator $\hat{O}$ to Ψ and solving the following eigenvalue problem

$$\hat{O}\Psi_i = o_i\Psi_i \tag{2.4}$$

to obtain the real eigenvalues o_i corresponding to the measurable values of the property associated with the eigenfunctions Ψ_i of $\hat{O}$, which represent different states of the system. If the wave function is not an eigenfunction of $\hat{O}$, it can be expanded in the complete set of eigenfunctions of $\hat{O}$, and an average (or expectation) value of property O, $\langle O\rangle$, can be calculated by integration over all coordinates τ:

$$\langle O\rangle = \int \Psi^* \hat{O} \Psi d\tau = \langle \Psi \,|\, \hat{O} \,|\, \Psi\rangle \tag{2.5}$$

where the *bra-ket* notation is introduced on the right-hand side.

Quantum mechanical operators can be constructed from their classical expressions by replacing the Cartesian coordinate q, and the linear momentum component p_q with the corresponding operators:

$$\hat{q} = q, \text{ and } \hat{p}_q = \frac{\hbar}{i}\frac{\partial}{\partial q} \tag{2.6}$$

The quantum mechanical operator for the total energy, the *Hamiltonian* operator, describing both kinetic and potential energy, T and V respectively, can then be constructed from the classical expression for the Hamiltonian for N particles:

$$H = T + V = \sum_{i=1}^{N} \frac{p_{xi}^2 + p_{yi}^2 + p_{zi}^2}{2m_i} + V(\mathbf{x}_1,\ldots,\mathbf{x}_N,t) \tag{2.7}$$

by substitution of (2.6) herein:

$$\hat{H} = \hat{T} + \hat{V} = -\sum_{i=1}^{N} \frac{\hbar^2}{2m_i}\nabla_i^2 + V(\mathbf{x}_1,\ldots,\mathbf{x}_N,t) \tag{2.8}$$

with ∇_i^2 the *Laplacian* operator for particle i:

$$\nabla_i^2 \equiv \left(\frac{\partial}{\partial x_i^2} + \frac{\partial}{\partial y_i^2} + \frac{\partial}{\partial z_i^2}\right) \tag{2.9}$$

From the *time-dependent Schrödinger equation*:

$$i\hbar\frac{\partial}{\partial t}\Psi(\mathbf{x}_1,...,\mathbf{x}_N,t)=\hat{H}\Psi(\mathbf{x}_1,...,\mathbf{x}_N,t) \tag{2.10}$$

if the potential energy $V(x_1,\ldots,z_N,t)$ is not a function of time, i.e. in the absence of time-dependent external forces (such as external magnetic and electric fields), the *time-independent Schrödinger equation*,

$$\hat{H}\psi(\mathbf{x}_1,...,\mathbf{x}_N)=E\psi(\mathbf{x}_1,...,\mathbf{x}_N) \tag{2.11}$$

where the lowest eigenvalue E_0 of $\hat{H}$ corresponds to the ground state energy of the system, can be obtained by writing the wave function as a product of a function of time and a function of space and spin coordinates:

$$\Psi(\mathbf{x}_1,...,\mathbf{x}_N,t)=\Theta(t)\psi(\mathbf{x}_1,...,\mathbf{x}_N)=e^{-iEt/\hbar}\psi(\mathbf{x}_1,...,\mathbf{x}_N) \tag{2.12}$$

In this case, the probability density becomes time-independent resulting in a *stationary state*:

$$\left|\Psi(\mathbf{x}_1,...,\mathbf{x}_N,t)\right|^2=\left|\psi(\mathbf{x}_1,...,\mathbf{x}_N)\right|^2 \tag{2.13}$$

For such stationary state, the electron density $\rho(\mathbf{r}_1)$, the probability for finding any electron with arbitrary spin in an infinitesimal space volume $d\mathbf{r}_1$ can be obtained from a normalized N-electron wave function by integration over all spin coordinates and all but one position vectors and multiplication by N to account for the indistinguishability of electrons:

$$\rho(\mathbf{r}_1)=N\int\ldots\int\psi(\mathbf{x}_1,...,\mathbf{x}_N)\psi^*(\mathbf{x}_1,...,\mathbf{x}_N)d\mathbf{x}_2..d\mathbf{x}_N ds_1 \tag{2.14}$$

Since the computational study of chemical reactions requires determination of the relative total energies of the involved reactants, transition states and products, the Hamiltonian operator of interest will be that of a molecular system with N electrons and M nuclei. The Hamiltonian, while neglecting spin-orbit interaction and relativistic effects, takes into account (in order of appearance) the kinetic energy of the nuclei T_N and electrons T_e, the electrostatic Coulomb repulsion between two nuclei V_{NN}, the Coulomb attraction between electron and nucleus V_{Ne} and the Coulomb repulsion between two electrons V_{ee}. The first two terms describe the kinetic energy, the last three the potential energy. In atomic units where $\hbar$, the electron mass m_e, electron charge Z_e and permittivity of the vacuum $4\pi\varepsilon_0$ have the numerical value of 1 this becomes:

$$\begin{aligned}\hat{H}&=\hat{T}_N+\hat{T}_e+\hat{V}_{NN}+\hat{V}_{Ne}+\hat{V}_{ee}=\\&-\frac{1}{2}\sum_{\alpha=1}^{M}\frac{1}{M_\alpha}\nabla_\alpha^2-\frac{1}{2}\sum_{i=1}^{N}\nabla_i^2+\sum_{\alpha=1}^{M}\sum_{\beta>\alpha}^{M}\frac{Z_\alpha Z_\beta}{r_{\alpha\beta}}-\sum_{\alpha=1}^{M}\sum_{i=1}^{N}\frac{Z_\alpha}{r_{\alpha i}}+\sum_{i=1}^{N}\sum_{j>i}^{N}\frac{1}{r_{ij}}\end{aligned} \tag{2.15}$$

with Z_α the atomic number and M_α the mass of the nucleus α, i and j denote electrons, r_{ij} the distance between the electrons and $r_{\alpha i}$ the distance between the nucleus α and the electron i.
Operation of the Hamiltonian in equation (2.15) on the wave function results in electronic, nuclear and mixed terms which can be separated to greatly facilitate solving the Schrödinger equation (2.11). Since the electrons are much lighter and move much faster than the nuclei, the latter can be regarded as fixed in space to good approximation. This means the electron-nuclear cross dependencies in the nuclear kinetic energy operator can be neglected, allowing for the wave function to be written as a nuclear and electronic wave function and allowing for a separation of the Hamiltonian in (2.15) in a nuclear and electronic component, the latter given by:

$$\hat{H}_{el} = \hat{T}_e + \hat{V}_{Ne} + \hat{V}_{ee} = -\frac{1}{2}\sum_{i=1}^{N}\nabla_i^2 - \sum_{\alpha=1}^{M}\sum_{i=1}^{N}\frac{Z_\alpha}{r_{\alpha i}} + \sum_{i=1}^{N}\sum_{j>i}^{N}\frac{1}{r_{ij}} \tag{2.16}$$

with $\hat{H}_{el}$ known as the purely electronic Hamiltonian. The resulting purely electronic energy E_{el} from the Schrödinger equation will then depend only parametrically on the positions of the nuclei via V_{Ne} and adding the nuclear repulsion V_{NN} to E_{el} gives the total electronic energy U. This approximation is known as the *Born-Oppenheimer approximation*.
Knowledge of the purely electronic Hamiltonian does not imply that the Schrödinger equation is easily solvable. In fact, exact solutions exist only for rather simple systems such as a particle in a box or the hydrogen atom. For molecules containing numerous electrons and atoms, we need to resort to approximate solution methods. Fortunately, there exists a principle, the *variational principle,* that can be exploited to systematically approach the ground state wave function ψ_0. It states that the expectation value for the energy E_{trial} for any normalized trial wave function ψ_{trial} is higher than or equal to the ground state energy E_0:

$$\langle \psi_{trial} | \hat{H} | \psi_{trial} \rangle = E_{trial} \geq E_0 = \langle \psi_0 | \hat{H} | \psi_0 \rangle \tag{2.17}$$

2.2 The Hartree-Fock Method

In the Hartree-Fock method, the true wave function is approximated by a single *Slater determinant* ψ_{SD} constructed from orthonormal one-electron wave functions or spin orbitals $\chi_i(\mathbf{x}_1)$:

$$\psi_{SD} = \frac{1}{\sqrt{N!}} \begin{vmatrix} \chi_1(\mathbf{x}_1) & \cdots & \chi_N(\mathbf{x}_1) \\ \vdots & \ddots & \vdots \\ \chi_1(\mathbf{x}_N) & \cdots & \chi_N(\mathbf{x}_N) \end{vmatrix} \tag{2.18}$$

Since the single Slater determinant changes sign when two rows are interchanged, it fulfils the the antisymmetry requirement on wave functions of multiple electrons. Its value becomes zero when two different electrons occupy the same spin orbital (when two columns become identical), reflecting the Pauli exclusion principle. The electrons are indistinguishable and the factor $(N!)^{-(1/2)}$ ensures normalization.

A consequence of approximating the true wave function by a single Slater determinant is that the probability of finding two electrons with opposite spin at the same point in space is not zero, despite the infinite Coulomb repulsion. Their motions will be uncorrelated (Coulomb correlation), in contrast to electrons with parallel spin which are correlated (Fermi correlation).

The expectation value of the Hamiltonian (2.16) with ψ_{SD} (2.18) by (2.5) is the Hartree-Fock energy E_{HF}:

$$E_{HF} = \langle \psi_{SD} | \hat{H} | \psi_{SD} \rangle = \sum_{i=1}^{N} \langle i | \hat{h}(1) | i \rangle + \frac{1}{2} \sum_{i=1}^{N} \sum_{j=1}^{N} \langle ii | jj \rangle - \langle ij | ji \rangle \tag{2.19}$$

with $\hat{h}(1)$ the core-Hamiltonian operator containing the one-electron terms of

$$\hat{h}(1) = -\frac{1}{2} \nabla_1^2 - \sum_{\alpha=1}^{M} \frac{Z_\alpha}{r_{\alpha 1}} \tag{2.20}$$

and the Coulomb integral

$$\langle ij | ij \rangle = \iint |\chi_i(\mathbf{x}_1)|^2 \frac{1}{r_{12}} |\chi_j(\mathbf{x}_2)|^2 \, d\mathbf{x}_1 d\mathbf{x}_2 \tag{2.21}$$

and exchange integral

$$\langle ij | ji \rangle = \iint \chi_i^*(\mathbf{x}_1) \chi_j^*(\mathbf{x}_2) \frac{1}{r_{12}} \chi_j(\mathbf{x}_1) \chi_i(\mathbf{x}_2) d\mathbf{x}_1 d\mathbf{x}_2 \tag{2.22}$$

The solution of the Schrödinger equation by the Hartree-Fock method involves the construction of a one-electron operator, the Fock operator $\hat{f}(1)$ which describes one electron in the average field of the other electrons j, called the Hartree-Fock potential $V_{HF}(1)$ (2.23). By doing so, a complicated N-electron problem is reduced to a one-electron problem requiring an iterative approach. The exact form of the Fock operator is as follows:

$$\hat{f}(1) = \hat{h}(1) + V_{HF}(1) = \hat{h}(1) + \sum_{j}^{N} \left(\hat{J}_j(1) - \hat{K}_j(1) \right) \tag{2.23}$$

with $\hat{J}_j(1)$ the Coulomb operator describing the classical electron-electron repulsion from the averaged field

$$\hat{J}_j(1) = \int \left|\chi_j(\mathbf{x}_2)\right|^2 \frac{1}{r_{12}} d\mathbf{x}_2 \tag{2.24}$$

and $\hat{K}_j(1)$ the non-classical exchange operator which is a non-local operator which is defined by its operation on an orbital.

$$\hat{K}_j(1)\chi_i(\mathbf{x}_1) = \left[\int \chi_j^*(\mathbf{x}_2) \frac{1}{r_{12}} \chi_i(\mathbf{x}_2) d\mathbf{x}_2 \right] \chi_j(\mathbf{x}_1) \tag{2.25}$$

The optimal orthonormal spin orbitals $\chi_i(\mathbf{x}_1)$ that minimize the energy E_{HF} are those that are eigenfunctions of the Fock operator, with eigenvalues ε_i. This leads to the Hartree-Fock equation:

$$\hat{f}(1)\chi_i(\mathbf{x}_1) = \varepsilon_i \chi_i(\mathbf{x}_1) \tag{2.26}$$

As noted above, the lack of Coulomb correlation in the Hartree-Fock method is a significant shortcoming. Several methods have been developed to introduce Coulomb correlation, such as perturbation theory (Møller-Plesset, MP), or by introducing additional Slater determinants (configuration interaction, CI and coupled cluster, CC). The main problem with such methods is their high computational cost preventing routine application to realistic transition metal systems. Density functional theory (DFT) offers an interesting option to introduce Coulomb correlation, essentially with the same computational cost as for the Hartree-Fock method.

2.3 Density Functional Theory

A consequence of the fact that only one and two electron interactions appear in the Hamiltonian (2.16) is that the molecular energy is only dependent of six spatial coordinates and two spin coordinates, the latter which can be eliminated from the expression. An N-electron wave function depends on the contrary on 3N spatial and N spin coordinates. This suggests that there is more information in the wave function than directly physically relevant and the properties of the system may be calculated from other functions containing fewer variables. This is the central idea in DFT, where the molecular properties are calculated as a functional of the electron density $\rho(\mathbf{r})$. The basis for DFT was laid in 1964 with two theorems due to Hohenberg and Kohn. The *first Hohenberg-Kohn theorem* (proof of existence) states that "the external potential $V_{ext}(\mathbf{r})$ is (to within a constant) a unique functional of $\rho(\mathbf{r})$; since, in turn $V_{ext}(\mathbf{r})$ fixes the Hamiltonian $\hat{H}$

we see that the full many particle ground state is a unique functional of $\rho(\mathbf{r})$." $V_{ext}(\mathbf{r})$ is nothing other than the nucleus-electron attraction V_{Ne} in the first term of (2.19) and second term of (2.20), which is termed external potential due to the fact that it is produced by charges external to the system of electrons, i.e. the nuclei fixed in space by the Born-Oppenheimer approximation. The theorem can be proven by reductio ad absurdum. Bright-Wilson quoted that this is not as surprising as it may seem: The total electron density defines the number of electrons in the system, the cusps in the density define the nuclear coordinates, the derivative of the density at the cusp the nuclear charge at the cusp and thus the configuration of the elements in the molecules. Hence, the system is fully defined. The first Hohenberg-Kohn theorem can be presented schematically as:

$$\rho \Rightarrow \{N, \mathbf{r}_\alpha, Z_\alpha\} \Rightarrow \hat{H} \Rightarrow \psi \Rightarrow E \tag{2.27}$$

With this theorem the ground state energy E_0 can be rewritten, as can be seen from (2.16), as follows, by defining the Hohenberg-Kohn functional $F_{HK}[\rho]$:

$$F_{HK}[\rho] = T[\rho] + V_{ee}[\rho] \tag{2.28}$$

$$E_0 = T[\rho_0] + V_{ee}[\rho_0] + V_{Ne}[\rho_0] = F_{HK}[\rho_0] + \int \rho_0(\mathbf{r}) V_{ext}(\mathbf{r}) d\mathbf{r} \tag{2.29}$$

If the exact expression for the Hohenberg-Kohn functional, which is system-independent, were known then the Schrödinger equation could be solved exactly. Therefore, the quest for the exact expression for $T[\rho]$ and $V_{ee}[\rho]$ is something of the quest for the Holy Grail in DFT.

The first Hohenberg-Kohn theorem states that the energy is a functional of the electron density $E[\rho]$, but it does not provide a practical manner to find that electron density. The *second Hohenberg-Kohn theorem* (variational theorem) deals with this by stating that $F_{HK}[\rho]$ delivers the lowest energy, if and only if the input density is the true ground state density ρ_0. This is the DFT analogue of the variational theorem. Furthermore, any trial density must correspond to an external potential $V_{ext}(\mathbf{r})$ (V_{ext}-representability) and to an antisymmetric N-electron wave function (N-representability).

The Hohenberg-Kohn functional $F_{HK}[\rho]$ consists of the kinetic energy $T[\rho]$ and the electron-electron interaction $V_{ee}[\rho]$ (2.29). Part of $V_{ee}[\rho]$ can be described by the classical electron electron repulsion $J[\rho]$ from (2.21), which includes self-interaction:

$$V_{ee}[\rho] = J[\rho] + E_{ncl}[\rho] = \frac{1}{2} \int\int \frac{\rho(\mathbf{r}_1)\rho(\mathbf{r}_2)}{r_{12}} d\mathbf{r}_1 d\mathbf{r}_2 + E_{ncl}[\rho] \tag{2.30}$$

The remainder of $V_{ee}[\rho]$ is contained in $E_{ncl}[\rho]$, the non-classical portion of the electron-electron interactions. Hence, two unknown functionals remain: $T[\rho]$ and $E_{ncl}[\rho]$. Especially finding an

appropriate expression for T[ρ] has proven difficult in the past. The idea behind the *Kohn-Sham method* is that the kinetic energy can be fairly accurately calculated by an orbital-based approach as the Hartree-Fock method. In this Kohn-Sham method a non-interacting reference system, exactly described by a single Slater determinant built from spin orbitals $\varphi(\mathbf{x}_1)$, with the same density as the real system is introduced. This departure from the electron density as main variable by introducing orbitals, means that the Kohn-Sham method breaks in a sense with the original goals of DFT. The kinetic energy of the non-interacting system, T_S, a first approximation to the real kinetic energy, is then given cf. the first terms in (2.19) and (2.20) by:

$$T_S = -\frac{1}{2}\sum_{i=1}^{N}\langle \varphi_i(\mathbf{x}_1) \mid \nabla_1^2 \mid \varphi_i(\mathbf{x}_1)\rangle \tag{2.31}$$

Now all unknown energy terms, such as the remainder of the kinetic energy ($T[\rho] - T_S[\rho]$) and the part of $V_{ee}[\rho]$ not covered by $J[\rho]$ (i.e. self-interaction, exchange and correlation) can be gathered in the exchange-correlation energy $E_{XC}[\rho]$:

$$E_{XC}[\rho] = \left(T[\rho] - T_S[\rho]\right) + \left(V_{ee}[\rho] - J[\rho]\right) \tag{2.32}$$

Analogously to the Fock operator (2.23), a one-electron Kohn-Sham operator $\hat{f}_{KS}$ can be constructed:

$$\hat{f}_{KS}(1) = -\frac{1}{2}\nabla_1^2 + V_S(\mathbf{r}_1) = -\frac{1}{2}\nabla_1^2 + \left[\int \frac{\rho(\mathbf{r}_2)}{r_{12}} d\mathbf{r}_2 - \sum_{\alpha=1}^{M}\frac{Z_\alpha}{r_{\alpha 1}} + V_{XC}(\mathbf{r}_1)\right] \tag{2.33}$$

with $V_{XC}(\mathbf{r}_1)$ the unknown potential from $E_{XC}[\rho]$, defined as its functional derivative with respect to ρ:

$$V_{XC} \equiv \frac{\delta E_{XC}}{\delta \rho} \tag{2.34}$$

The optimal spin orbitals $\varphi_i(\mathbf{x}_1)$ are then found under the orthonormality constraint by the second Hohenberg-Kohn theorem to minimize E_0 (2.29) via (2.35), where ε_i^{KS} are the orbital energies, completely analogous to the Hartree-Fock equation (2.26):

$$\hat{f}_{KS}(1)\varphi_i(\mathbf{x}_1) = \varepsilon_i^{KS}\varphi_i(\mathbf{x}_1) \tag{2.35}$$

In constrast to the Hartree-Fock method, where the single Slater determinant from the optimized spin orbitals $\chi_i(\mathbf{x}_1)$ is an approximation to the N-electron wave function, the single Slater determinant from the DFT optimized spin orbitals $\varphi_i(\mathbf{x}_1)$ does not have any direct connection to the wave function. However, often DFT optimized spin orbitals $\varphi_i(\mathbf{x}_1)$ resemble their HF counterparts, and another similarity is that the sum of the product of the orbitals with their

complex conjugate yields the electron density. Finally, it can be noted that the Kohn-Sham method is in principle exact, if the exact form of E_{XC} and V_{XC} would be known.

Many approximations to the critical exchange-correlation energy functional $E_{XC}[\rho]$ have been made. One of the earliest is the *Local-Density Approximation* (LDA), where the value of $E_{XC}[\rho]$ depends solely on the local value of ρ:

$$E_{XC}^{LDA}[\rho] = \int \rho(\mathbf{r}) \varepsilon_{XC}(\rho(\mathbf{r})) d\mathbf{r} \tag{2.36}$$

with $\varepsilon_{XC}(\rho(\mathbf{r}))$ the exchange and correlation energy per electron in a homogeneous electron gas, which can be written as a sum of exchange and correlation parts $\varepsilon_{XC}(\rho(\mathbf{r})) = \varepsilon_X(\rho(\mathbf{r})) + \varepsilon_C(\rho(\mathbf{r}))$. This approximation makes use of the exact analytical expression of the exchange energy per electron $\varepsilon_X(\rho(\mathbf{r}))$ of a homogeneous electron gas:

$$\varepsilon_X(\rho(\mathbf{r})) = -\frac{3}{4}\left(\frac{3}{\pi}\right)^{1/3} (\rho(\mathbf{r}))^{1/3} \tag{2.37}$$

For the correlation part, accurate numerical Monte-Carlo simulations have led to approximate expressions for $\varepsilon_C(\rho(\mathbf{r}))$ by Vosko, Wilk and Nusair (VWN), and Perdew and Wang (PW).

The homogeneous electron gas of the LDA is a rather poor model for the electron density in a molecule, which can vary drastically in space. In an attempt to alleviate this situation, gradient-corrected functionals also include the gradient of the electron density in the expression for $E_{XC}[\rho]$. Such functionals are said to make use of the generalized gradient approximation (GGA). As with the LDA, $E_{XC}[\rho]$ is split into an exchange $E_X[\rho]$ and correlation part $E_C[\rho]$, and approximate expressions are sought for both separately. The LDA is an important basis for $E_X[\rho]$, which is further corrected for the inhomogeneity of the electron density. Popular functionals for $E_X[\rho]$ include Becke, 1988 (B(88)) and Perdew, Burke and Ernzerhof, 1996 (PBE). The forms of $E_C[\rho]$ are rather complicated and most popular ones include Perdew, 1986 (P(86)), Perdew, Burke and Ernzerhof, 1996 (PBE) and Lee, Yang and Parr (LYP), the latter derived from an accurate He wave function. Combining these correlation and exchange functionals provides the GGA functionals commonly used in the thesis: BP86, BLYP and PBEPBE (or simplified PBE). An extension to the GGA functionals are the meta-GGA functionals, which also include, in addition to the electron density and its gradient, the Laplacian of the electron density in the expression for $E_{XC}[\rho]$.

Since the exchange energy of a single Slater determinant can be calculated exactly from the last term in (2.19), the inclusion of such exact exchange E_X^{exact} in $E_X[\rho]$ seems a promising

approach. Functionals using exact exchange, while still using LDA and GGA as basis, are termed hybrid functionals. The most popular hybrid functional is probably B3LYP, a combination of the B88 exchange functional and the LYP correlation functional, the 3 standing for three empirical parameters, a=0.20, b=0.72 and c=0.81:

$$E_{XC}^{B3LYP} = (1-a)E_X^{LSD} + aE_X^{exact} + bE_X^{B88} + cE_C^{LYP} + (1-c)E_C^{LSD} \tag{2.38}$$

with LSD a spin-adapted LDA.

A significant shortcoming of DFT is that the *dispersion or London forces* between instantaneously induced dipoles are not accounted for. This can be understood by the local character of $V_{XC}(\mathbf{r})$, which is dependent of the density and its gradient at a single point **r**. Another, distant system with no overlap will hence not be able to lower the energy in order to account for the long-range, non-local correlation contained in the dispersion or London forces. This has quite dramatic effects when studying realistic catalytic systems, especially for dissociation and association reactions.[108] Several remedies have been devised. One is the development of a new series of heavily parameterized functionals including dispersion, the Minnesota type of functionals (M06, M08). Another is an empirical dispersion correction devised by Grimme. The latter is routinely used in the thesis, and consists of adding a negative (stabilizing) dispersion correction E_{disp} to the electronic DFT energy.

$$E_{disp} = -s_6 \sum_{\alpha=1}^{M} \sum_{\beta>\alpha}^{M} \frac{C_6^{\alpha\beta}}{r_{\alpha\beta}^{-6}} f_{dmp}(r_{\alpha\beta}) \tag{2.39}$$

with s_6 a global scaling parameter that depends on the functional used (BP86 and B3LYP = 1.05, BLYP = 1.20, PBE = 0.75). $C_6^{\alpha\beta}$ is a dispersion coefficient for the two involved atoms which is defined as the geometric mean from the two atomic dispersion parameters. f_{dmp} is a damping factor with r_{vdw} the sum of the van der Waals radii of the two involved atoms:

$$f_{dmp}(r_{\alpha\beta}) = \frac{1}{1 + e^{-d\left(\frac{r_{\alpha\beta}}{r_{vdw}} - 1\right)}} \tag{2.40}$$

which, at interatomic distances typical for covalent bonding where $r_{\alpha\beta} < r_{vdw}$, drops to zero, hereby making the dispersion correction E_{disp} negligible, as required. d is a parameter set to 20. (2.39) shows the typical interatomic $r_{\alpha\beta}^{-6}$ dependence as in the attractive (second) term for the Lennard-Jones potential V_{LJ}:

$$V_{LJ} = 4\varepsilon\left[\left(\frac{\sigma}{r_{\alpha\beta}}\right)^{12} - \left(\frac{\sigma}{r_{\alpha\beta}}\right)^{6}\right] \tag{2.41}$$

with ε the well-depth and σ the distance at which V_{LJ} becomes zero, which is related to the van der Waals distance. Unfortunately, the Grimme dispersion correction can not be used for third row transition metals due to the appearance of systematic errors in test calculations.[109]

2.4 Semiempirical Methods

The spin orbitals $\chi_i(\mathbf{x}_1)$ in the Hartree-Fock and Kohn-Sham equations (2.26) and (2.35) are a product of a spatial molecular orbital $\psi_i(\mathbf{r}_1)$ and a spin function α(ω) or ß(ω) (where ω is an unspecified spin coordinate). α(ω) and ß(ω) form a complete set and are orthonormal. In order to solve equations (2.26) and (2.35) these spatial molecular orbitals $\psi_i(\mathbf{r}_1)$ are expanded linearly in a basis of known atomic basis functions or atomic orbitals $\eta_\nu(\mathbf{r}_1)$, which are in turn most commonly constructed from several Gaussian or Slater functions:

$$\psi_i(\mathbf{r}_1) = \sum_{\nu=1}^{K} C_{\nu i}\eta_\nu(\mathbf{r}_1) \tag{2.42}$$

By inserting this expansion in (2.26) and (2.35), left multiplication with an arbitrary basis function $\eta_\mu^*(\mathbf{r}_1)$ and integration over space one obtains several equations, the Roothaan equations (2.43) with i=1,…,K which apply to closed shell systems with doubly occupied orbitals:

$$\sum_{\nu=1}^{K} F_{\mu\nu}C_{\nu i} = \varepsilon_i \sum_{\nu=1}^{K} S_{\mu\nu}C_{\nu i} \tag{2.43}$$

with $F_{\mu\nu}$ the Fock matrix element:

$$F_{\mu\nu} = \int \eta_\mu^*(\mathbf{r}_1)\hat{f}(1)\eta_\nu(\mathbf{r}_1)d\mathbf{r}_1 \tag{2.44}$$

and $S_{\mu\nu}$ the overlap matrix element:

$$S_{\mu\nu} = \int \eta_\mu^*(\mathbf{r}_1)\eta_\nu(\mathbf{r}_1)d\mathbf{r}_1 \tag{2.45}$$

(2.43) can be written more compactly as a matrix equation

$$\mathbf{FC} = \mathbf{SC\varepsilon} \tag{2.46}$$

with **C** a K×K matrix with the expansion coefficients $C_{\nu i}$ and **ε** a diagonal matrix with the orbital energies ε_i. Since **F** is dependent of **C** via the Fock operator (2.23) this is a non-linear matrix equation and it is therefore solved iteratively for **C** and **ε** by successive diagonalization of a transformed **F** until *self-consistency*, i.e. consistency between the Hartree-Fock potential $V_{HF}(1)$ (2.23) and the electron density (determined by **C**), is reached. Taking into account the explicit

form of the Fock operator (2.23) for (2.46), and integrating out spin coordinates, a matrix element of the Fock matrix can be expressed in atomic orbitals (2.42) as:

$$F_{\mu\nu} = H_{\mu\nu}^{core} + \sum_{a=1}^{N/2}\sum_{\sigma=1}^{K}\sum_{\lambda=1}^{K} C_{\lambda a} C_{\sigma a}^{*} \left[2(\mu\nu \mid \sigma\lambda) - (\mu\lambda \mid \sigma\nu)\right] \tag{2.47}$$

where the round brackets now indicate integrations over spatial functions, and with $H_{\mu\nu}^{core}$:

$$H_{\mu\nu}^{core} = (\mu \mid \hat{h}(1) \mid \nu) \tag{2.48}$$

The solving of the two electron integrals in (2.47) consumes most of the computational time in a Hartree-Fock or DFT calculation. Because of these integrals, both methods scale to the fourth power with basis set size ($O(K^4)$).

Semiempirical methods reduce the computational time by reducing the number of two electron integrals. They take into account only subpart of the electrons, such as the π-electrons in early semiempirical methods or the valence electrons in later, more general methods. The methods are heavily dependent on parameterization which relies on reference data, either experimental or computational. The semiempirical method used in Paper V, PM6 (Parametric Method 6),[110] uses the same Hamiltonian as in (2.16), but only takes into account the valence electrons, the amount of which is N_{val}. Hence the first summation in (2.47) is limited to a much smaller $N_{val}/2$ instead of N/2 (again for closed shell systems). K in the following summations of (2.47) is likewise limited by considering a subpart of the electrons in addition to having a minimal valence basis set of Slater functions. In PM6, as a NDDO (*Neglect of Diatomic Differential Overlap*) method, the number of two electron integrals is further reduced by neglecting the differential overlap of the atomic orbitals $\eta_{\mu,A}$ and $\eta_{\nu,B}$ when they are centred on different atoms:

$$\eta_{\mu,A}^{*}(\mathbf{r}_1)\eta_{\nu,B}(\mathbf{r}_1)d\mathbf{r}_1 = 0, \qquad (A \neq B) \tag{2.49}$$

The elements of the core Hamiltonian matrix $H_{\mu\nu}^{core}$ (2.48) are obtained by making use of several parameters. First, if the atomic orbitals $\eta_{\mu,A}$ and $\eta_{\nu,B}$ are centred on different atoms the matrix element is proportional to the overlap integral $S_{\mu,A\nu,B}$ as in (2.45):

$$H_{\mu,A\nu,B}^{core} = \frac{1}{2}(\beta_{\mu,A} + \beta_{\nu,B})S_{\mu,A\nu,B}, \qquad (A \neq B) \tag{2.50}$$

with ß an element and orbital type dependent parameter. If the atomic orbitals $\eta_{\mu,A}$ and $\eta_{\nu,A}$ are centred on the same atom A, $H_{\mu\nu}^{core}$ can be written as:

$$H_{\mu,A\nu,A}^{core} = \langle \mu_A \mid -\frac{1}{2}\nabla^2 + V_A \mid \nu_A \rangle + \sum_{A \neq B} V_B \tag{2.51}$$

where the first term can be shown to be zero. The second term, the electron-nuclei attraction, is calculated by an electron-electron repulsion integral involving a valence s-orbital on B, multiplied by the negative core charge C_B, which is the atomic number minus the number of core electrons on B:

$$H^{core}_{\mu,A\nu,A} = \sum_{A\neq B} V_B = -\sum_{A\neq B} C_B(\mu_A\nu_A \mid s_B s_B) \text{ for } \mu \neq \nu \tag{2.52}$$

In case the atomic orbitals $\eta_{\mu,A}$ and $\eta_{\nu,A}$ are the same ($\mu = \nu$), the first term in (2.51) is not zero, and it can be parameterized as an element and orbital type dependent parameter $U_{\mu,A\mu,A}$:

$$H^{core}_{\mu,A\mu,A} = U_{\mu,A\mu,A} - \sum_{A\neq B} C_B(\mu_A\nu_A \mid s_B s_B) \tag{2.53}$$

The two electron, one center integrals appearing in (2.47) are parametrized as $g_{\mu\nu}$ and $h_{\mu\nu}$ for the Coulomb and exchange integrals $(\mu_A\mu_A|\nu_A\nu_A)$ (cf. (2.21)) and $(\mu_A\nu_A|\mu_A\nu_A)$ (cf. (2.22)) respectively. The two center integrals in (2.47) which also appear in (2.52) and (2.53) are then found from the values of the one center integrals by an approximate method. Finally, the role of the nuclear-nuclear repulsion V_{NN} in (2.15) is played by the core-core repulsion energy V_{cc}, which, similarly to (2.52), involves a two electron Coulomb repulsion integral (cf. (2.21)) with the valence s orbitals of A and B:

$$V_{cc} = \sum_A \sum_{B>A} \left[C_A C_B(s_A s_A \mid s_B s_B) + f_{AB}\right] \tag{2.54}$$

with f_{AB} a parameterized function. Appropriate values for these and other parameters such as the Slater exponents in the basis functions are found by fitting to experimental reference data supplemented by computational data where experimental data is lacking or incomplete. The reference data include *inter alia* standard enthalpies of formation, dipole moments and geometries.

2.5 Molecular Mechanics

The molecular mechanics method is an even faster method than semiempirical methods and allows for rapid evaluation of relative molecular stabilities. Because of the speed, it is very suitable for conformational searches for which it is exclusively used in this thesis. As semiempirical methods, it relies heavily on parameterization, and often there exists a trade-off between accuracy and generality. It does not treat electrons explicitly, but instead considers a molecule as atoms held together by springs. Deviations of reference bond lengths, angles, etc…

contribute directly to the energy of the molecule, which is termed steric energy or strain energy V. The most general expression for V defining the force field is:

$$V = V_{str} + V_{bend} + V_{oop} + V_{tors} + V_{cross} + V_{vdW} + V_{es} + V_{hb} \tag{2.55}$$

with V_{str} the potential energy of bond stretching, V_{bend} that of bond-angle bending, V_{oop} that of out-of-plane bending, V_{tors} that of torsion about bonds, V_{cross} that of the interactions between these terms giving rise to cross terms, V_{vdW} that of van der Waals attractions and repulsions between non-bonded atoms, V_{es} describing the electrostatic interactions and finally V_{hb} describing hydrogen bonding.

The bond stretching is either described by a harmonic oscillator with a displacement l_{ij} of two atoms i and j from a reference bond length l_{IJ}^0 with a force constant k_{IJ} with the latter two parameters depending on the atom types I and J involved:

$$V_{str} = \frac{1}{2} k_{IJ} (l_{ij} - l_{IJ}^0)^2 \tag{2.56}$$

or by a Morse function:

$$V_{str} = D_e \left(1 - e^{-\alpha (l_{ij} - l_{IJ}^0)^2} \right) \tag{2.57}$$

where D_e is the well depth and α the scale parameter.

The bond-angle bending is commonly described, similarily to (2.56) as:

$$V_{bend} = \frac{1}{2} k_{IJK} (\theta_{ijk} - \theta_{IJK}^0)^2 \tag{2.58}$$

It describes the bond-angle bending energy with three involved atoms i, j and k as a displacement θ_{ijk} from the reference value θ_{IJK} with force constant K_{IJK}, with the latter two depending on the atom types I, J and K.

The torsion about a bond with dihedral angle φ can be described using one parameter V_n with the periodicity n the number of minima and φ_0 determining the location of the minima:

$$V_{tors} = \frac{1}{2} V_n \left[1 + \cos\left(n\varphi - \varphi_0 \right) \right] \tag{2.59}$$

Alternatively, the torsional energy can be expressed as a Fourier series expansion.

Furthermore, the electrostatic interactions are described by a Coulombic expression and the van der Waals interactions by a Lennard-Jones potential (2.41) with the r_{IJ}^{-6} dependence for the attraction as in the Grimme dispersion correction (2.39) and a r_{IJ}^{-12} dependence for the repulsion.

In Paper V use was made of the (enhanced) DREIDING force field,[111] a general force field capable of handling a wide range of atom types including transition metals. This force field uses

the above expressions for the calculation of the steric energy, with the exception that there are no cross terms in (2.55) and with (2.56) as default for bond stretching.

As stated before, the speed of the different methods is in the following order: HF/DFT < Semiempirical < Molecular Mechanics. The number of atoms in the systems which can still be studied practically by the computational means used in this thesis is roughly 150 for HF/DFT, 1500 for semiempirical methods and 15000 for molecular mechanics. This has inspired the approach in Paper V, where the conformational search was done with molecular mechanics, the fitness calculation with PM6, and the final, most reliable validation fitness calculation with DFT.

2.6 Thermodynamic Corrections

The spontaneity of a chemical reaction at constant pressure and temperature will be determined by the change in Gibbs free energy ΔG. Therefore, Gibbs free energy profiles contain more useful information for chemical reactions than electronic energy profiles. Gibbs free energies and enthalpies can be obtained by adding thermodynamic corrections to the electronic energy. The thermodynamic corrections, within the ideal gas approximation with non-interacting particles, are obtained by calculation of the internal thermal energy E

$$E = Nk_BT^2\left(\frac{\partial \ln q}{\partial T}\right)_V \tag{2.60}$$

and the entropy S

$$S = R\ln(qe) + RT\left(\frac{\partial \ln q}{\partial T}\right)_V \tag{2.61}$$

from the partition function q. k_B is the Boltzmann constant, T the temperature, R the universal gas constant, V the volume, e = 2.718 and N the number of particles. By considering the expressions of the partition functions for translation q_t, electronic motion q_e, rotation q_r and vibration q_v, the product of which is the partition function q in (2.60) and (2.61), under the rigid rotor and harmonic oscillator approximations, and assuming that all electronic excited states are inaccessible, the partition functions become:

$$q_t = RT\left(\frac{2\pi mk_BT}{h^2}\right)^{3/2} V \tag{2.62}$$

$$q_e = \omega_0 \tag{2.63}$$

with ω_0 the degeneracy of the ground state. For a non-linear molecule the rotational partition function q_r becomes:

$$q_r = \frac{\pi^{1/2}}{\sigma_r}\left(\frac{T^{3/2}}{(\Theta_{r,x}\Theta_{r,y}\Theta_{r,z})^{1/2}}\right) \tag{2.64}$$

with σ_r the symmetry number and $\Theta_{r,K}$ the characteristic rotational temperature in the x, y and z direction. The vibrational partition function q_v is given by, considering the characteristic vibrational temperature $\Theta_{v,K}$ of a vibrational mode K:

$$q_v = \prod_K \frac{e^{-\Theta_{v,K}/2T}}{1 - e^{-\Theta_{v,K}/2T}} \tag{2.65}$$

By insertion of the partition functions in (2.60) and (2.61) the respective contributions to S and E can be determined. The enthalpy corrections H_{corr} can then be obtained by summing all the contributions to the internal thermal energy ($E_{tot} = E_t + E_e + E_r + E_v$) as:

$$H_{corr} = E_{tot} + k_B T \tag{2.66}$$

and the Gibbs free energy corrections G_{corr} likewise by gathering all the contributions ($S_{tot} = S_t + S_e + S_r + S_v$) as:

$$G_{corr} = H_{corr} - TS_{tot} \tag{2.67}$$

2.7 Effective Core Potential

Similarly to the idea in semiempirical methods, where a large number of two electron integrals could be dropped by explicitly considering solely the valence electrons in the Hamiltonian (2.16), an effective core potential (ECP) or pseudopotential, can be introduced.

This ECP describes the interactions between the valence electrons and core electrons and the interactions among the core electrons. For those interactions, it replaces the two electron Coulomb and exchange operators in (2.23) by a one electron operator which is much easier to evaluate. ECPs are derived from accurate atomic calculations. The underlying justification for this approximation is that the inner shell orbitals hardly change upon molecule formation.

In heavy elements with a high atomic number, the velocities of the electrons, especially the inner core electrons approach the speed of light and the relativistic effects cannot be neglected anymore as was done in the non-relativistic Schödinger equation (2.11). In those cases ECPs also include relativistic effects.

2.8 Solvent calculations

Since polymerization reactions commonly take place in a liquid solvent and the methods described above produce gas-phase energies, it can be important to take solvent effects into account in order to obtain reliable Gibbs free energy profiles. The inclusion of several solvent molecules in the vicinity of the solute requires considerable computational resources, also because of the many possible conformations and configurations, and therefore solvent effects in Papers I and IV were estimated by modeling the solvent implicitly as a *polarizable continuum*.[112, 113] More specifically, the solvent is a *continuous dielectric* with a relative permittivity ε_r (D-PCM). The passing of a solute from the gas phase to the liquid phase will change the electron density of the solute. In particular, the solvent will polarize the solute and *vice versa*. The electric field the solvent generates is termed the *reaction field*. The change of the electron density means another operator describing the interaction with the solvent must be added to the gas-phase Hamiltonian (2.15). The Schrödinger equation is then solved iteratively, as in (2.46), until self-consistency including the reaction field is reached (SCRF, self-consistent reaction field).

The standard Gibbs free energy of solvation ΔG°_{solv} can be split in four terms:

$$\Delta G^\circ_{solv} = \Delta G^\circ_{solv,es} + \Delta G^\circ_{solv,cav} + \Delta G^\circ_{solv,disp} + \Delta G^\circ_{solv,rep} \tag{2.68}$$

where $\Delta G^\circ_{solv,es}$ covers the electrostatic interactions between the solute and solvent, $\Delta G^\circ_{solv,cav}$ the work needed to create the solute cavity in the solvent, $\Delta G^\circ_{solv,disp}$ the dispersion forces between solute and solvent and $\Delta G^\circ_{solv,rep}$ the quantum-mechanical repulsion between the solute and solvent. $\Delta G^\circ_{solv,es}$ is the hardest term to calculate, since it requires an accurate charge distribution of the solute in the solvent and the electric potential produced by the polarized dielectric continuum φ_σ, which are dependent of each other. The latter is equal to an electric potential by an apparent surface charge on the surface of the solute cavity. Once φ_σ is found, the operator due to the reaction field can be constructed, with N and M still the number of electrons and atoms in the system:

$$\hat{V}_{int} = -\sum_{i=1}^{N} \varphi_\sigma(\mathbf{r}_i) + \sum_{\alpha=1}^{M} Z_\alpha \varphi_\sigma(\mathbf{r}_\alpha) \tag{2.69}$$

and $\Delta G^\circ_{solv,es}$ can be calculated as follows:

$$\Delta G^\circ_{solv,es} = \langle \psi_{solv} | \hat{H}_{gas} + \frac{1}{2}\hat{V}_{int} | \psi_{solv} \rangle - \langle \psi_{gas} | \hat{H}_{gas} | \psi_{gas} \rangle \tag{2.70}$$

with ψ_{gas} the original gas-phase wave function from the Hamiltonian $\hat{H}_{gas}$ and ψ_{solv} the self-consistent wave function for the solute in solution. The solute cavity is constructed by intersecting spheres on the atoms of the solute based on van der Waals radii. Several methods exist. In Papers I and IV Bondi radii[114] were used which explicitly consider hydrogen atoms, while the united atom Hartee-Fock method (UAHF) includes hydrogen in the sphere of the neighboring atom. $\Delta G°_{solv,cav}$ can then be calculated from scaled particle theory. $\Delta G°_{solv,rep}$ and $\Delta G°_{solv,disp}$ are calculated similarly to the respective terms in the Lennard-Jones potential (2.41).

Quite different to the ab initio approach in D-PCM, is the semiempirical approach for the Solvent Model 8 (SM8),[115] used in Papers II and III, and claimed to outperform the default implementation of D-PCM in Gaussian03 and to provide very accurate Gibbs free energies of solvation, also for neutral solutes in non-polar solvents.[115] It is a universal solvent model in the sense that $\Delta G°_{solv}$ for any solute in any solvent can be calculated. In general, it involves a partitioning of the solvent Gibbs free energy in ΔE_E, the change in internal electronic energy of the solute at gas-phase equilibrium geometry, ΔE_N, the change in internal electronic energy of the solute due to geometry changes resulting from the solvation, G_P, the Gibbs free energy due to the electrostatic interactions between the solute and solvent, including polarization and G_{CDS} the Gibbs free energy due to creation of the solute cavity, dispersion and change in solvent structure:

$$\Delta G^{\circ}_{solv} = \Delta E_E + \Delta E_N + G_P + G_{CDS} \tag{2.71}$$

Since all solvent effects have been calculated at the gas-phase equilibrium geometry, ΔE_N is zero. The sum of ΔE_E and G_P, which equals $\Delta G°_{solv,es}$ in (2.68), is calculated by an equation based on the generalized Born equation:

$$\Delta E_E + G_P = \Delta G^{\circ}_{solv,el} = -\frac{1}{2}\left(1-\frac{1}{\varepsilon_r}\right)\sum_{\alpha}^{M}\sum_{\beta}^{M}\frac{Q_\alpha Q_\beta}{(R_{\alpha\beta}^2 + a_\alpha a_\beta e^{-R_{\alpha\beta}^2/(d a_\alpha a_\beta)})^{1/2}} \tag{2.72}$$

with Q_i the partial charge of an atom i, $R_{\alpha\beta}$ the internuclear distance, d an empirical constant set to 3.7 and a_i the Born radius of an atom i, which is a quantity describing the burial depth of the atom in the solute or the average distance of the atom to the dielectric continuum around the solute. The appearance of Q_i in (2.72) requires accurate, partial atomic charges and therefore class IV partial atomic charges are recommended rather than commonly used class II Mulliken or Löwdin partial atomic charges. In particular SM8 was parameterized for Charge Model 4 (CM4) charges, which use class II partial atomic charges and a set of parameters to obtain the class IV CM4 charges.[116] Since $\Delta G°_{solv,es}$ determines the overall energy of the system and depends on Q_i, while Q_i depends on the wave function, an iterative approach is needed as for

(2.46). The partial atomic charges from the solute in gas-phase are used as initial values for Q_i for the iterative process involving $\Delta G°_{solv,es}$ added to the Fock or Kohn-Sham matrix, until self-consistency is reached and the total energy is minimized. Therefore it is also a self-consistent reaction field or SCRF method.

Finally, G_{CDS} is calculated by the solvent accessible surface model:

$$G_{CDS} = \sum_{\alpha}^{M} \sigma_{\alpha} A_{\alpha} + \sigma_{solute} \sum_{\alpha}^{M} A_{\alpha} \tag{2.73}$$

where σ_α and σ_{solute} are the atomic and molecular surface tensions respectively, which contain a number of solvent-dependent parameters such as Abraham's hydrogen bond acidity and basicity parameters, the refractive index, and the macroscopic surface tension. It can also be noted that σ_α is dependent of the atoms in the proximity of α. A_α is the solvent accessible surface for an atom α, which is determined by the smoothened solute cavity surface depending on the molecular radius of the solvent.

2.9 Regression

Since in Papers IV and V use was made of regression methods, this short section will very briefly introduce such methods. The problem at hand is to find a solution for the unknown coefficients vector **x** in the matrix equation (2.74) for an overdetermined system where there are more equations than variables, i.e. for an M×N matrix **A** with M>N.

$$\mathbf{Ax} = \mathbf{b} \tag{2.74}$$

Because of the overdeterminedness a solution for **x** can only be approximate. Therefore, for the equality in (2.74) to be true, a residual vector **ε** must be introduced:

$$\mathbf{Ax} + \boldsymbol{\varepsilon} = \mathbf{b} \tag{2.75}$$

Finding the approximate **x** involves the minimization of the square of the norm of the residuals **ε**, hence the name least-squares:

$$\min_{\mathbf{x}} \|\boldsymbol{\varepsilon}\|^2 = \min_{\mathbf{x}} \|\mathbf{b} - \mathbf{Ax}\|^2 \tag{2.76}$$

This condition is fulfilled when the vector $\mathbf{b} - \mathbf{Ax}$ is orthogonal to the range or column space of **A**. This can be accomplished by constructing an orthogonal projection operator $\mathbf{P}_A$ given by:

$$\mathbf{P}_A = \mathbf{A}(\mathbf{A}^T\mathbf{A})^{-1}\mathbf{A}^T \tag{2.77}$$

to project **b** onto the range of **A** and obtain the normal equation with $\mathbf{A}^+$ the matrix pseudoinverse:

$$(\mathbf{A}^{\mathrm{T}}\mathbf{A})^{-1}\mathbf{A}^{\mathrm{T}}\mathbf{b} = \mathbf{A}^{+}\mathbf{b} = \mathbf{x} \tag{2.78}$$

by which the approximate **x** can be found.

Chapter 3: Modeling Coordination-Insertion Polymerization Catalysts

In order to use computer time efficiently and keep calculations within the boundaries of practical feasibility, two approximations are often introduced. The first pertains to the growing chain lengths, and the second to the counterion which is involved with cationic catalysts.

3.1 Chain Lengths

The formation of a high molecular weight polyethylene chain can involve the insertion of tens of thousands of ethylene monomers. A complete modeling of these insertion steps would not only be unfeasible at probably any level of theory, but also be quite inefficient with respect to obtaining new information. Indeed, the barriers for ethylene insertion into a growing chain can be expected to remain essentially constant after a certain number of monomer units have been incorporated. The same consideration can be made for other barriers such as for ß-H elimination or for energy differences dictating equilibria. This implies that a catalyst's characteristics during propagation can be investigated by solely considering a single chain length, which is then a model for the growing polymer chain during propagation. Indirect experimental support for this assumption can be found in the observation that oligomer distributions are often adequately described by a Schulz-Flory distribution exhibiting a constant probability for chain growth. Such a distribution is characterized by a growth factor α = mol fraction C_{n+2} alkene / mol fraction C_n alkene = $(1 + ß)^{-1}$, with ß = reaction rate for termination / reaction rate for propagation.[117-119] The question at hand is now how long the growing polymer chain in the model should be to capture the propagation energetics. In this work, the chain was mainly (Papers I, II and III) modeled as a propyl ligand. This choice was inspired by the fact that such a ligand reproduces the most important α- and ß-agostic interactions (e.g. references [120-125]) and also allows for a modeling of the ß-H elimination reactions in a realistic environment.[126] In Paper IV, where ß-H elimination reactions do not play a role, an ethyl ligand is used.

3.2 Counterion

When the involved catalyst is cationic, some degree of ion pair association is expected due to the low relative permittivity of solvents typically used in olefin polymerization such as toluene. On

one hand, the explicit consideration of the counterion has, in some cases, been found to be necessary for an accurate description of activity and stereoselectivity of early transition metal polymerization catalysts as metallocenes,[127-130] CGCs,[127, 131-135] or post-metallocene catalysts.[136] On the other hand there are also examples where consideration of the transition metal alkyl cation alone (the so-called 'naked cation' approach) affords a sufficiently accurate description, as for example seen for the stereoselectivity of polypropylene catalyzed by ansa-zirconocenes.[26, 27] It can also be noted that using the 'naked cation' approach is commonplace in computational work on olefin polymerization with late transition metal catalysts. For a more general discussion on ion pairing in organometallic catalysis and the implications for computational chemistry one can turn to references [137] and [138].

In Paper I, which deals with ruthenium olefin coordination-insertion polymerization catalysts and more specifically with the (bis(oxazoline)pyridine)$Ru^{II}X_2$(ethylene)/MAO catalysts due to Nomura and coworkers,[90-92] inclusion of the counterion is further complicated because of the ill-defined chemical structure of the counterion presumably generated by MAO (*vide supra*).[19]

Chapter 4: Mechanistic Aspects of Coordination-Insertion Ethylene Polymerization with Late Transition Metals

4.1 Ruthenium Olefin Coordination-Insertion Polymerization Catalysts

Ruthenium, because of its excellent polar functional group tolerance and low moisture- and air-sensitivity as exemplified by ruthenium olefin metathesis catalysts,[139] is a very promising candidate metal on which to base a catalyst for the random copolymerization of polar and non-polar olefins. This was an important motivation for taking a closer look in Paper I at the only example of a Ru^{II} based catalyst for olefin polymerization due to Nomura and coworkers, i.e. the (bis(oxazoline)pyridine)$Ru^{II}X_2$(ethylene)/MAO system **I** in Chart 4.[90-92]

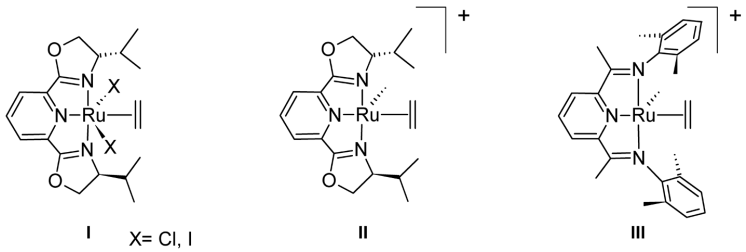

I II III

Chart 4. The precatalyst due to Nomura and coworkers. **(I)**,[90-92] the methyl ethylene cation **(II)** supposedly generated by MAO upon activation of **I**, and the corresponding complex synthesized by Brookhart and coworkers **(III)**.[140]

Puzzlingly, the alleged cationic methyl ethylene complex generated by reacting the precatalyst (bis(oxazoline)pyridine)$Ru^{II}X_2$(ethylene) (**I** in Chart 4) with MAO, the latter which supposedly methylates and dehalogenates the precatalyst to form [(bis(oxazoline)pyridine)Ru^{II}Me(ethylene)]$^+$ (**II** in Chart 4), is structurally very similar to the [(bis(imino)pyridine)Ru^{II}Me(ethylene)]$^+$ cations synthesized by Brookhart and coworkers (**III** in Chart 4), which were contrastingly found to be inactive for ethylene insertion into a Ru−Me bond.[140] This finding suggests that the polymerization activity observed in the (bis(oxazoline)pyridine)$Ru^{II}X_2$(ethylene)/MAO systems cannot solely be ascribed to the allegedly formed cation **II**. Indeed, no sufficiently large energy difference between the most facile overall barrier for propagation by the Cossee-Arlman mechanism[141, 142] for the corresponding propyl complexes of **II** and **III** which could account for the observed difference in

activity was found. Mind that the overall barriers were calculated from the ethylene propyl complex resting state **1a** in Scheme 1, so considering necessary isomerization barriers, the height of which were calculated to be even larger than the insertion barriers in case of bulky ligands as with **III**. This finding remains when the Cossee-Arlmann mechanism was studied with an extra ethylene coordinated to Ru compared to in Scheme 1.

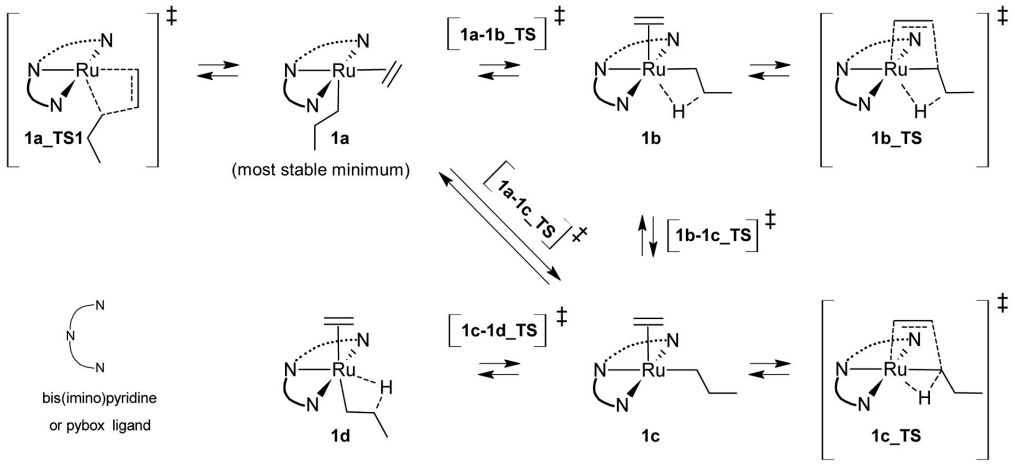

Scheme 1. Different minima, isomerization transition states and Cossee-Arlman insertion transition states calculated for the corresponding propyl complexes of **II** and **III** (see Chart 4).

Upon investigation of other propagation mechanisms, such as the Green-Rooney mechanism[143] and a carbene insertion propagation mechanism (see the top and bottom of Scheme 2 respectively),[144-146] still no sufficiently large difference in propagation barriers emerged.

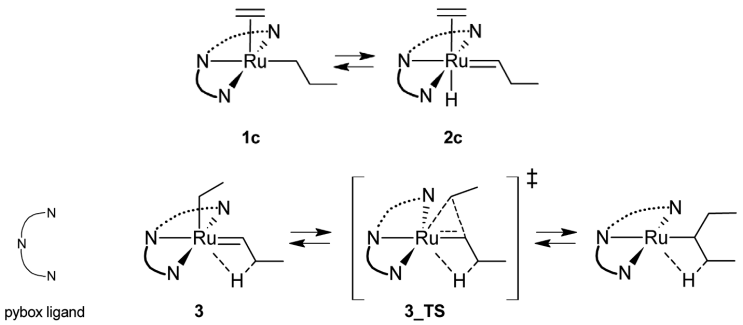

Scheme 2. Calculated hydride carbene intermediate **2c** in the Green-Rooney mechanism (top). Calculated intermediates in the carbene insertion propagation mechanism (bottom).

Also, a facile chain termination via ß-H transfer (BHT) to monomer (see Scheme 3) was found to be possible for both corresponding propyl complexes of **II** and **III**. This means that if a first

insertion of ethylene in methyl were possible, the next insertion would be strongly disfavored relative to chain termination by BHT.

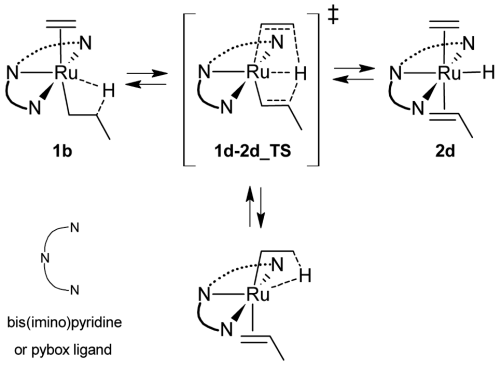

Scheme 3. Calculated intermediates and transition states in the ß-H transfer to monomer (BHT) chain termination reaction.

With these results we can strongly corroborate the suggestion that the polymerization activity observed in the (bis(oxazoline)pyridine)$Ru^{II}X_2$(ethylene)/MAO systems cannot solely be ascribed to the allegedly formed cation [(bis(oxazoline)pyridine)Ru^{II}Me(ethylene)]$^+$.

In the remainder of Paper I, in order to gain insight in the nature of the active site, we investigated different oxidation states of Ru, which might be formed in small amounts upon reaction with MAO. This was partly inspired by earlier work on the group 8 (bis(imino)pyridine)$Fe^{II}X_2$/MAO systems suggesting that the active catalyst might consist of anything from dicationic,[147, 148] monocationic,[149-153] neutral,[154, 155] to anionic complexes,[156] with the corresponding formal oxidation states ranging from Fe^{III}, Fe^{II}, Fe^{I}, to Fe^0, respectively. In addition the characteristics of the formed polyethylene (small total mass of polyethylene, but high molecular weight) might suggest that a minority species is responsible for the observed activity. Furthermore, in order to exhaust all of the most probable propagation mechanisms, we have investigated a propagation mechanism involving metallacyclic intermediates (Scheme 4). Such a carbon-carbon bond formation mechanism was demonstrated for homogeneous Cr,[32, 157-161] Ti[162-167] and Ta[168-170] trimerization catalysts, as well as homogeneous Cr tetramerization[171, 172] and oligomerization[159, 173, 174] catalysts. Polymerization by such a metallacyclic mechanism has been suggested for heterogeneous Cr/SiO_2-based polymerization catalysts,[175, 176] homogeneous Cr polymerization catalysts[159] and predicted for Hf-based species.[162]

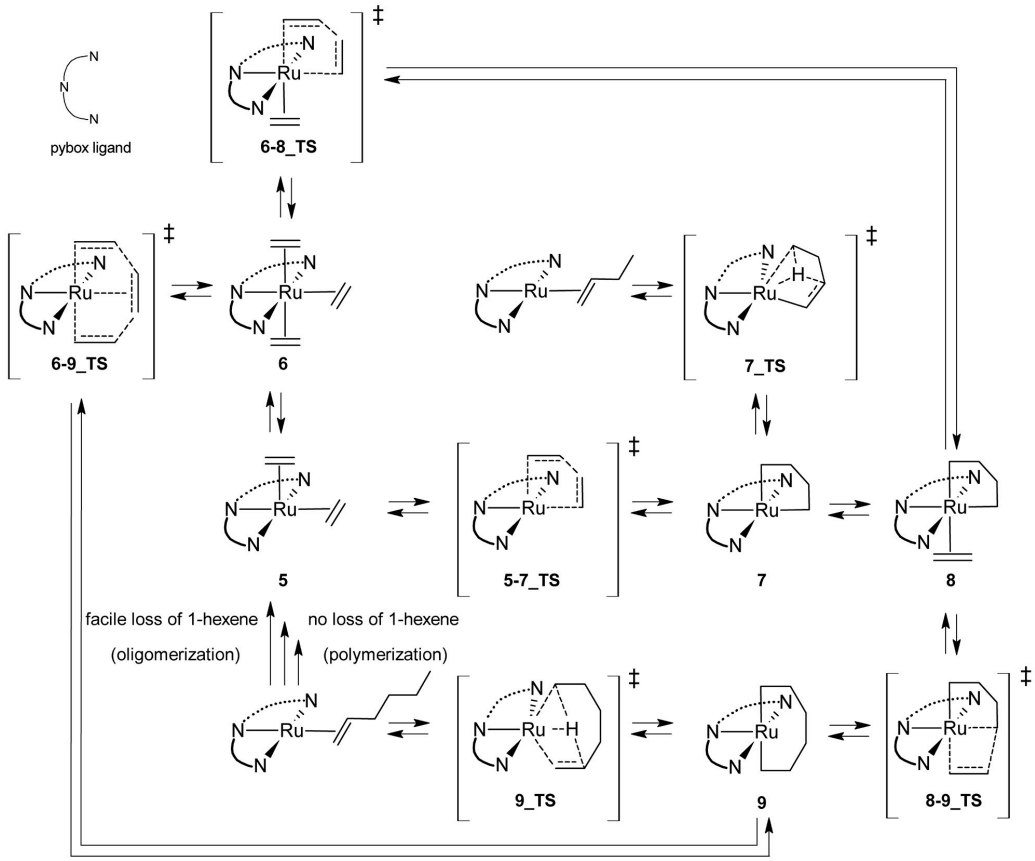

Scheme 4. Calculated intermediates for the metallacyclic propagation mechanism.

However, from the results in Paper I it can be summarized that none of the combinations of oxidation state and propagation mechanism offers a reasonably low barrier to propagation to explain the observed activity.

Hence we conclude that the activity of the (bis(oxazoline)pyridine)$Ru^{II}X_2$(ethylene)/MAO systems towards ethylene polymerization most probably does not originate from a mononuclear ruthenium complex bearing an intact pybox ligand. Instead, a range of different modifications of the ligand, either chemical modifications such as alkylation, (de)protonation or dimerization, or bidentate coordination modes, could, possibly, explain the observed activity, as could complexes involving more than one metal center.

4.2 Neutral Ni Ethylene Oligo- and Polymerization Catalysts

Neutral Ni ethylene oligo- and polymerization catalysts tend to show excellent polar functional group tolerance in combination with high activities and cost-effectiveness.[47, 50, 54, 177-180] This makes them prime candidates for the random copolymerization of polar and non-polar olefins. Nonetheless, such copolymerization by means of neutral Ni ethylene oligo- and polymerization catalysts was only achieved with polar monomers where the polar functional group is well-separated from the double bond.[50, 181-187] For MA for example, where the polar functional group is neighboring the double bond, despite efforts,[47, 188] no successful reports exist. The only exception is the bimetallic neutral Ni catalyst of Marks and coworkers, where the incorporation of MA is facilitated by the cooperative effects of the other Ni center in close proximity.[86] Neutral Ni catalysts play a prominent role in oligo- and polymerization with late transition metals. Two reasons contributing to the allure of this family of catalysts are (1) the importance of the Shell-Higher-Olefin-Process (SHOP), developed already in the 1970s, which uses neutral, single-component Ni SHOP-type catalysts for the oligomerization of ethylene and represents one of the most important examples of industrial homogeneous catalysis in general; and (2) the neutral, single-component Ni salicylaldiminato catalysts of Grubbs and coworkers,[50, 54] which are commonly regarded as an influential breakthrough. Up to today, neutral Ni catalysts continue to attract a lot of attention because of their partly unexploited potential.[189, 190] Because of the above considerations, we have taken a closer look at some of the poorly understood mechanistic aspects surrounding neutral Ni ethylene oligo- and polymerization catalysts in Papers II and III. More specifically, in Paper II chain termination reactions from alkyl phosphine complexes are investigated, and in Paper III this understanding is complemented with the termination reactions from the alkyl agostic complexes.

4.2.1 Termination Pathways from Alkyl Phosphine Complexes

It is now a well-established phenomenon that molecular weights of oligo- and polymers produced by neutral Ni catalysts as a general rule decrease with an increase of coordinative strength and/or concentration of the ligands that dissociate for olefin coordination and insertion to take place.[53, 191-198] This was already exemplified in the 1980s illustrating the versatility of the SHOP-type catalyst: whereas increasing concentration and basicity of the dissociating phosphine leads to oligomers with lower molecular weight, abstracting the phosphine with a phosphine scavenger leads to higher molecular weight polymers.[45-48] Somewhat surprisingly,

despite the prominent role of neutral Ni catalysts, no mechanistic rationale is available for the relationship between the basicity and concentration of the phosphine on one hand, and the molecular weights on the other. Kuhn *et al*. phrased this fittingly as: "*A rationale for this observation, in mechanistic terms, has not yet been given"*[199] and "*The reason why an increase of the PR_3 basicity induces a decrease of the molecular weight of the oligomers formed is still a matter of debate*".[200]

In Paper II an unconventional ß-H elimination chain termination pathway is explored for three prominent neutral Ni catalysts: the SHOP-type catalyst (**I**),[56, 201] the anilinotropone catalyst (**II**)[51-53] and the salicylaldiminato catalyst (**III**) (see Chart 5).[49, 50] For the first time this pathway offers a mechanistic rationale for the decreasing chain lengths observed upon increasing phosphine concentration and basicity.

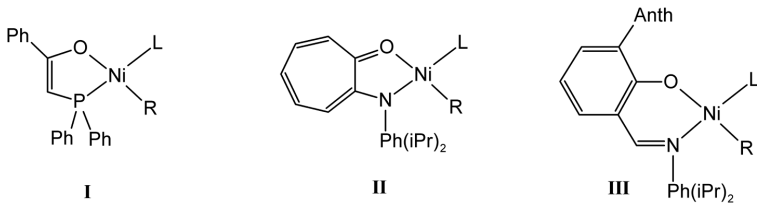

Chart 5. The studied neutral Ni catalysts in Paper II: the SHOP-type catalyst (**I**), the anilinotropone catalyst (**II**), and the salicylaldiminato catalyst (**III**). Anth signifies a 9-anthryl substituent and $Ph(iPr)_2$ indicates a 2,6-diisopropylphenyl group.

Because of the C_1 or C_S symmetry of the bidentate ligand, the possible reaction pathways can be considered to double, now involving ß-H elimination trans to both N/P and O. This results in distinct pathways which are designated by suffix a and b in the structure labels in Scheme 5. As opposed to the conventional ß-H elimination chain termination pathway[52, 53, 199, 200, 202, 203] from the alkyl agostic complex studied in Paper III (see section 4.2.2), this pathway was found to involve a ß-H elimination from the alkyl phosphine complex resting state **1a** and does not require phosphine dissociation. The actual ß-H elimination elementary step occurs from an approximate square pyramidal alkyl phosphine complex with a ß-agostic interaction, **2a** or **2b**, after an initial chain rearrangement step to create a ß-agostic interaction in the original square plane. Chain termination is complete after propene dissociation from the pentacoordinate hydride complex **3a** or **3b**. Summarizing, the preferred termination sequence for **I** and **III** is **1a** → **1a_2a_TS** → **2a** → **2a_3b_TS** → **3b** → **3b_4b_TS** → **4b**. For **II** the preferred termination sequence is **1a** → **1a_2a_TS** → **2a** → **2a_3a_TS** → **3a** → **3a_4a_TS** → **4a** or, showing an identical overall

barrier, **1a** → **1a_2a_TS** → **2a** → **2a_2b_TS** → **2b** → **2b_3b_TS** → **3a** → **3a_4a_TS** → **4a**. This unconventional termination pathway was found also to exist for PPh_3 instead of PMe_3 as phosphine ligand as in Scheme 5. The overall barrier was calculated to be 19.3 kcal/mol for **I** and 25.3 kcal/mol for **II**, measured from the resting state **1a_PPh**, the PPh_3 analogue of **1a**. The latter value was in excellent agreement with the experimentally measured rate constant for chain termination without phosphine dissociation from NMR studies for **II** translating to an overall barrier of 24.6 kcal/mol.[53]

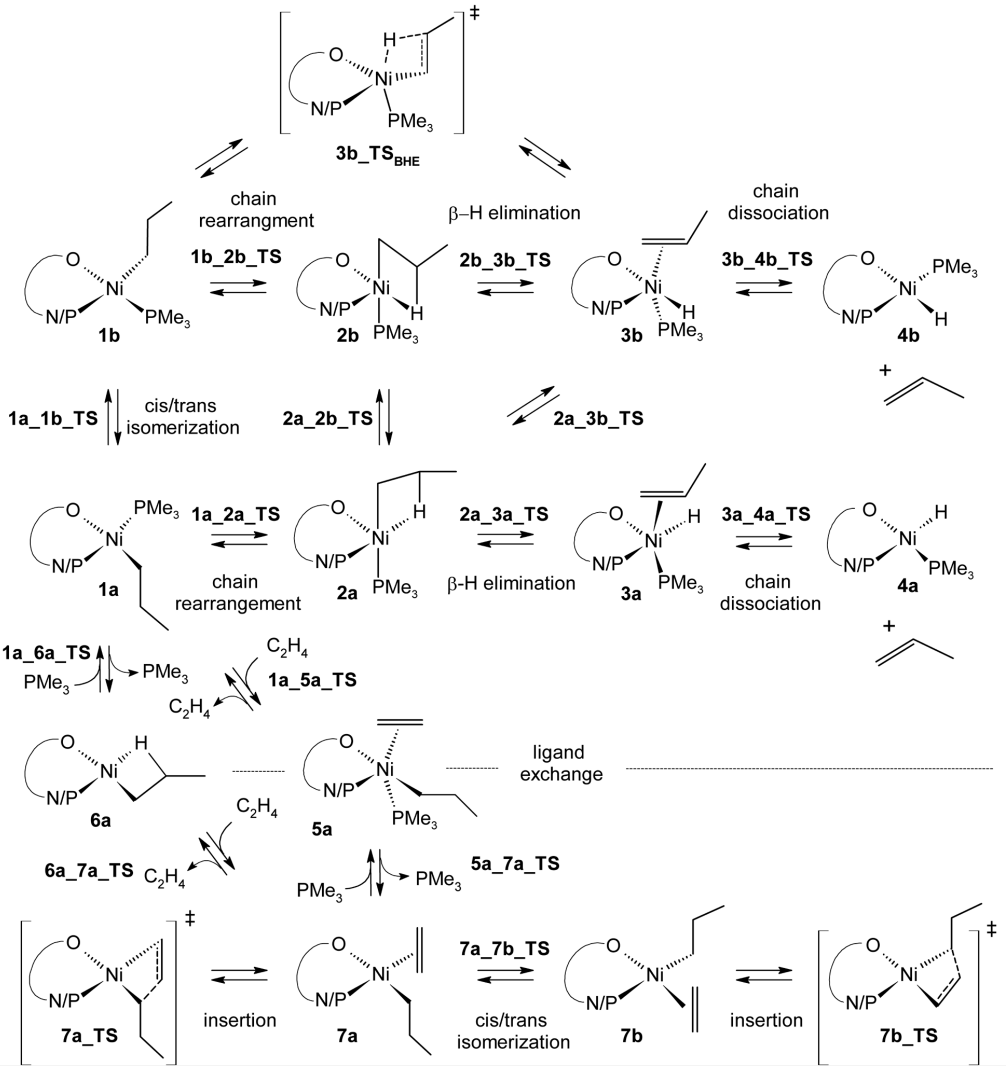

Scheme 5. Reaction pathways studied, including labeling of the stationary points.

The C_1 or C_S symmetry of the bidentate ligand not only doubles the chain termination pathways, but also the possible propagation pathways. From previous computational work on square planar d^8 complexes with asymmetric bidentate ligands it has become clear that the most energetically favorable insertion transition states involve the alkyl chain to be positioned trans to the more sterically hindered and stronger donating P or N of the bidentate ligand (cf. **7b_TS** in Scheme 5), while the most stable ethylene π-complexes most often involve the alkyl chain to be positioned trans to O (cf. **7a** in Scheme 5), although for **II** and **III** the different cis/trans isomers of the ethylene π-complex are very close in energy.[80, 125, 203-208] This means a cis/trans isomerization (**7a_7b_TS** in Scheme 5), will be required before insertion takes place. For **I**, the barrier for this cis/trans isomerization is comparable to the insertion barrier, which underscores the importance of such isomerization reactions. Considering the most facile ligand exchange pathway, i.e. dissociative for **I**, associative for **II** and **III**, the calculations support the experimental observation of the trapping of the first insertion products by PPh_3 for **II**,[53] indicating that the phosphine complex **1a_PPh** and the ethylene complex **7a** are in equilibrium with an equilibrium constant K_{eq}:

$$K_{eq} = \frac{[\mathbf{7a}][PPh_3]}{[\mathbf{1a\_PPh}][eth]} \tag{4.1}$$

Then the ratio of the rate of termination over the rate of propagation r_{term}/r_{prop} (= the Schulz-Flory value ß, see section 3.1), by taking into account the unconventional chain termination pathway, can be expressed with (4.1), as:

$$\beta = \frac{r_{term}}{r_{prop}} = \frac{\sum_i r_{term,i}}{r_{prop}} \geq \frac{k_t[\mathbf{1a\_PPh}]}{k_{ins}[\mathbf{7a}]} = \frac{k_t}{k_{ins}} \frac{1}{K_{eq}} \frac{[PPh_3]}{[eth]} \tag{4.2}$$

with k_t and k_{ins} the calculated reaction rate constants for the unconventional chain termination and insertion respectively.

Using (4.2), ß was calculated to be≥ 0.0043 for **I**, near one order of magnitude in accuracy with the experimental value of 0.0645.[209] This result suggests that our unconventional termination pathway is not only realistic, but also a major termination pathway. For **II**, ß was found to be≥ 10^{-7}, which is consistent with the observed average degree of polymerization <DP> of 10^3 since 1/ß > <DP>.[51]

One characteristic aspect of oligomerization with the SHOP-type catalyst **I** is the production of predominantly linear α-olefins. If the unconventional termination pathway is indeed a major termination pathway, then chain branching originating from intermediates along this pathway must be unfavorable to be in accord with the observed oligomer structures. A well-documented branching mechanism for Ni polymerization catalysts involves ß-hydrogen elimination and subsequent insertion of the olefinic polymer chain, with opposite regiochemistry, into the Ni–H

bond, followed by ethylene insertion into a nickel–carbon bond of a secondary carbon atom. This mechanism creates a methyl branch, while longer branches require multiple insertions and ß-H eliminations involving different ß-agostic hydrogens (chain walking).[67, 202, 210, 211] These examples all involve phosphine-free complexes, but the exact same mechanism could easily apply to phosphine complexes. Upon comparison of the transition state **1b'_3b_TS** for reinsertion of propene with opposite regiochemistry into the Ni–H bond of the hydride intermediate **3b** with the transition state **3b_4b_TS** for propene dissociation which completes the chain termination, the latter is found to be 3.2 kcal/mol lower in Gibbs free energy (see Scheme 6). This indicates that chain dissociation and termination is more likely than reinsertion which possibly leads to branched and internal olefins. Hence, the finding that the unconventional termination pathway plays a major role for chain termination is completely in accord with the formation of linear α-olefins.

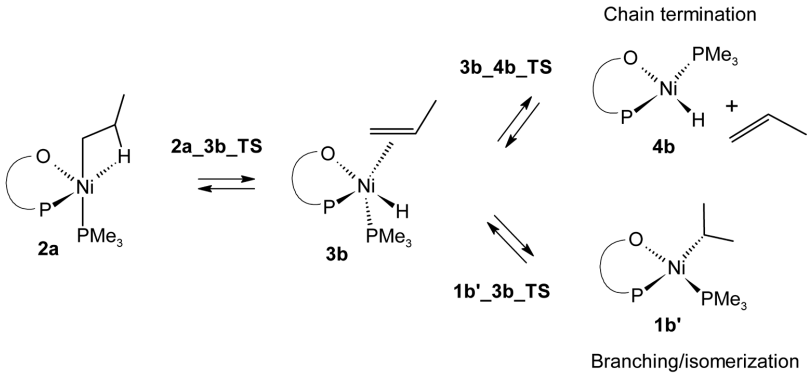

Scheme 6. Important intermediates in chain branching and olefin isomerization for **I**.

Based on these findings we are able to propose a catalytic cycle for **I** which is extended compared to the generally accepted cycle originally proposed by Keim (see Scheme 7). [56, 212]

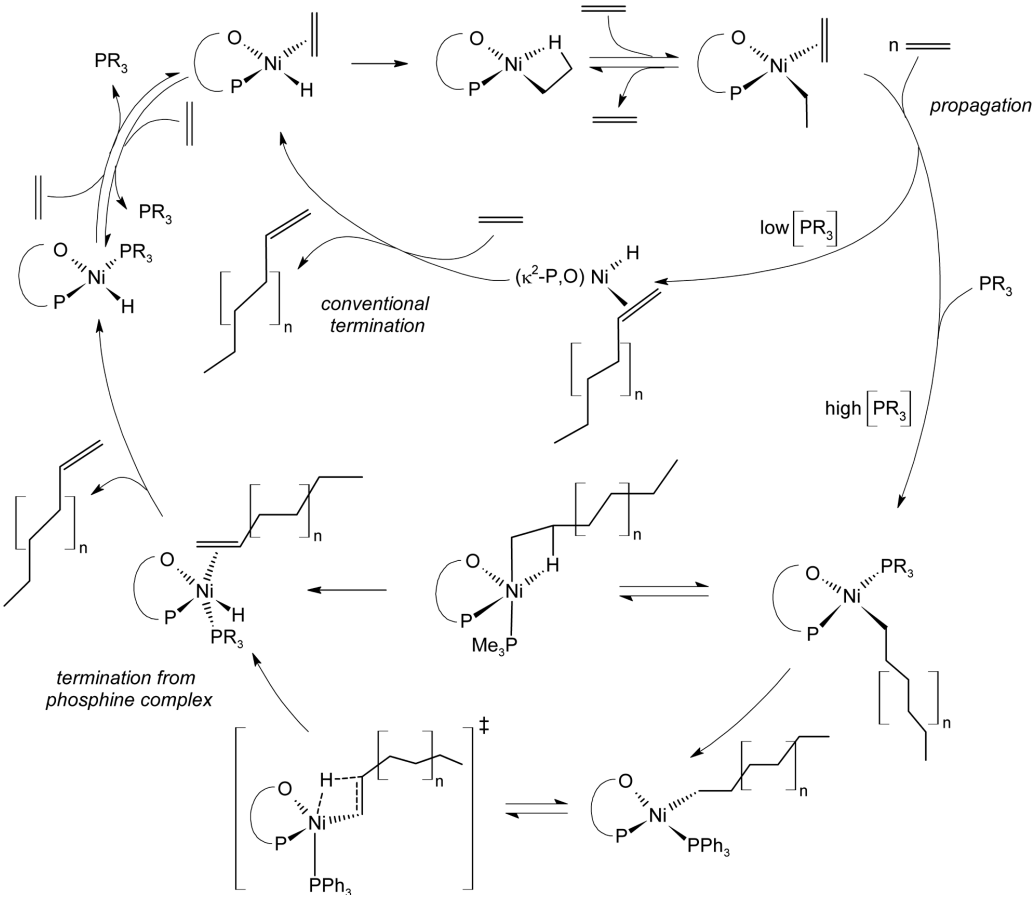

Scheme 7. Proposed catalytic cycle for **I**. [PR_3] signifies the phosphine concentration.

Furthermore, the unconventional termination pathway offers a rationalization for the shorter oligomers produced by the pyrazolonato-phosphane catalysts (**IV**)[199, 209] (see Chart 6) relative to **I**, hereby adding to its credibility. The origin for the shorter oligomers produced by **IV** relative to **I**, mainly pertains to the increased relative stability of the ß-agostic intermediate **2a** (see Scheme 5) which lowers the overall, effective barrier to termination. It can be noted that this is in line with earlier speculations.[199, 200]

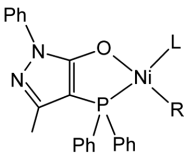

IV

Chart 6. The pyrazolonato-phosphane catalyst (**IV**).

4.2.2 Termination Pathways from Alkyl Agostic Complexes

Whereas the preceding section 4.2.1 dealt with termination reactions from alkyl phosphine complexes, this section deals with termination reactions from alkyl agostic complexes, i.e. in absence of the donor ligand L in Chart 7 which shows the studied catalysts in Paper III.

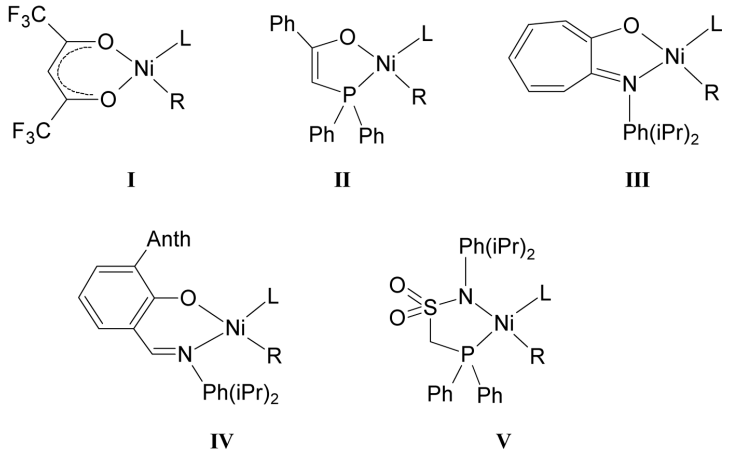

Chart 7. The studied neutral Ni catalysts in Paper III: the Ni(acac) catalyst (**I**), the SHOP-type catalyst (**II**), the anilinotropone catalyst (**III**), the salicylaldiminato catalyst (**IV**) and the phosphinosulfonamide catalyst (**V**). Anth signifies a 9-anthryl substituent and $Ph(iPr)_2$ indicates a 2,6-diisopropylphenyl group.

It is safe to say that for Ni and Pd oligo- and polymerization catalysts, termination pathways have remained more controversial and elusive than their propagation and branching counterparts.[53, 210, 213-218] An important experimental finding with regard to termination from the cationic Ni and Pd α-diimine catalysts is that shorter chains were produced with increasing ethylene pressure, which, in combination with a relatively low barrier to associative ligand exchange led to the suggestion that the preferred chain termination occurred via associative displacement i.e. the dissociation of an olefinic chain *after* coordination of ethylene.[67, 215, 216, 218] However, numerous computational investigations for the Ni α-diimine catalysts suggested an alternative termination mechanism involving BHT to the monomer in one way or the other,[219-222] an alternative which could not be excluded based on the experimental data,[223] although other computational reports did point towards associative displacement after ß-H elimination (BHE).[124, 224] For the neutral Pd phosphine-sulfonate catalysts a recent computational work found the dissociative displacement pathway, i.e. dissociation of an olefinic chain *before* coordination of ethylene, most favorable, followed by the associative displacement which could possibly compete.[208] Relevant for Paper III, in an early couple of computational works, the

dominating termination mechanism of **I** (see Chart 7) was found to be the stepwise BHT pathway (the so-called monomer-assisted BHE), while the dissociative displacement route was unlikely due to the high energy of the resulting tricoordinated hydride complex.[225, 226] For **IV** (see Chart 7) on the other hand, a stepwise BHT pathway via a stable pentacoordinated bisolefin hydride complex was found to be more facile than the dissociative displacement pathway.[203] The possibility of an associative displacement termination pathway or a direct BHT pathway was not considered.[203] Summarizing, it appears that the previous computational investigations typically have been focused on limited number of the many possible termination mechanisms.

Insight in the intimate termination mechanism could facilitate the *in silico* rationalization and/or prediction of catalysts since the ratio of termination and propagation rates will determine if dimers, oligomers or polymers are obtained. Two examples of this methodology exist for cationic Ni catalysts: (1) The contrasting behavior of several Ni catalysts, including cationic Ni iminophosphonamide and amidinate catalysts was rationalized by energy differences of a bisolefin hydride complex, rather than a transition state.[227] (2) the oligomer distribution for cationic (κ^2-P,N) Ni ethylene oligomerization catalysts was rationalized by considering the BHE transition state for the alkyl agostic complex, despite the fact that this transition state was not shown to be rate-limiting and there could be other termination pathways more favorable.[228, 229] Even though good results were obtained with these rather approximate approaches, it seems clear that there is a need for more comprehensive approaches in order to establish the intimate mechanisms of termination for the various catalysts and also for theory to contribute to prediction and tuning of Ni oligo- and polymerization catalysts.

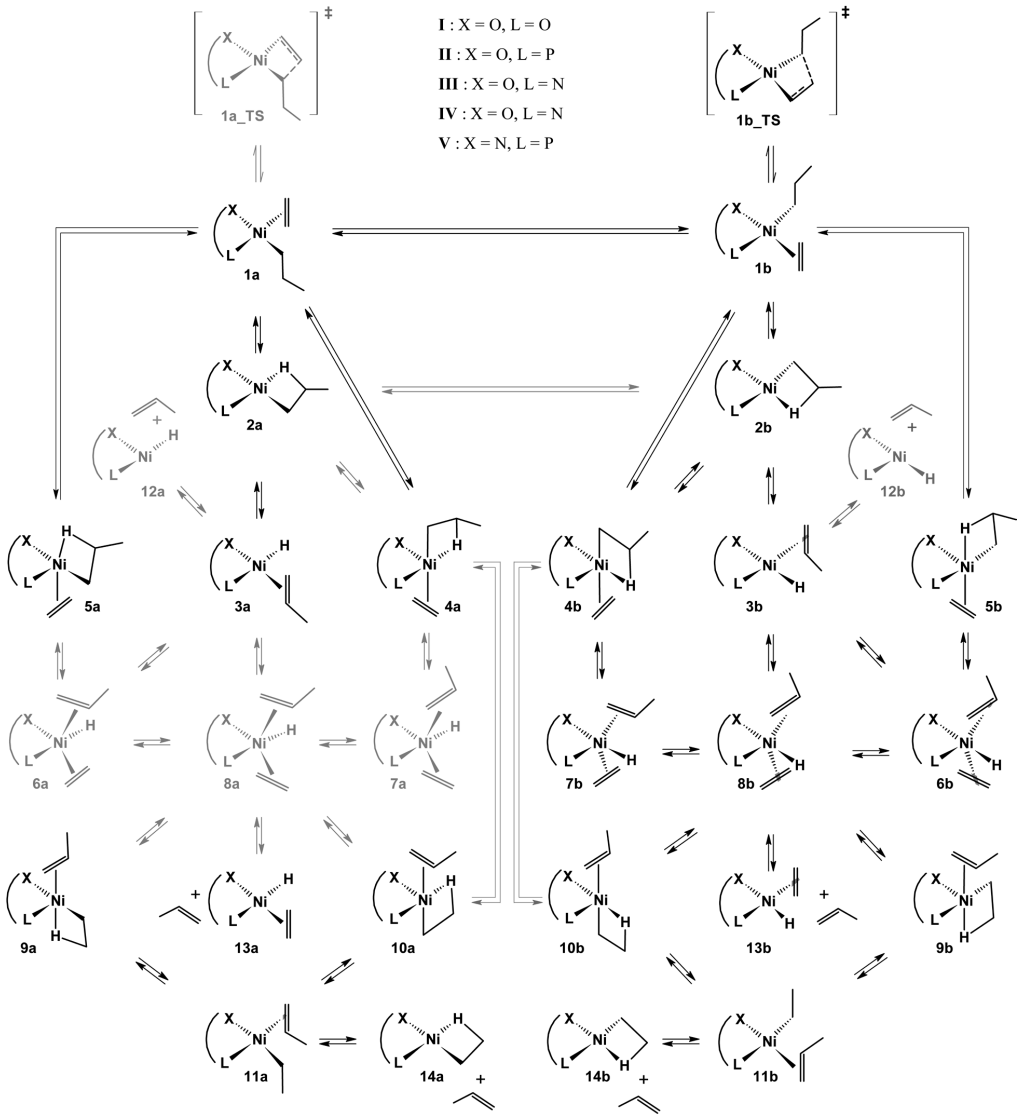

Scheme 8. Studied minima and transition states relevant for termination, branching and propagation pathways of neutral Ni oligo- and polymerization catalysts **I**, **II**, **III**, **IV** and **V**. Gray coloring indicates unfavorable intermediates and transition states. Mind that the left and right section of the scheme become equal for L = X as is the case for **I**.

Part of the explanation for these difficulties surrounding termination pathways could lie in their rather complex nature involving many intermediates and transition states leading to many possible routes to termination.

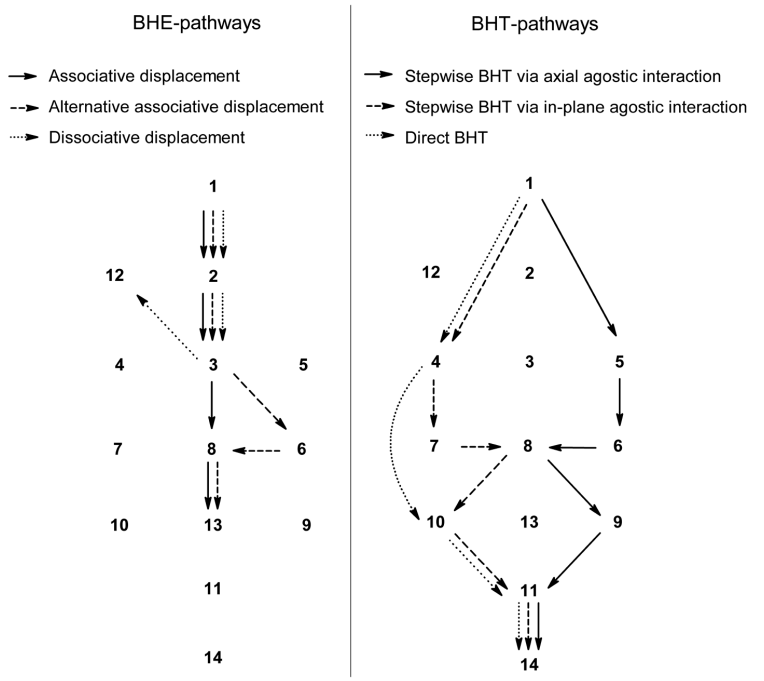

Scheme 9. Possible ß-H elimination (left) and ß-H transfer to monomer (right) pathways. See Scheme 2 for the line structures associated with the labels. The mixed BHE/BHT, BHT/BHE and BHT/BHT pathways (pathways 7, 8 and 9) are not shown explicitly but can be envisioned to switch side (left to right for BHE/BHT, right to left for BHT/BHE) or arrow type (for BHT/BHT) at the common intermediate **8** (see Scheme 8).

In summary nine different termination pathways can be distinguished, including the ones mentioned above (see Scheme 9 for a graphical presentation of the described termination pathways below):

(1) Dissociative BHE or dissociative displacement: **1 → 1_2_TS → 2 → 2_3_TS → 3 → 12**

(2) Associative BHE or associative displacement: **1 → 1_2_TS → 2 → 2_3_TS → 3 → 3_8_TS → 8 → 8_13_TS → 13**

(3) Alternative associative BHE or alternative associative displacement: **1 → 1_2_TS → 2 → 2_3_TS → 3 → 3_6_TS → 6 → 6_8_TS → 8 → 8_13_TS → 13**

(4) Stepwise BHT via axial agostic interaction: **1 → 1_5_TS → 5 → 5_6_TS → 6 → 6_8_TS → 8 → 8_9_TS → 9 → 9_11_TS → 11 → 14**

(5) Stepwise BHT via in-plane agostic interaction: **1 → 1_4_TS → 4 → 4_7_TS → 7 → 7_8_TS → 8 → 8_10_TS → 10 → 10_11_TS → 11 → 14**

(6) Direct BHT: **1 → 1_4_TS → 4 → 4_10_TS → 10 → 10_11_TS → 11 → 14**

(7) Mixed BHE/BHT: **1** → **1_2_TS** → **2** → **2_3_TS** → **3** → **3_8_TS** → **8** → **8_9_TS** → **9** → **9_11_TS** → **11** → **14** (or …→ **8** → **8_10_TS** → **10** → **10_11_TS** → **11** → **14**) (or …→ **3** → **3_6_TS** → **6** → **6_8_TS** → **8** → …)
(8) Mixed BHT/BHE: **1** → **1_5_TS** → **5** → **5_6_TS** → **6** → **6_8_TS** → **8** → **8_13_TS** → **13** (or **1** → **1_4_TS** → **4** → **4_7_TS** → **7** → **7_8_TS** → **8** → …)
(9) Mixed BHT/BHT: **1** → **1_5_TS** → **5** → **5_6_TS** → **6** → **6_8_TS** → **8** → **8_10_TS** → **10** → **10_11_TS** → **11** → **14** (or **1** → **1_4_TS** → **4** → **4_7_TS** → **7** → **7_8_TS** → **8** → **8_9_TS** → **9** → **9_11_TS** → **11** → **14**)

Summarizing our results on the preferred termination mechanism of the catalysts, we can state that they will be varied and dependent of the catalyst. For **I** and **III** many of the nine termination pathways were energetically degenerate, resulting in many realistic termination pathways. For **II** the stepwise BHT via an axial agostic interaction (pathway 4) showed the lowest overall barrier, while for **IV** both the associative displacement (pathway 2) and the mixed BHE/BHT (pathway 7) were found most facile. Finally, for **V**, the preferred termination pathway can best be described as the mixed BHT/BHE pathway (pathway 8).

An interesting observation from the calculations is that the transition states highest in energy for the most viable termination pathways occur before the bisolefin hydride complex **8** (Scheme 8). More in particular, the transition state highest in energy is either the ß-H elimination transition state **1b_6b_TS** (or **5b_6b_TS**) or **2a_3a_TS**, the chain rearrangement transition state **1b_4b_TS** (or **1b_7b_TS**) or the ethylene association transition state **1b_2b_TS**. This means that despite the complexity and multitude of possible termination pathways (see Scheme 8), the most critical information for termination is contained in relatively few transition states.

Furthermore, the ß-H elimination transition state where a hydride is formed trans to L **2a_3a_TS** and the ethylene association transition state where the propyl is trans to L **1b_2b_TS** are the rate-limiting transition states for the hydride formation, **3a** and **3b** respectively. Formation of this hydride **3a** or **3b** is a necessary step in the conventional branching mechanism. It can be noted that it will be difficult to *a priori* predict from which ethylene π-complex, **1a** or **1b**, hydride formation will be most facile. Indeed, even for the structurally related catalysts **III** and **IV**, the regiochemistry was found different, i.e. from **1a** for **III** and from **1b** for **IV** (Figure 1). It can be noted that this contrasts with the report of Michalak *et al*.[205] for **III** and that of Chan *et al.* for **IV**.[203]

From Figure 1 the effect of a C_1- or C_S-symmetric bidentate ligand with different σ-donor properties on each side of the ligand on the hydride formation can be seen. The lowest overall barrier is observed for **I** possessing a C_{2v}-symmetric ligand where both bridgehead atoms have identical σ-donor ability. The second lowest overall barrier is observed for **V**, where the L phosphine moiety and the X amido moiety can both be considered as exhibiting a strong σ-donation. Then, highest overall barriers are observed for **II**, **III** and **IV**, all displaying a strong σ-donor L on one side of the bidentate ligand, and a weak σ-donor X on the other. In line with the highest overall barrier to hydride formation, these catalysts also produce polyethylene with low amounts of branching under typical conditions. We state that these results can be explained by considering that a *difference* in σ-donation of both bridgehead atoms will lead to a relative destabilization of both **1b_2b_TS** and **2a_3a_TS** to **1a** and **2a**. To conclude, it can be noted that this fits well with other neutral Ni catalysts in the literature, such as the polyethylene with low amounts of branching produced by phosphine-sulfonate catalyst, which shows a large difference in σ-donor abilities of the phosphine moiety (strong) and the sulfonate moiety (very weak).[197, 230] Another corroborating example from the literature is that substituting the aryl substituents of P of the bidentate ligand for the phosphine-sulfonate catalyst by cyclohexyl groups, which increase the σ-donor properties of P without significantly affecting those of O, leads, as expected since the difference in σ-donor abilities increases, to less branching.[197]

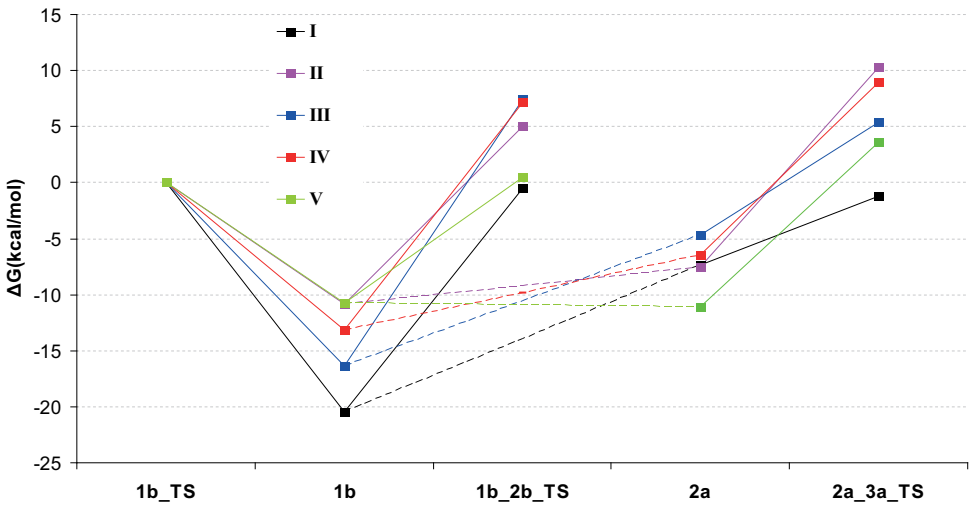

Figure 1. Gibbs free energy profiles for propagation via **1b_TS** and hydride formation via the rate-limiting transition states **1b_2b_TS** or **2a_3a_TS** (Scheme 8) for the catalysts studied in this work (Chart 7). Note that the energies are given relative to **1b_TS**, to ensure facile comparison

between the transition state leading to propagation on one hand, and to hydride formation on the other.

Chapter 5: Challenges in the Random Copolymerization of Polar and Non-Polar Olefins with Late Transition Metals

5.1 Strong σ-Coordination of the Polar Olefin

In order for the coordination-insertion random copolymerization of polar and non-polar olefins to be successful, it is necessary that both the non-polar olefin and the polar olefin are able to coordinate to the metal center via their olefinic function prior to insertion. This type of bonding of the polar olefin is often termed π-coordination and the resulting complex a π-complex because the polar olefin then mainly binds to the metal via its π and π* orbitals. Alternatively, since the polar olefin also has a polar functional group, this group can coordinate to the metal center instead of the olefinic function. Because such a bonding usually predominantly consists of σ-contributions, it is termed σ-coordination, creating a σ-complex.

Under most circumstances the coordination of different comonomers and binding modes are in equilibrium with each other, so a preference for σ-coordination of the polar olefin will reduce the polymerization activity since most metal centers will rest in an inactive σ-complex form. From previous computational work it has become clear that especially acrylonitrile, but also methyl acrylate and vinyl acetate form very stable σ-complexes with cationic α-diimine Pd catalysts.[231-233] Indeed, such σ-complexes have been observed experimentally for acrylonitrile on several occasions.[234-237] The reduced preference for σ-coordination of acrylonitrile for the Pd phosphine-sulfonate catalysts relative to other catalysts was used to explain the successful copolymerization of ethylene and acrylonitrile with the former catalyst.[238] Furthermore, for methyl acrylate, the preference for σ-coordination with cationic α-diimine Ni catalysts has been pointed out to be the reason for their inactivity in ethylene-methyl acrylate copolymerization under mild conditions.[239, 240] It can be noted that a σ-complex of an acrylate or methacrylate leads to an inactive metal center for coordination-insertion copolymerization, but σ-coordination of such monomers is contrastingly necessary for group transfer polymerization (GTP) which is a type of coordination-addition polymerization involving enolate intermediates.[241]

5.2 Weak π-Coordination of the Polar Olefin

In section 5.1 the competition between the σ-coordination of the polar olefin on one hand and the π-coordination of both polar and non-polar olefins on the other was discussed. However, in copolymerization there is also a competition between the π-coordination of the polar olefin and the π-coordination of the non-polar olefin. If one shows much stronger π-coordination than the other, this might compromise the copolymer composition in the sense that very little of the weaker coordinating comonomer is incorporated.

For Pd catalysts, where π-donation from the olefin to the metal is more important for the bond strength than the backdonation from the metal into the π*-orbital of the olefin, the polar olefin will bind weaker to the metal as it is more electron deficient.[242] An experimental illustration of this is the weak (relative to ethylene) binding of vinyl acetate to Pd, and an even weaker binding of vinyl trifluoroacetate.[243] Since insertion rates will increase with electron deficiency of the polar olefin,[242, 244] their weak π-coordination is responsible for the low levels of polar olefin incorporation into the copolymer typically seen for the coordination-insertion random copolymerization of polar and non-polar olefins (see section 1.2.2.2). For vinyl trifluoroacetate as an extreme example, π-coordination is so weak that only ethylene homopolymer is formed during the attempted copolymerization.[243]

5.3 Stable Chelate Formation

Very characteristic of the copolymerization of methyl acrylate and ethylene is the greatly reduced polymerization activity, which decreases as more methyl acrylate is incorporated. It was soon realized that this, after preferred 2,1-insertion of methyl acrylate, was due to the formation of a stable 4-membered chelate which for cationic α-diimine Pd catalysts could isomerize to even more stable 5- and 6-membered chelates.[68] The rarer 1,2-insertion of methyl acrylate gives directly rise to 5-membered chelates. The formation of these stable chelates hinders further coordination of a new monomer which is necessary to continue copolymerization.

Stable 5-membered chelates are also observed after preferred 2,1-insertion of vinylacetate.[243] In case of acrylonitrile, the nitrile function from the incorporated monomer after insertion, instead of coordinating intramolecularly to form a chelate (‘backbiting’), rather coordinates intermolecularly to another metal center, hereby forming a stable, inactive aggregate.[234-237]

5.4 Enolate Formation

2,1-insertion of acrylates and methacrylates lead to 4-membered chelates. Depending on the resonance structure chosen, this can be a C-chelate with C an X moiety and O an L moiety (see Scheme 10), or it can be an O-chelate, with O the X moiety and the C=C double bond the L moiety. The opening of the C-chelate, i.e. the decoordination of the O=C L moiety from the metal, was pointed out in section 5.3 to be a major factor slowing down copolymerization. In the extreme case, the L moiety prefers to be decoordinated from the metal, which could greatly facilitate the coordination of a new monomer. Whereas C-chelates are generally preferred for coordination-insertion catalysts, O-chelates fit better for coordination-addition catalysts following the GTP mechanism. Hence 4-membered chelates carry a lot of useful information for potential catalysts.

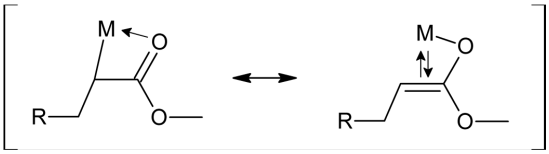

Scheme 10. Different resonance structures for the 4-chelate. C-chelate left, O-chelate right.

5.5 Reduced Migratory Insertion Reactivity

2,1-insertion of polar olefins creates an electron withdrawing functional group in α-position, while 1,2-insertion leads to a functional group in ß-position. For Ni and Pd, where the π-donation is generally more important than the backdonation from the metal to the olefin,[242] the migratory insertion of an alkene into an alkyl-metal bond for Ni and Pd can be interpreted as a nucleophilic attack from that alkyl on the coordinated alkene.[245] Hence, the presence of an electron withdrawing group on the alkyl, reducing its nucleophilicity, will increase the barrier for migratory insertion and retard propagation. This was nicely illustrated for vinylacetate and vinyl trifloroacetate. When these acetoxy groups were positioned in α-position, the insertion barriers increased with ca. 3 kcal/mol in comparison with barriers for insertion into a simple alkyl-metal bond.[243] For MA-ethylene copolymerization with neutral Pd phosphine-sulfonate catalysts, the higher insertion barriers due to α-carboxyl functions after preferred 2,1-insertion of MA were recognized as the rate-limiting bottleneck.[79] Note that, contrary to the cationic Pd α-diimine catalysts,[68] the neutral Pd phosphine-sulfonate catalysts do not readily isomerize from 4-membered chelates to 5- and 6-membered chelates and are hereby forced to make this difficult

insertion step which would be easier if the carbonyl group would be in ß- (5-membered chelate) or γ-position (6-membered chelate).[74, 243]

5.6 ß-Polar Functional Group Elimination

Due to the generally higher strength of metal halogen, acetate and alkoxyl bonds relative to metal carbon bonds,[246] such polar functional groups, if they are in ß-position, are in threat of ß-elimination, which derails the copolymerization process by leading to inactive complexes. This has been experimentally shown to be a problem for copolymerization involving vinylchloride,[247] vinylacetate,[190, 243] and vinylether.[248] ß-elimination was suppressed and copolymerization became possible with somewhat different monomers, such as vinylfluoride,[77] which shows a weaker metal fluoride bond compared to chloride, and silyl vinylether.[248]
It can be noted that ß-elimination could be avoided when 2,1-insertion exclusively occurs. In that case, the polar functional group would initially be in α-position and eventually move to γ-position upon insertion of the next monomer without passing through the ß-position.

5.7 Radical Formation

Although acrylates are not susceptible to ß-elimination, they are known to form radicals via homolytic Pd-carbon bond cleavage when the carboxyl group is in the ß-position.[245, 249, 250] The radical formed on the dissociated alkyl ligand with the carboxyl group in the ß-position, is significantly stabilized by delocalization. Since acrylates are quite reactive in radical polymerization and more reactive than α-alkenes, acrylate homopolymerization is possible with these neutral Pd systems, in addition to copolymerization of acrylate and α-alkenes resulting in an acrylate-rich copolymer.[245, 249, 250]

5.8 Catalyst Decomposition Involving Reductive Elimination

Neutral Ni and Pd catalysts for the copolymerization of ethylene and MA are generally inactive and decompose to metallic Ni^0 and Pd^0. The only exceptions are the neutral Pd phosphine-sulfonate catalysts, which are known to form linear copolymer.[74] Linear copolymer most likely implies that ß-H elimination necessary for chain branching for this catalyst will be difficult, and this has been supported by calculations.[208, 238] Because of this, only very little hydride

complexes will be present in the media. In contrast, it is known that neutral Ni catalysts such as those based on salicylaldiminato and anilinotropone ligands, as well as other neutral Pd catalysts based on pyrrole-imine ligands do readily undergo ß-H elimination leading to hydride complexes. This distinction combined with the contrasting behavior in copolymerization, leads to the suspicion that the hydride complexes play an important role in explaining the inactivity of neutral Ni and Pd catalysts for copolymerization.

Several investigations have been carried out in order to elucidate the mechanism of the decomposition. For the anilinotropone catalyst, it was found that the phosphine hydride complex formed after ß-H elimination could undergo reductive elimination of the free ligand forming metallic Ni^0, the free ligand which thereafter reacted by protonolysis with the alkyl complexes involved in propagation forming saturated terminated chains and bisligand complexes.[53] Such bisligand complexes are since long known for neutral Ni catalysts,[47, 251] and constitute a very stable thermodynamic sink. In addition it can be noted that, since protonolysis in decomposition involves the free ligand, the acidity of this ligand will play a role in this decomposition mechanism.[53] For the structurally similar salicylaldiminato catalysts, a very similar mechanism was proposed, however, since specifically the copolymerization was investigated, the hydride complex now originated from the 4-membered chelate by ß-H elimination.[188] It could however not be excluded that the hydride complex directly attacked the alkyl complexes.[188] Such a mechanism leads to a 1:1 ratio of saturated and unsaturated chains. Further investigation of related salicylaldiminato catalysts showed that alkyl complexes could be directly attacked by hydride complexes in a bimolecular pathway characterized by a negative activation entropy, forming saturated terminated chains and bisligand complexes.[189] Interestingly, 4-membered chelates were found to be stable in absence of hydride complexes, and a similar bimolecular pathway was assumed for the decomposition of the former.[190] Also interesting was the observation that the alkyl fragment occurring in 4-membered chelates is far more sensitive to protonolysis than a simple alkyl from ethylene homopolymerization.[190] This can help explain why the occurrence of hydride complexes in the ethylene homopolymerization does not lead to catalyst decomposition, while in ethylene-MA copolymerization, it does. Switching focus to Pd, both metallic Pd^0, free ligand and unsaturated terminated chains were observed in the attempted copolymerization of ethylene and acrylonitrile with neutral Pd salicylaldiminato catalysts.[238]

Finally, formation of metallic Pd^0 was also observed in the attempted polymerization of acrylate and methacrylate with pyrrole-imine Pd complexes, with involvement of bimolecular complexes leading to both unsaturated and saturated terminated chains.[245, 250, 252] Similarly to the preceding examples, the formation of a mono- or bimolecular hydride complex from the alkyl ligand formed after insertion of (M)MA, ultimately led to reductive elimination and chain

termination.[245, 250, 252] Interestingly, (radical, see section 5.7) polymerization did become possible after addition of coordinating ligand (pyridine, PPh_3) to the media, which retarded ß-H elimination and decomposition by reductive elimination,[250] the latter a finding which was echoed for the neutral Ni anilinotropone catalysts.[53]

Chapter 6: The Polar Functional Group Tolerance of Transition Metal Catalysts for Olefin Polymerization

The coordination-insertion random copolymerization of non-polar and polar olefins (where the polar functional group is directly bonded to the sp^2 C of the C=C double bond) can be regarded as holding fantastic potential.[70, 71, 101] Most important breakthroughs in this field have been realized with Pd^{II} catalysts, while some examples also exist of Ni^{II} catalysts (see section 1.2.2.2). In Paper IV the potential of other transition metals for this reaction is assessed since there is currently no rationalization for the apparent superiority of Pd^{II}. Investigation of other transition metals for copolymerization is interesting because such catalysts might provide a way of circumventing the typical inherent limitations of current copolymerization catalysts such as a low polar olefin incorporation (see section 5.2) and a significantly reduced activity compared to ethylene homopolymerization (see section 5.5), not to mention the appeal of replacing Pd by a less expensive transition metal.

Two essential aspects of catalysts for copolymerization of non-polar and polar olefins are (1) the height of the migratory insertion barrier and (2) the tolerance against polar functional groups. A successful copolymerization catalyst should combine low insertion barriers with high polar functional group tolerance. Therefore we have investigated the ligand exchange Gibbs free energies ΔG_{exch} between ethylene and MA coordinated via its carbonyl O (σ-coordination) as an indication of the polar functional group tolerance on one hand, and the migratory insertion barriers $\Delta G^{\ddagger}_{ins}$ as an indication of the activity on the other. At this point it can be noted that the ΔG_{exch} was defined as the difference between the dissociation Gibbs free energy ΔG_{diss} of ethylene and ΔG_{diss} of MA (i.e. $\Delta G_{exch} = \Delta G_{diss}$ ([M]−C_2H_4) − ΔG_{diss} ([M]−MA)) and hence a high ΔG_{exch} indicates a high polar functional group tolerance. From the preceeding chapter it is clear that ΔG_{exch} and its accompanying polar functional group tolerance play an important part for the copolymerization since it can be related to stable σ-coordination (see section 5.1) and chelate and enolate formation (see sections 5.3 and 5.4 respectively).

We have done this for complexes of all 30 transition metals, indicated in Chart 8, which are reminiscent (in order of appearance) of existing polymerization catalysts such as the constrained geometry complexes (CGCs),[29] the bis(imido)pyridine Fe and Co catalysts[87-89] and the α-diimine Pd and Ni catalysts.[67]

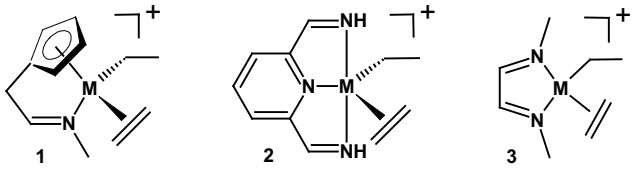

Chart 8. Model systems of the ethylene complexes employed in the calculation of ΔG_{exch}.

Relevant in this context is that a computational work on cationic Pd α-diimine catalysts has shown that the polar functional group tolerance correlates positively with the height of the insertion barrier[231] hereby imposing a compromise between the catalyst's activity and its aptitude towards copolymerization. In Paper IV, we have found a good correlation between ΔG_{exch} and $\Delta G^{\ddagger}_{ins}$ ($R^2 = 0.85$), supporting the validity of the previous claim across the full set of transition metals.

First looking at ΔG_{exch}, the results in Figure 2 show that ΔG_{exch}, when generalizing, is largest for the third row transition metals, closely followed by the second row transition metals while the first row transition metals show the lowest ΔG_{exch}. The highest ΔG_{exch} values, implying the highest polar functional group tolerance, are seen for Tc^{III}(1), Mo^{III}(2), Ta^{III}, W^{III}, Re^{III} and Os^{III}, lying in the middle of the transition metal groups (groups 5-8). The lowest ΔG_{exch} values (<-10 kcal/mol) are observed for the d^0 systems Sc^{III}, Y^{III} and Lu^{III} reflecting their oxophilicity. When considering that the spin state is retained during the ligand exchange reaction, a large effect on ΔG_{exch} was observed for the first and second row transition metals of groups 5-7 upon varying the spin state. High spin states which only have singly occupied orbitals invariably led to lower ΔG_{exch} compared to the low spin complexes which have one doubly occupied orbital. A large jump in ΔG_{exch} values is seen when going from d^1 to d^2 complexes in the same row, e.g. from Zr^{III} to Nb^{III}(1) or from Hf^{III} to Ta^{III}(1). Furthermore, there is a downward trend as one moves further to the right of the periodic table. All these findings taken together suggest that the ability of the transition metal to engage in π-backbonding plays an important role for the functional group tolerance.

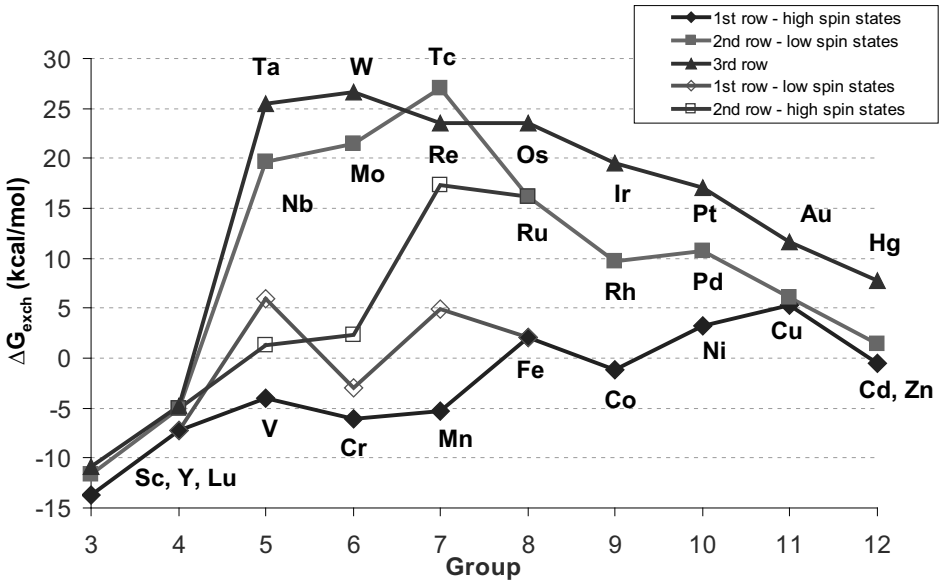

Figure 2. ΔG_{exch} in kcal/mol for all transition metals as function of their group in the periodic table.

This hypothesis found support in the construction of a multilinear regression model, where a good model for ΔG_{exch} could be found by using just one descriptor. Two very similar descriptors were found suitable, both a product describing the efficiency of backdonation, i.e. the nd-orbital radius and *n*d/*(n+1)*s radius ratio[253] multiplied with the formal number of d-electrons available for backbonding. These descriptors were denoted $r_d n_{d\pi}$ and $r_{ds} n_{d\pi}$, respectively. For $r_{ds} n_{d\pi}$, the model showed $R^2 = 0.82$ and $q^2 = 0.81$ and for $r_d n_{d\pi}$ it showed $R^2 = 0.84$ and $q^2 = 0.83$.

Turning now to $\Delta G^{\ddagger}_{ins}$ (Figure 3), a quite similar trend is seen as for ΔG_{exch}, except for group 11 and 12 transition metals. For the group 11 metals Au^{II} and Ag^{II}, insertion transition states could not be obtained, while for group 12 the insertion barriers were very high which can be ascribed to the electronic saturation of these d^{10} metals, since there are no low-lying d-orbitals available for mediating the insertion. In general, insertion barriers can be lowered through accepting π-electron density by the metal in the transition state geometry.[254-256] With this similar trend in mind, it is not surprising that a good correlation exists between ΔG_{exch} and $\Delta G^{\ddagger}_{ins}$ when leaving the offending group 11 and 12 elements out. Furthermore, this is in line with the finding that the insertion barrier was positively correlated with the amount of backbonding from the metal,[257, 258] of which $r_d n_{d\pi}$ and $r_{ds} n_{d\pi}$ describe the efficiency. This correlation between ΔG_{exch} and $\Delta G^{\ddagger}_{ins}$ can be considered somewhat unfortunate, since it implies that a compromise must be struck

between polar functional group tolerance and the height of the insertion barrier which is critical for the catalyst's activity. Undoubtedly this is an essential part of the puzzle why the copolymerization of non-polar and polar olefins is proving to be a serious challenge.

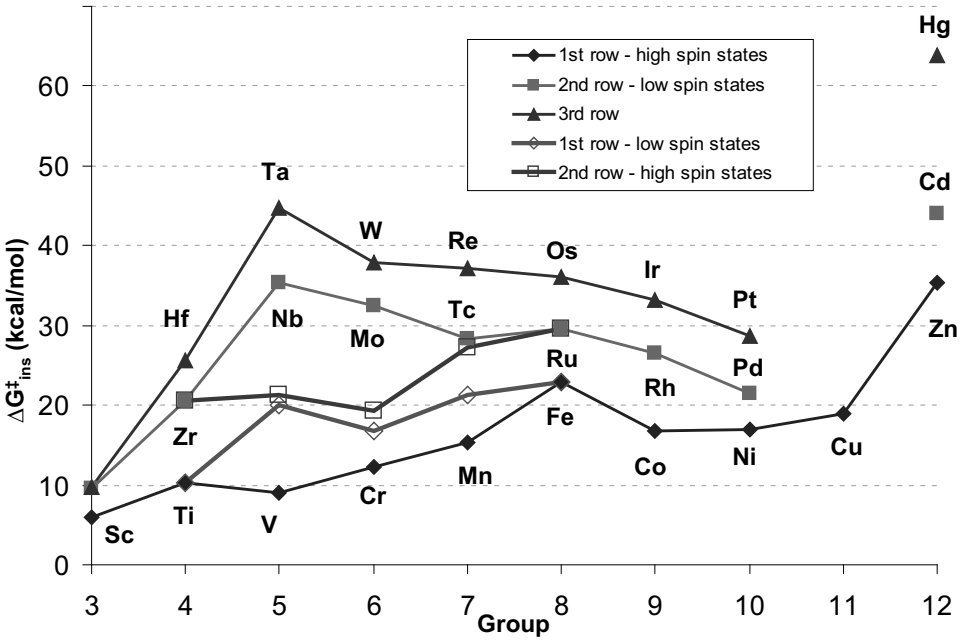

Figure 3. The barriers for ethylene insertion in a ethyl – metal bond ($\Delta G^{\ddagger}_{ins}$) in kcal/mol for all transition metals except Au^{II} and Ag^{II} as function of their group in the periodic table.

To investigate which transition metals strike this compromise well and can hence be considered apt for copolymerization, an interval can be defined for both ΔG_{exch} and $\Delta G^{\ddagger}_{ins}$. For ΔG_{exch} a lower limit can be set, e.g. the value for Ni^{II}, which was reported to be problematically low since such Ni^{II} diimine catalysts were inactive for the copolymerization under mild conditions,[83, 84] due to σ-coordination[239, 240] or chelate formation.[68, 69, 83, 84] For $\Delta G^{\ddagger}_{ins}$ an upper limit can be set, e.g. the value for Ru^{II}, which was reported to be problematically high.[90, 140, 259] To summarize, Pd^{II} was located furthest away from these limit values, thereby rendering it the most suited metal to base a copolymerization catalyst on and rationalizing its apparent superiority.

Chapter 7: *In silico* Catalyst Development

The total number of possible small organic molecules that populate the so-called 'chemical space' in drug-design has been estimated to be near 10^{60},[260] a number which lies in between the number of positions that can occur in chess within the first 40 moves (ca. 10^{46}) and the number of atoms in universe (ca. 10^{81}). In any case, in typical instances of drug-design or catalyst development the chemical space is extremely vast. Therefore, any reasonable development strategy should maximize the speed with which this space is explored. Combinatorial chemistry, where specific techniques speed up the synthesis of distinct molecules as well as their characterization and testing, has contributed significantly to the speed of assessment of potential drugs or catalysts. Further speeding-up can be obtained by means of robotics and automation in general. Another important aspect is scale reduction which cuts the cost of required chemicals. Because of the high speed of screening that becomes possible, this methodology is termed high-throughput screening.
In silico screening can constitute a viable alternative to such an experimental approach, provided that the activity of the potential drugs or catalysts can be both reliably and quickly predicted. An advantage is that there are no chemicals required in this first stage.

While screening speed is an important factor in catalyst development, realistic speeds are still far too low in most situations to systematically consider the whole chemical space of interest. Therefore several methods exist to screen this space efficiently, i.e. to increase the chance that a more active candidate is screened in the next step and candidates that are less likely to be active are never screened. Such methods include quantitative structure-activity relationship (QSAR)[261] and evolutionary algorithm (EA)[262] methods. In absence of such methods, one must rely solely on chemical intuition.

Whereas *in silico* screening is well-established in medicinal chemistry,[263, 264] it is much less commonplace in chemistry at large, and only very few examples in organometallic chemistry exist, e.g. [265]. Undoubtedly, this can be partially ascribed to historical reasons due to the relative complexity in describing the latter complexes computationally.[266] In order to demonstrate the untapped potential of *in silico* organometallic catalyst screening we have developed and presented an evolutionary algorithm capable of handling coordination compounds in Paper V.

Evolutionary algorithms[262] for drug or catalyst development (including the one in Paper V) generally mimic the evolutionary process by applying operators to an initial population of structures. By retention of the fittest structures throughout the optimization process, the population becomes fitter and fitter. The fitness function used to evaluate the structures can be whatever, but in catalyst development it is likely to represent the catalysts' activity.

The evolutionary algorithm in Paper V is characterized by dividing the coordination compounds of interest into three types of fragments: (1) a "rigid" part common to all structures and typically containing the coordination center itself, (2) zero or more "trial" parts consisting of ligand scaffolds, and (3) zero or more "flexible" parts which are allowed to vary freely (see Figure 4). The available trial patterns are typically specified beforehand by the user, and are used to limit the chemical space as well as to ensure reasonable coordination of the transition metal. The flexible parts on the other hand consist of building blocks that are typically generated from large and diverse libraries, currently the KEGG database by Ligand.Info.[267] Three different operators, termed growing (or constitution), mutation and crossover, are used to evolve the population. These operators are pattern-sensitive, i.e. they recognize these different fragments as to protect essential aspects of the structures lying within the rigid and trial parts. This could be accomplished by representing the structures as a combined graph of scaffolds (containing more than one substitution point) and side chains (containing one substitution point). Looking more into the working of the operators, the constitution operator creates new graphs by selection of a trial part and linking of flexible parts to it. Crossover requires two graphs and can be seen as the mutual exchange of a side chain between these two. Finally, mutation requires one graph and replaces a side chain or scaffold by another with an equal amount of substitution points. After action of the operators on the graphs, 3-dimensional structures are generated, and a conformational search with the DREIDING force field[111] (see section 2.5) is carried out.

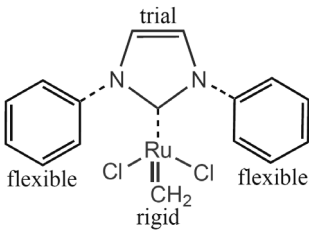

Figure 4. Example of a coordination compound constructed from a rigid part, a trial part and two identical flexible parts.

The above approach allows for application of the evolutionary algorithm to a wide range of inorganic and organometallic problems. As an example we have optimized ruthenium-based catalysts for olefin metathesis. The active complexes of these catalysts are 14-electron alkylidene complexes $LCl_2Ru{=}CH_2$, where L is a dative ligand. This dative ligand heavily impacts on the complex' activity and stability and most research efforts so far have been aimed at this dative ligand.[268] There are currently two main classes of ruthenium olefin metathesis catalysts, the so-called first[269, 270] and second[271] generation Grubbs catalysts, differing only in the kind of dative ligand L in the active catalyst complex (phosphine for the first generation, N-heterocyclic carbene (NHC) based on the imidazol-2-ylidene ring for the second generation). Therefore, the invariable rigid part was specified to contain $Cl_2Ru{=}CH_2$ (see Figure 4), while the donor ligand scaffold constituted the trial part.

Previous work in the group[272] has shown that the catalytic activity of these metathesis catalysts is related to the calculated 'productivity' which is a measure of the metallacyclobutane stability relative to several inactivated states of the catalyst. In that previous work, the productivity also showed a good correlation with DFT-derived molecular descriptors. Since *in silico* catalyst screening requires a rapid assessment of the catalyst potential (*vide supra*) we have investigated if a good correlation with the productivity could be found by means of descriptors based on (computationally cheaper) semiempirical methods rather than on DFT. By using six PM6 (see section 2.4) descriptors (the average Ru−Cl bond distance, the Cl−Ru−Cl bond angle, the average Cl−Ru=C bond angle, the absolute value of X−Ru=C-H torsion angle, the average partial charge on Cl, and the average partial charge on H, where Ru, C, Cl and H are atoms of the rigid part, and X is the donor atom of the trial part formally bound to Ru) a partial least squares (PLS) model with $Q^2 = 0.85$ and root mean square error of cross-validation (RMSECV) = 1.46 kcal/mol could be obtained. This allows for efficient fitness calculation where more than 100 structures can be evaluated per hour and ultimately makes the EA approach feasible.

In Paper V, several different trial parts were specified and allowed to compete against each other in five evolution experiments. In the first experiment a trial part containing a phosphorous atom as scaffold for a phosphine ligand competed against a trial part containing an imidazol-2-ylidene ring as scaffold for the NHC ligand. This corresponded to the first and second generation of Grubbs catalysts, respectively. As desired due to their superior activity, the NHC trial parts eventually dominated the population after a sufficient number of generations, hereby retracing the transition from the first generation Grubbs catalysts to the second generation. In the other evolution experiments the population similarly evolves towards structures based on dative ligands known to provide more active catalysts. The second evolution experiment was aimed at

the substituents of the phosphine ligand. In particular it was found that the alkyl phosphine complexes outcompeted the para-substituted aryl phosphine complexes, which is in line with known catalyst activities.[272] In the third experiment, the backbone substituents of the NHC ligand were investigated. Again, in line with known catalyst activities,[273] evolution favored hydrogen substituents rather than chlorine substituents. The fourth evolution experiment was a combination of the second and third evolution experiment and hence used four different trial parts. As desired, NHC ligands with hydrogen substituents prevailed after sufficient evolution time. The final evolution experiment looked at substituents for saturated NHC ligands. Similarily to the third evolution experiment, the fluorine substituents were outcompeted by the hydrogen substituents on the backbone.

The structures at the end of the evolution experiments are characterized by high fitness values, and since the fitness value is related to the productivity these offer structural hints for novel catalysts, or could be candidates for potential catalysts themselves provided that they can be obtained synthetically. Indeed, when subjecting three of these structures to explicit DFT productivity calculations, particularly high values were found, which for two structures were at level with the best productivities reported for unsaturated NHC-based catalysts,[272] while the remaining structure showed a productivity higher than those of the best previous predictions.[272] These results demonstrate the potential of the EA for the *in silico* development of catalysts and by extension of other functional coordination and organometallic compounds in general.

Chapter 8: Concluding Remarks

The work presented in this thesis can be classified as, on one hand, efforts to increase understanding of the mechanistic aspects of late transition metal based catalysts for olefin polymerization (Papers I, II and III) and on the other, as efforts towards catalyst development (Papers IV and V). These two directions are connected in the sense that although increasing mechanistic understanding of catalysts is very important from a fundamental point of view, it can also be put to use for the development of new catalysts.

In Paper I, after careful investigation into the active center of the (bis(oxazoline)pyridine)$RuCl_2$(ethylene)/MAO catalytic system, it had to be concluded that the observed ethylene polymerization activity is not due to a mononuclear ruthenium complex carrying an intact pybox ligand. Instead, similarly to the related (bis(imino)pyridine)$FeCl_2$/MAO catalytic systems, the active center remains unknown and can be of arbitrary complexity.

In Papers II and III the mechanism of ethylene oligo- and polymerization by neutral Ni catalysts was investigated. Paper II explores the mechanism in the presence of a phosphine ligand, while Paper III does the same in the absence of a phosphine ligand. These two papers together provide a fairly complete understanding of neutral Ni catalysts for ethylene oligo- and polymerization with regard to experimentally observed activity, chain length and branching. Contrary to the (bis(oxazoline)pyridine)$RuCl_2$(ethylene)/MAO catalytic system in Paper I, these neutral Ni catalysts have well-established active centers, facilitating an in-depth investigation.

Paper IV explores the possibility of other transition metals than Ni and Pd as metals for catalysts for random copolymerization of polar and non-polar olefins. Two critical properties of these catalysts were calculated: the polar functional group tolerance and the height of the ethylene insertion barrier. It was found that the ability of the transition metal to engage in backdonation influences both the polar functional group tolerance and the height of the insertion barrier. More specifically, they are positively correlated. Therefore, a compromise must be struck between these two properties, a compromise which is best struck by Pd and which explains its prominent position in the random copolymerization of polar and non-polar olefins.

Finally, Paper V presents an evolutionary algorithm designed to handle coordination compounds by dividing the molecular structure in three fragments, the rigid, trial and flexible part. Because

of this, the evolutionary algorithm is applicable to a wide range of problems in inorganic and organometallic chemistry, as long as a meaningful and computationally efficient fitness function is available. By using a PM6-derived fitness function, we have demonstrated the potential of such an approach for ruthenium olefin metathesis catalysts, where we succeeded in evolving the populations to structures based on dative ligands known to provide more active catalysts. In addition we were able to retrieve interesting potential catalyst structures from the final generations of the evolution experiments.

Chapter 9: Suggestions for Future Work

In Paper I we have excluded the possibility of mononuclear ruthenium complex carrying an intact pybox ligand as the active center in the (bis(oxazoline)pyridine)$RuCl_2$(ethylene)/MAO catalytic system, leaving the active center unknown. This naturally prompts the question what the active center might be. Although the active center could be of arbitrary complexity, an article by Janse van Rensburg *et al*.[274] might provide arguments for first investigating bimetallic Ru-Al centers. In particular their computational work on (pyrrolyl)$Cr^{II}Cl$ complexes active for ethylene trimerization showed, upon coordination of $AlMe_3$ to Cl, a dramatic (>10 kcal/mol (!)) drop of the ethylene insertion barrier into chromacyclopentane. Coordination of Al species originating from MAO to Cl in the (bis(oxazoline)pyridine)$RuCl_2$(ethylene)/MAO system could have a similar effect and could be studied computationally.

While in Papers II and III existing neutral Ni catalysts were investigated, hereby rationalizing the observed activity, chain length and branching, these results pave the way to the prediction of oligo- or polymerization behavior of any stable square planar neutral Ni complex carrying a bidentate ligand. Such predictions could be obtained for specific complexes, or they could be obtained by exploring the vast chemical space constituting of all stable square planar neutral Ni complexes with bidentate ligands more systematically, e.g. by the evolutionary algorithm presented in Paper V. The trial patterns would then come from a library of bidentate ligands of interest. It can be noted that, in case less arbitrariness in the selection of bidentate ligands is desired, use can be made of computational tools capable of automatically generating huge libraries of bidentate ligands.[265] The fitness function would then ideally be derived from the full DFT-calculated reaction profile since these describe all thermodynamics and kinetics, but could more realistically be based on a certain function from PM6 calculations containing the same information. Alas, such simplified fitness function normally comes at the cost of narrowing the applicability domain and/or reducing the accuracy and therefore requires a thorough prior investigation such as was done in Paper V.

Another possibility would be to construct a QSAR model from a number a full energy profiles including those from Paper II and III in order to make more educated guesses at promising structures. Such an approach could be facilitated by an in-house developed Fortran code capable of fully automatically replacing bidentate ligands in xyz files, hence providing excellent starting geometries without the need of possibly tedious manual geometry creation.

It can be noted that this understanding of neutral Ni^{II}-based catalysts could be a good starting point for exploring the potential of other square planar d^8 systems, such as those based on Pd^{II} and Rh^{I}, for oligo- and polymerization of ethylene.

For the copolymerization of polar and non-polar olefins, a complication for the *in silico* development of catalysts is that key catalyst characteristics are correlated. As shown in Paper IV, the height of the insertion barrier dictating the activity is positively correlated with the polar functional group tolerance. An illustrative experimental example from the literature showed that the weaker chelate formation of vinyl trifluoroacetate relative to vinyl acetate came at the expense of a weaker binding of the monomer, so weak relative to ethylene that incorporation was unattainable.[243] Another, now computational, example showed that stronger monomer binding led to higher insertion barriers.[242] Hence a fine balance fulfilling several possibly tight criteria must be struck to achieve successful copolymerization.

The decomposition mechanism involving reductive elimination of neutral Ni and Pd polymerization catalysts described in section 5.8 remains elusive, despite its important role in the copolymerization of non-polar and polar olefins. To understand this mechanism could give a grip on catalyst development for the copolymerization of non-polar and polar olefins, and could therefore facilitate 'a quantum advance in the polyolefin field'[70] or facilitate the accomplishment of 'the ultimate goal of coordination-insertion polymerization'.[71]

The accumulated experimental puzzle pieces (e.g. the measured reaction rate constant for the decomposition of a Ni anilinotropone hydride phosphine complex)[53] provide good reference points for an in-depth computational study which would provide a great compliment to the experiments so far. Even though such an investigation could be challenging due to the involvement of binuclear geometries and the range of possible transition states, in the least a number of reasonable proposals should be able to be made, and unreasonable pathways excluded. Only little computational work has been preformed previously, as one lone work solely investigated the most simple reductive elimination pathway for neutral Pd phosphine-sulfonate catalysts.[238]

List of Abbreviations

(D-)PCM	(Dielectric-)Polarizable Continuum Model
Acac	1,1,1,5,5,5-hexafluoro-2,4-pentanedionato or 1,1,1,5,5,5-hexafluoro-2,4-acetylacetonato
Anth	9-Anthryl
Ar	Aryl
BHE	ß-H Elimination
BHT	ß-H Transfer
CGC	Constrained Geometry Complex
CM4	Charge Model 4
COD	1,5-Cyclooctadiene
Cp	Cyclopentadienyl
Cp*	Pentamethylcyclopentadienyl
DFT	Density Functional Theory
<DP>	Average Degree of Polymerization
EA	Evolutionary Algorithm
ECP	Effective Core Potential
Et	Ethyl
GGA	Generalized Gradient Approximation
GTP	Group Transfer Polymerization
HF	Hartree-Fock
iPr	Isopropyl
LDA	Local Density Approximation
MA	Methyl Acrylate
MAO	Methylaluminoxane
Me	Methyl
MLR	Multiple Linear Regression
MMA	Methyl Methacrylate
MMAO	Modified Methylaluminoxane
M_v	Viscosity Average Molecular Weight
NDDO	Neglect of Diatomic Differential Overlap
NHC	N-Heterocyclic Carbene
NMR	Nuclear Magnetic Resonance
PE	Polyethylene
Ph	Phenyl
PLS	Partial Least Squares
PM6	Parametric Method 6
Pr	Propyl
Pybox	Bis(oxazoline)pyridine
PymNox	2-iminopyridine N-oxide
QSAR	Quantitative Structure-Activity Relationship
RMSECV	Root Mean Square Error of Cross-Validation
SCF	Self-Consistent Field
SCRF	Self-Consistent Reaction Field
SD	Slater Determinant
SHOP	Shell Higher Olefin Process
S.I.	Supporting Information
SM8	Solvent Model 8
TS	Transition State
UAHF	United Atom Hartree-Fock

References

[1] K. Ziegler, *Belg. Pat.,* 533362, **1953**.
[2] K. Ziegler, E. Holzkamp, H. Breil and H. Martin, *Angew. Chem. Int. Ed.* **1955**, *67*, 426-426.
[3] K. Ziegler, E. Holzkamp, H. Breil and H. Martin, *Angew. Chem. Int. Ed.* **1955**, *67*, 541-547.
[4] G. Natta, *Journal of Polymer Science* **1955**, *16*, 143-154.
[5] G. Natta, *Makromol. Chem.* **1955**, *16*, 213-237.
[6] G. Natta, *Angew. Chem. Int. Ed.* **1956**, *68*, 393-403.
[7] J. Boor Jr., *Makromol. Revs.* **1967**, 115.
[8] O. G. Piringer and A. L. Baner in *Plastic Packaging: Interaction with Food and Pharmaceuticals* Wiley-VCH, **2008**, p. 32.
[9] R. H. Crabtree in *The Organometallic Chemistry of the Transition Metals*, John Wiley & Sons, Inc, Hoboken, NJ, USA, **2005**, p. 351.
[10] K. H. Theopold, *Eur. J. Inorg. Chem.* **1998**, 15-24.
[11] D. S. Breslow and N. R. Newburg, *J. Am. Chem. Soc.* **1957**, *79*, 5072-5073.
[12] G. Natta, P. Pino, G. Mazzanti, U. Giannini, E. Mantica and M. Peraldo, *Journal of Polymer Science* **1957**, *26*, 120-123.
[13] G. Natta, P. Pino, G. Mazzanti and U. Giannini, *J. Am. Chem. Soc.* **1957**, *79*, 2975-2976.
[14] H. Sinn, W. Kaminsky, H. J. Vollmer and R. Woldt, *Angew. Chem. Int. Ed. Engl.* **1980**, *19*, 390-392.
[15] H. Sinn and W. Kaminsky, *Adv. Organomet. Chem.* **1980**, *18*, 99.
[16] W. Kaminsky, *J. Chem. Soc.-Dalton Trans.* **1998**, 1413-1418.
[17] D. Cam and U. Giannini, *Makromolekulare Chemie-Macromolecular Chemistry and Physics* **1992**, *193*, 1049-1055.
[18] W. Kaminsky, *Macromol. Chem. Phys.* **1996**, *197*, 3907-3945.
[19] E. Y. X. Chen and T. J. Marks, *Chem. Rev.* **2000**, *100*, 1391-1434.
[20] K. Soga and T. Shiono, *Prog. Polym. Sci.* **1997**, *22*, 1503-1546.
[21] M. Bochmann, *J. Chem. Soc.-Dalton Trans.* **1996**, 255-270.
[22] H. G. Alt and A. Köppl, *Chem. Rev.* **2000**, *100*, 1205-1221.
[23] H. H. Brintzinger, D. Fischer, R. Mülhaupt, B. Rieger and R. M. Waymouth, *Angew. Chem. Int. Ed. Engl.* **1995**, *34*, 1143-1170.
[24] R. H. Crabtree in *The Organometallic Chemistry of the Transition Metals*, John Wiley & Sons, Inc, Hoboken, NJ, USA, **2005**, p. 352.
[25] H. Werner in *Landmarks in organo-transition metal chemistry: a personal view*, Springer Science + Business Media, New York, NY, USA, **2009**, p. 161.
[26] K. Angermund, G. Fink, V. R. Jensen and R. Kleinschmidt, *Chem. Rev.* **2000**, *100*, 1457-1470.
[27] K. Angermund, G. Fink, V. R. Jensen and R. Kleinschmidt, *Macromol. Rapid Commun.* **2000**, *21*, 91-97.
[28] K. P. Bryliakov, *Russ. Chem. Rev.* **2007**, *76*, 253-277.
[29] H. Braunschweig and F. M. Breitling, *Coord. Chem. Rev.* **2006**, *250*, 2691-2720.
[30] A. L. McKnight and R. M. Waymouth, *Chem. Rev.* **1998**, *98*, 2587-2598.
[31] V. C. Gibson and S. K. Spitzmesser, *Chem. Rev.* **2003**, *103*, 283-315.
[32] R. Emrich, O. Heinemann, P. W. Jolly, C. Krüger and G. P. J. Verhovnik, *Organometallics* **1997**, *16*, 1511-1513.
[33] M. P. Coles and V. C. Gibson, *Polym. Bull.* **1994**, *33*, 529.
[34] M. C. W. Chan, K. C. Chew, C. I. Dalby, V. C. Gibson, A. Kohlmann, I. R. Little and W. Reed, *Chem. Commun.* **1998**, 1673-1674.
[35] K. Mashima, S. Fujikawa and A. Nakamura, *J. Am. Chem. Soc.* **1993**, *115*, 10990-10991.

[36] K. Mashima, S. Fujikawa, Y. Tanaka, H. Urata, T. Oshiki, E. Tanaka and A. Nakamura, *Organometallics* **1995**, *14*, 2633-2640.
[37] K. Mashima, S. Fujikawa, H. Urata, E. Tanaka and A. Nakamura, *J. Chem. Soc.-Chem. Commun.* **1994**, 1623-1624.
[38] A. J. Sillanpää and K. E. Laasonen, *Organometallics* **2001**, *20*, 1334-1344.
[39] E. Le Grognec, R. Poli and L.-S. Wang, *Inorg. Chem. Commun.* **1999**, *2*, 95-96.
[40] E. Le Grognec, R. Poli and P. Richard, *Organometallics* **2000**, *19*, 3842-3853.
[41] E. Le Grognec and R. Poli, *Chem.-Eur. J.* **2001**, *7*, 4572-4583.
[42] T. Matsugi and T. Fujita, *Chem. Soc. Rev.* **2008**, *37*, 1264-1277.
[43] H. Makio and T. Fujita, *Acc. Chem. Res.* **2009**, *42*, 1532-1544.
[44] R. H. Crabtree in *The Organometallic Chemistry of the Transition Metals*, John Wiley & Sons, Inc, Hoboken, NJ, USA, **2005**, pp. 357-358.
[45] K. A. Ostoja Starzewski and J. Witte, *Angew. Chem. Int. Ed. Engl.* **1987**, *26*, 63-64.
[46] K. A. Ostoja Starzewski and J. Witte, *Angew. Chem. Int. Ed. Engl.* **1985**, *24*, 599-601.
[47] U. Klabunde and S. D. Ittel, *J. Mol. Catal.* **1987**, *41*, 123-134.
[48] U. Klabunde, R. Mülhaupt, T. Herskovitz, A. H. Janowicz, J. Calabrese and S. D. Ittel, *J. Polym. Sci., Part A: Polym. Chem.* **1987**, *25*, 1989-2003.
[49] C. M. Wang, S. Friedrich, T. R. Younkin, R. T. Li, R. H. Grubbs, D. A. Bansleben and M. W. Day, *Organometallics* **1998**, *17*, 3149-3151.
[50] T. R. Younkin, E. F. Conner, J. I. Henderson, S. K. Friedrich, R. H. Grubbs and D. A. Bansleben, *Science* **2000**, *287*, 460-462.
[51] F. A. Hicks and M. Brookhart, *Organometallics* **2001**, *20*, 3217-3219.
[52] F. A. Hicks, J. C. Jenkins and M. Brookhart, *Organometallics* **2003**, *22*, 3533-3545.
[53] J. C. Jenkins and M. Brookhart, *J. Am. Chem. Soc.* **2004**, *126*, 5827-5842.
[54] T. R. Younkin, E. F. Connor, J. I. Henderson, S. K. Friedrich, R. H. Grubbs and D. A. Bansleben, *Science* **2000**, *288*, 1749-1751.
[55] J. Skupińska, *Chem. Rev.* **1991**, *91*, 613-648.
[56] W. Keim, *Angew. Chem. Int. Ed. Engl.* **1990**, *29*, 235-244.
[57] S. D. Ittel, L. K. Johnson and M. Brookhart, *Chem. Rev.* **2000**, *100*, 1169-1203.
[58] W. Keim, B. Hoffmann, R. Lodewick, M. Peuckert, G. Schmitt, J. Fleischhauer and U. Meier, *J. Mol. Catal.* **1979**, *6*, 79-97.
[59] R. B. Cracknell, A. G. Orpen and J. L. Spencer, *J. Chem. Soc.-Chem. Commun.* **1984**, 326-328.
[60] G. F. Schmidt and M. Brookhart, *J. Am. Chem. Soc.* **1985**, *107*, 1443-1444.
[61] M. Brookhart, A. F. Volpe and D. M. Lincoln, *J. Am. Chem. Soc.* **1990**, *112*, 5634-5636.
[62] M. Brookhart, E. Hauptman and D. M. Lincoln, *J. Am. Chem. Soc.* **1992**, *114*, 10394-10401.
[63] M. Brookhart and D. M. Lincoln, *J. Am. Chem. Soc.* **1988**, *110*, 8719-8720.
[64] L. Wang, R. S. Lu, R. Bau and T. C. Flood, *J. Am. Chem. Soc.* **1993**, *115*, 6999-7000.
[65] L. Wang and T. C. Flood, *J. Am. Chem. Soc.* **1992**, *114*, 3169-3170.
[66] S. Timonen, T. T. Pakkanen and T. A. Pakkanen, *J. Mol. Catal. A-Chem.* **1996**, *111*, 267-272.
[67] L. K. Johnson, C. M. Killian and M. Brookhart, *J. Am. Chem. Soc.* **1995**, *117*, 6414-6415.
[68] L. K. Johnson, S. Mecking and M. Brookhart, *J. Am. Chem. Soc.* **1996**, *118*, 267-268.
[69] S. Mecking, L. K. Johnson, L. Wang and M. Brookhart, *J. Am. Chem. Soc.* **1998**, *120*, 888-899.
[70] L. S. Boffa and B. M. Novak, *Chem. Rev.* **2000**, *100*, 1479-1493.
[71] V. Busico, *Dalton Trans.* **2009**, 8794–8802.
[72] C. S. Popeney, D. H. Camacho and Z. B. Guan, *J. Am. Chem. Soc.* **2007**, *129*, 10062-10063.
[73] C. S. Popeney and Z. B. Guan, *J. Am. Chem. Soc.* **2009**, *131*, 12384-12393.
[74] E. Drent, R. van Dijk, R. van Ginkel, B. van Oort and R. I. Pugh, *Chem. Commun.* **2002**, 744-745.
[75] T. Kochi, S. Noda, K. Yoshimura and K. Nozaki, *J. Am. Chem. Soc.* **2007**, *129*, 8948-8949.

[76] S. Ito, K. Munakata, A. Nakamura and K. Nozaki, *J. Am. Chem. Soc.* **2009**, *131*, 14606-14607.
[77] W. Weng, Z. Shen and R. F. Jordan, *J. Am. Chem. Soc.* **2007**, *129*, 15450-15451.
[78] S. Luo, J. Vela, G. R. Lief and R. F. Jordan, *J. Am. Chem. Soc.* **2007**, *129*, 8946-8947.
[79] D. Guironnet, P. Roesle, T. Rünzi, I. Göttker-Schnetmann and S. Mecking, *J. Am. Chem. Soc.* **2009**, *131*, 422-423.
[80] D. Guironnet, L. Caporaso, B. Neuwald, I. Göttker-Schnetmann, L. Cavallo and S. Mecking, *J. Am. Chem. Soc.* **2010**, *132*, 4418-4426.
[81] S. Ikeda, F. Ohhata, M. Miyoshi, R. Tanaka, T. Minami, F. Ozawa and M. Yoshifuji, *Angew. Chem. Int. Ed.* **2000**, *39*, 4512-4513.
[82] O. Daugulis, M. Brookhart and P. S. White, *Organometallics* **2002**, *21*, 5935-5943.
[83] L. Johnson, L. Wang, S. McLain, A. Bennett, K. Dobbs, E. Hauptman, A. Ionkin, S. Ittel, K. Kunitsky, W. Marshall, E. McCord, C. Radzewich, A. Rinehart, K. J. Sweetman, Y. Wang, Z. H. Yin and M. Brookhart, *Beyond Metallocenes: Next Generation Polmerization Catalysts* **2003**, *857*, 131-142.
[84] L. Johnson, A. Bennett, K. Dobbs, E. Hauptman, A. Ionkin, S. Ittel, E. McCord, S. McLain, C. Radzewich, Z. Yin, L. Wang, Y. Wang and M. Brookhart, *Polym. Mater. Sci. Eng.* **2002**, *86*, 319.
[85] M. Brasse, J. Cámpora, P. Palma, E. Álvarez, V. Cruz, J. Ramos and M. L. Reyes, *Organometallics* **2008**, *27*, 4711-4723.
[86] B. A. Rodriguez, M. Delferro and T. J. Marks, *J. Am. Chem. Soc.* **2009**, *131*, 5902-5919.
[87] B. L. Small, M. Brookhart and A. M. A. Bennett, *J. Am. Chem. Soc.* **1998**, *120*, 4049-4050.
[88] G. J. P. Britovsek, M. Bruce, V. C. Gibson, B. S. Kimberley, P. J. Maddox, S. Mastroianni, S. J. McTavish, C. Redshaw, G. A. Solan, S. Strömberg, A. J. P. White and D. J. Williams, *J. Am. Chem. Soc.* **1999**, *121*, 8728-8740.
[89] G. J. P. Britovsek, V. C. Gibson, B. S. Kimberley, P. J. Maddox, S. J. McTavish, G. A. Solan, A. J. P. White and D. J. Williams, *Chem. Commun.* **1998**, 849-850.
[90] K. Nomura, S. Warit and Y. Imanishi, *Macromolecules* **1999**, *32*, 4732-4734.
[91] Y. Imanishi and K. Nomura, *Journal of Polymer Science Part A: Polymer Chemistry* **2000**, 4613-4626.
[92] K. Nomura, S. Warit and Y. Imanishi, *Bull. Chem. Soc. Jpn.* **2000**, *73*, 599-605.
[93] V. C. Gibson, A. Tomov, D. F. Wass, A. J. P. White and D. J. Williams, *J. Chem. Soc.-Dalton Trans.* **2002**, 2261-2262.
[94] R. T. Stibrany, D. N. Schulz, S. Kacker, A. O. Patil, L. S. Baugh, S. P. Rucker, S. Zushma, E. Berluche and J. A. Sissano, *Macromolecules* **2003**, *36*, 8584-8586.
[95] S. V. Larionov, Z. A. Savel'eva, N. V. Semikolenova, R. F. Klevtsova, L. A. Glinskaya, E. G. Boguslavskii, V. N. Korskii, V. A. Zakharov, S. A. Popov and A. V. Tkachev, *Russian Journal of Coordination Chemistry* **2007**, *33*, 436-448.
[96] M. B. Bushuev, V. P. Krivopalov, N. V. Semikolenova, E. V. Peresypkina, A. V. Virovets, L. A. Sheludyakova, L. G. Lavrenova, V. A. Zakharov and S. V. Larionov, *Russian Journal of Coordination Chemistry* **2006**, *32*, 199-207.
[97] A. M. R. Galletti, C. Carlini, S. Giaiacopi, M. Martinelli and G. Sbrana, *J. Polym. Sci., Part A: Polym. Chem.* **2007**, *45*, 1134-1142.
[98] L. S. Baugh, J. A. Sissano, S. Kacker, E. Berluche, R. T. Stibrany, D. N. Schulz and S. P. Rucker, *J. Polym. Sci., Part A: Polym. Chem.* **2006**, *44*, 1817-1840.
[99] M. Nagel, W. F. Paxton, A. Sen, L. Zakharov and A. L. Rheingold, *Macromolecules* **2004**, *37*, 9305-9307.
[100] G. J. P. Britovsek, V. C. Gibson and D. F. Wass, *Angew. Chem. Int. Ed.* **1999**, *38*, 429-447.
[101] A. Nakamura, S. Ito and K. Nozaki, *Chem. Rev.* **2009**, *109*, 5215-5244.
[102] I. N. Levine, *Quantum Chemistry*, Prentice Hall, Upper Saddle River, NJ, USA, **2000**.

[103] A. Szabo and N. S. Ostlund, *Modern Quantum Chemistry: Introduction to Advanced Structure Theory*, Dover Publications Inc., New York, NY, USA, **1982**.
[104] W. Koch and M. C. Holthausen, *A Chemist's Guide to Density Functional Theory* Wiley-VCH, Weinheim, **2001**.
[105] R. G. Parr and W. Yang, *Density-Functional Theory of Atoms and Molecules*, Oxford University Press, Oxford, UK, **1989**.
[106] D. A. McQuarrie and J. D. Simon, *Molecular Thermodynamics*, University Science Books, Mill Valley, CA, USA, **1999**.
[107] N. L. Trefethen and D. Bau, *Numerical Linear Algebra*, SIAM: Society for Industrial and Applied Mathematics, **1997**.
[108] Y. Minenkov, G. Occhipinti and V. R. Jensen, *J. Phys. Chem. A* **2009**, *113*, 11833-11844.
[109] S. Grimme, *J. Comput. Chem.* **2006**, *27*, 1787-1799.
[110] J. J. P. Stewart, *Journal of Molecular Modeling* **2007**, *13*, 1173-1213.
[111] S. L. Mayo, B. D. Olafson and W. A. Goddard, *J. Phys. Chem.* **1990**, *94*, 8897.
[112] J. Tomasi, *Theor. Chem. Acct.* **2004**, *112*, 184-203.
[113] J. Tomasi, B. Mennucci and R. Cammi, *Chem. Rev.* **2005**, *105*, 2999-3093.
[114] A. Bondi, *J. Phys. Chem.* **1964**, *68*, 441.
[115] A. V. Marenich, R. M. Olson, C. P. Kelly, C. J. Cramer and D. G. Truhlar, *J. Chem. Theor. Comput.* **2007**, *3*, 2011-2033.
[116] R. M. Olson, A. V. Marenich, C. J. Cramer and D. G. Truhlar, *J. Chem. Theor. Comput.* **2007**, *3*, 2046-2054.
[117] G. V. Schulz, *Z. Phys. Chem.* **1939**, *B43*, 25–46.
[118] G. V. Schulz, *Z. Phys. Chem.* **1935**, *B30*, 379–388.
[119] P. J. Flory, *J. Am. Chem. Soc.* **1940**, *62*, 1561–1565.
[120] V. R. Jensen, D. Koley, M. N. Jagadeesh and W. Thiel, *Macromolecules* **2005**, *38*, 10266-10278.
[121] J. C. W. Lohrenz, T. K. Woo and T. Ziegler, *J. Am. Chem. Soc.* **1995**, *117*, 12793.
[122] T. K. Woo, P. M. Margl, J. C. W. Lohrenz, P. E. Blöchl and T. Ziegler, *J. Am. Chem. Soc.* **1996**, *118*, 13021-13030.
[123] D. G. Musaev, M. Svensson, K. Morokuma, S. Strömberg, K. Zetterberg and P. E. M. Siegbahn, *Organometallics* **1997**, *16*, 1933-1945.
[124] D. G. Musaev, R. D. J. Froese, M. Svensson and K. Morokuma, *J. Am. Chem. Soc.* **1997**, *119*, 367-374.
[125] A. Zeller and T. Straßner, *J. Organomet. Chem.* **2006**, *691*, 4379-4385.
[126] T. K. Woo, P. M. Margl, T. Ziegler and P. E. Blöchl, *Organometallics* **1997**, *16*, 3454-3468.
[127] M. S. W. Chan, K. Vanka, C. C. Pye and T. Ziegler, *Organometallics* **1999**, *18*, 4624-4636.
[128] I. E. Nifant'ev, L. Y. Ustynyuk and D. N. Laikov, *Organometallics* **2001**, *20*, 5375-5393.
[129] M. Bochmann, *J. Organomet. Chem.* **2004**, *689*, 3982-3998.
[130] P. A. Wilson, M. H. Hannant, J. A. Wright, R. D. Cannon and M. Bochmann, *Macromol. Symp.* **2006**, *236*, 100-110.
[131] G. Lanza, I. L. Fragala and T. J. Marks, *J. Am. Chem. Soc.* **2000**, *122*, 12764-12777.
[132] G. Lanza, I. L. Fragala and T. J. Marks, *Organometallics* **2002**, *21*, 5594-5612.
[133] G. Lanza, I. L. Fragala and T. J. Marks, *J. Am. Chem. Soc.* **1998**, *120*, 8257-8258.
[134] Z. T. Xu, K. Vanka, T. Firman, A. Michalak, E. Zurek, C. B. Zhu and T. Ziegler, *Organometallics* **2002**, *21*, 2444-2453.
[135] Z. T. Xu, K. Vanka and T. Ziegler, *Organometallics* **2004**, *23*, 104-116.
[136] G. Ciancaleoni, N. Fraldi, P. H. M. Budzelaar, V. Busico and A. Macchioni, *Dalton Trans.* **2009**, 8824-8827.
[137] A. Macchioni, *Chem. Rev.* **2005**, *105*, 2039-2073.
[138] E. Clot, *Eur. J. Inorg. Chem.* **2009**, 2319-2328.

[139] T. M. Trnka and R. H. Grubbs, *Acc. Chem. Res.* **2001**, *34*, 18-29.
[140] E. L. Dias, M. Brookhart and P. S. White, *Organometallics* **2000**, *19*, 4995-5004.
[141] P. Cossee, *J. Catal.* **1964**, *3*, 80-88.
[142] E. J. Arlman and P. Cossee, *J. Catal.* **1964**, *3*, 99-104.
[143] K. J. Ivin, J. J. Rooney, C. D. Stewart, M. L. H. Green and R. Mahtab, *J. Chem. Soc.-Chem. Commun.* **1978**, 604-606.
[144] D. G. H. Hetterscheid, C. Hendriksen, W. I. Dzik, J. M. M. Smits, E. R. H. van Eck, A. E. Rowan, V. Busico, M. Vacatello, V. V. Castelli, A. Segre, E. Jellema, T. G. Bloemberg and B. de Bruin, *J. Am. Chem. Soc.* **2006**, *128*, 9746-9752.
[145] E. Jellema, P. H. M. Budzelaar, J. N. H. Reek and B. de Bruin, *J. Am. Chem. Soc.* **2007**, *129*, 11631-11641.
[146] E. Jellema, A. L. Jongerius, J. N. H. Reek and B. de Bruin, *Chem. Soc. Rev. 39*, 5067-5067.
[147] R. Raucoules, T. de Bruin, P. Raybaud and C. Adamo, *Organometallics* **2008**, *27*, 3368-3377.
[148] R. Raucoules, T. de Bruin, P. Raybaud and C. Adamo, *Organometallics* **2009**, *28*, 5358-5367.
[149] P. M. Castro, P. Lahtinen, K. Axenov, J. Viidanoja, T. Kotiaho, M. Leskela and T. Repo, *Organometallics* **2005**, *24*, 3664-3670.
[150] M. W. Bouwkamp, E. Lobkovsky and P. J. Chirik, *J. Am. Chem. Soc.* **2005**, *127*, 9660-9661.
[151] D. V. Khoroshun, D. G. Musaev, T. Vreven and K. Morokuma, *Organometallics* **2001**, *20*, 2007-2026.
[152] L. Q. Deng, P. Margl and T. Ziegler, *J. Am. Chem. Soc.* **1999**, *121*, 6479-6487.
[153] E. A. H. Griffiths, G. J. P. Britovsek, V. C. Gibson and I. R. Gould, *Chem. Commun.* **1999**, 1333-1334.
[154] M. W. Bouwkamp, S. C. Bart, E. J. Hawrelak, R. J. Trovitch, E. Lobkovsky and P. J. Chirik, *Chem. Commun.* **2005**, 3406-3408.
[155] K. P. Bryliakov, E. P. Talsi, N. V. Semikolenova and V. A. Zakharov, *Organometallics* **2009**, *28*, 3225-3232.
[156] J. Scott, S. Gambarotta, I. Korobkov and P. H. M. Budzelaar, *Organometallics* **2005**, *24*, 6298-6300.
[157] J. R. Briggs, *J. Chem. Soc.-Chem. Commun.* **1989**, 674-675.
[158] T. Agapie, S. J. Schofer, J. A. Labinger and J. E. Bercaw, *J. Am. Chem. Soc.* **2004**, *126*, 1304-1305.
[159] A. K. Tomov, J. J. Chirinos, D. J. Jones, R. J. Long and V. C. Gibson, *J. Am. Chem. Soc.* **2005**, *127*, 10166-10167.
[160] W. Janse van Rensburg, C. Grové, J. P. Steynberg, K. B. Stark, J. J. Huyser and P. J. Steynberg, *Organometallics* **2004**, *23*, 1207-1222.
[161] T. Agapie, J. A. Labinger and J. E. Bercaw, *J. Am. Chem. Soc.* **2007**, *129*, 14281-14295.
[162] S. Tobisch and T. Ziegler, *J. Am. Chem. Soc.* **2004**, *126*, 9059-9071.
[163] S. Tobisch and T. Ziegler, *Organometallics* **2003**, *22*, 5392-5405.
[164] P. J. W. Deckers, B. Hessen and J. H. Teuben, *Organometallics* **2002**, *21*, 5122-5135.
[165] P. J. W. Deckers, B. Hessen and J. H. Teuben, *Angew. Chem. Int. Ed.* **2001**, *40*, 2516-2519.
[166] A. N. J. Blok, P. H. M. Budzelaar and A. W. Gal, *Organometallics* **2003**, *22*, 2564-2570.
[167] T. J. M. de Bruin, L. Magna, P. Raybaud and H. Toulhoat, *Organometallics* **2003**, *22*, 3404-3413.
[168] C. Andes, S. B. Harkins, S. Murtuza, K. Oyler and A. Sen, *J. Am. Chem. Soc.* **2001**, *123*, 7423-7424.
[169] R. Arteaga-Müller, H. Tsurugi, T. Saito, M. Yanagawa, S. Oda and K. Mashima, *J. Am. Chem. Soc.* **2009**, *131*, 5370-5371.

[170] Z. X. Yu and K. N. Houk, *Angew. Chem. Int. Ed.* **2003**, *42*, 808-811.
[171] M. J. Overett, K. Blann, A. Bollmann, J. T. Dixon, D. Haasbroek, E. Killian, H. Maumela, D. S. McGuinness and D. H. Morgan, *J. Am. Chem. Soc.* **2005**, *127*, 10723-10730.
[172] S. Kuhlmann, J. T. Dixon, M. Haumann, D. H. Morgan, J. Ofili, O. Spuhl, N. Taccardi and P. Wasserscheid, *Adv. Synth. Catal.* **2006**, *348*, 1200-1206.
[173] A. K. Tomov, J. J. Chirinos, R. J. Long, V. C. Gibson and M. R. J. Elsegood, *J. Am. Chem. Soc.* **2006**, *128*, 7704-7705.
[174] D. S. McGuinness, J. A. Suttil, M. G. Gardiner and N. W. Davies, *Organometallics* **2008**, *27*, 4238-4247.
[175] E. Groppo, C. Lamberti, S. Bordiga, G. Spoto and A. Zecchina, *Chem. Rev.* **2005**, *105*, 115-183.
[176] Ø. Espelid and K. J. Børve, *J. Catal.* **2002**, *206*, 331-338.
[177] A. Held, F. M. Bauers and S. Mecking, *Chem. Commun.* **2000**, 301-302.
[178] S. Mecking, A. Held and F. M. Bauers, *Angew. Chem. Int. Ed.* **2002**, *41*, 544-561.
[179] J. P. Claverie and R. Soula, *Prog. Polym. Sci.* **2003**, *28*, 619-662.
[180] V. C. Gibson and A. Tomov, *Chem. Commun.* **2001**, 1964-1965.
[181] E. F. Connor, T. R. Younkin, J. I. Henderson, S. J. Hwang, R. H. Grubbs, W. P. Roberts and J. J. Litzau, *J. Polym. Sci., Part A: Polym. Chem.* **2002**, *40*, 2842-2854.
[182] G. M. Benedikt, E. Elce, B. L. Goodall, H. A. Kalamarides, L. H. McIntosh, L. F. Rhodes, K. T. Selvy, C. Andes, K. Oyler and A. Sen, *Macromolecules* **2002**, *35*, 8978-8988.
[183] S. J. Diamanti, P. Ghosh, F. Shimizu and G. C. Bazan, *Macromolecules* **2003**, *36*, 9731-9735.
[184] S. J. Diamanti, V. Khanna, A. Hotta, D. Yamakawa, F. Shimizu, E. J. Kramer, G. H. Fredrickson and G. C. Bazan, *J. Am. Chem. Soc.* **2004**, *126*, 10528-10529.
[185] J. Q. Sun, Y. H. Shan, Y. J. Xu, Y. G. Cui, H. Schumann and M. Hummert, *J. Polym. Sci., Part A: Polym. Chem.* **2004**, *42*, 6071-6080.
[186] S. Sujith, D. J. Joe, S. J. Na, Y. W. Park, C. H. Chow and B. Y. Lee, *Macromolecules* **2005**, *38*, 10027-10033.
[187] C. Y. Guo, N. Peulecke, K. R. Basvani, M. K. Kinderman and J. Heinicke, *Macromolecules* **2010**, *43*, 1416-1424.
[188] A. W. Waltman, T. R. Younkin and R. H. Grubbs, *Organometallics* **2004**, *23*, 5121-5123.
[189] A. Berkefeld and S. Mecking, *J. Am. Chem. Soc.* **2009**, *131*, 1565-1574.
[190] A. Berkefeld, M. Drexler, H. M. Möller and S. Mecking, *J. Am. Chem. Soc.* **2009**, *131*, 12613-12622.
[191] J. Heinicke, M. Köhler, N. Peulecke and W. Keim, *J. Catal.* **2004**, *225*, 16-23.
[192] J. Heinicke, M. Köhler, N. Peulecke, M. Z. He, M. K. Kindermann, W. Keim and G. Fink, *Chem.-Eur. J.* **2003**, *9*, 6093-6107.
[193] J. Heinicke, M. Z. He, A. Dal, H. F. Klein, O. Hetche, W. Keim, U. Flörke and H. J. Haupt, *Eur. J. Inorg. Chem.* **2000**, 431-440.
[194] J. Pietsch, P. Braunstein and Y. Chauvin, *New J. Chem.* **1998**, *22*, 467-472.
[195] D. P. Song, J. Q. Wu, W. P. Ye, H. L. Mu and Y. S. Li, *Organometallics* **2010**, *29*, 2306-2314.
[196] R. S. Rojas, G. B. Galland, G. Wu and G. C. Bazan, *Organometallics* **2007**, *26*, 5339-5345.
[197] X. Y. Zhou, S. Bontemps and R. F. Jordan, *Organometallics* **2008**, *27*, 4821-4824.
[198] L. Zhang, M. Brookhart and P. S. White, *Organometallics* **2006**, *25*, 1868-1874.
[199] P. Kuhn, D. Sémeril, C. Jeunesse, D. Matt, M. Neuburger and A. Mota, *Chem.-Eur. J.* **2006**, *12*, 5210-5219.
[200] P. Kuhn, D. Sémeril, D. Matt, M. J. Chetcuti and P. Lutz, *Dalton Trans.* **2007**, 515-528.
[201] W. Keim, F. H. Kowaldt, R. Goddard and C. Krüger, *Angew. Chem. Int. Ed. Engl.* **1978**, *17*, 466-467.
[202] J. C. Jenkins and M. Brookhart, *Organometallics* **2003**, *22*, 250-256.

[203] M. S. W. Chan, L. Q. Deng and T. Ziegler, *Organometallics* **2000**, *19*, 2741-2750.
[204] D. V. Deubel and T. Ziegler, *Organometallics* **2002**, *21*, 4432-4441.
[205] A. Michalak and T. Ziegler, *Organometallics* **2003**, *22*, 2069-2079.
[206] J. Ramos, V. L. Cruz, J. Martínez-Salazar, M. Brasse, P. Palma and J. Cámpora, *J. Polym. Sci., Part A: Polym. Chem.* **2010**, *48*, 1160-1165.
[207] A. Haras, G. D. W. Anderson, A. Michalak, B. Rieger and T. Ziegler, *Organometallics* **2006**, *25*, 4491-4497.
[208] S. Noda, A. Nakamura, T. Kochi, L. W. Chung, K. Morokuma and K. Nozaki, *J. Am. Chem. Soc.* **2009**, *131*, 14088-14100.
[209] P. Kuhn, D. Sémeril, C. Jeunesse, D. Matt, P. Lutz and R. Welter, *Eur. J. Inorg. Chem.* **2005**, 1477-1481.
[210] M. D. Leatherman, S. A. Svejda, L. K. Johnson and M. Brookhart, *J. Am. Chem. Soc.* **2003**, *125*, 3068-3081.
[211] M. J. Rachita, R. L. Huff, J. L. Bennett and M. Brookhart, *J. Polym. Sci., Part A: Polym. Chem.* **2000**, *38*, 4627-4640.
[212] G. Rothenberg in *Catalysis: Concepts and Green Applications*, Wiley-VCH, **2008**, p. 98.
[213] L. K. Johnson, C. M. Killian and M. Brookhart, *J. Am. Chem. Soc.* **1995**, *117*, 6414-6415.
[214] Z. B. Guan, P. M. Cotts, E. F. McCord and S. J. McLain, *Science* **1999**, *283*, 2059-2062.
[215] S. A. Svejda, L. K. Johnson and M. Brookhart, *J. Am. Chem. Soc.* **1999**, *121*, 10634-10635.
[216] D. J. Tempel, L. K. Johnson, R. L. Huff, P. S. White and M. Brookhart, *J. Am. Chem. Soc.* **2000**, *122*, 6686-6700.
[217] L. H. Shultz and M. Brookhart, *Organometallics* **2001**, *20*, 3975-3982.
[218] L. H. Shultz, D. J. Tempel and M. Brookhart, *J. Am. Chem. Soc.* **2001**, *123*, 11539-11555.
[219] L. Q. Deng, T. K. Woo, L. Cavallo, P. M. Margl and T. Ziegler, *J. Am. Chem. Soc.* **1997**, *119*, 6177-6186.
[220] L. Q. Deng, P. Margl and T. Ziegler, *J. Am. Chem. Soc.* **1997**, *119*, 1094-1100.
[221] D. G. Musaev and K. Morokuma, *Topics in Catalysis* **1999**, *7*, 107-123.
[222] D. G. Musaev, R. D. J. Froese and K. Morokuma, *Organometallics* **1998**, *17*, 1850-1860.
[223] D. P. Gates, S. K. Svejda, E. Oñate, C. M. Killian, L. K. Johnson, P. S. White and M. Brookhart, *Macromolecules* **2000**, *33*, 2320-2334.
[224] J. Ramos, V. Cruz, A. Muñoz-Escalona, S. Martínez and J. Martínez-Salazar, *Polymer* **2003**, *44*, 2169-2176.
[225] L. Fan, A. Krzywicki, A. Somogyvari and T. Ziegler, *Inorg. Chem.* **1996**, *35*, 4003-4006.
[226] L. Fan, A. Krzywicki, A. Somogyvari and T. Ziegler, *Inorg. Chem.* **1994**, *33*, 5287-5294.
[227] S. Collins and T. Ziegler, *Organometallics* **2007**, *26*, 6612-6623.
[228] V. Tognetti, G. Fayet and C. Adamo, *Int. J. Quantum Chem.* **2010**, *110*, 540-548.
[229] V. Tognetti, P. Le Floch and C. Adamo, *J. Comput. Chem.* **2009**, *31*, 1053–1062.
[230] S. Noda, T. Kochi and K. Nozaki, *Organometallics* **2009**, *28*, 656-658.
[231] M. J. Szabo, R. F. Jordan, A. Michalak, W. E. Piers, T. Weiss, S. Y. Yang and T. Ziegler, *Organometallics* **2004**, *23*, 5565-5572.
[232] M. J. Szabo, N. M. Galea, A. Michalak, S. Y. Yang, L. F. Groux, W. E. Piers and T. Ziegler, *Organometallics* **2005**, *24*, 2147-2156.
[233] D. M. Philipp, R. P. Muller, W. A. Goddard, J. Storer, M. McAdon and M. Mullins, *J. Am. Chem. Soc.* **2002**, *124*, 10198-10210.
[234] G. Stojcevic, E. M. Prokopchuk and M. C. Baird, *J. Organomet. Chem.* **2005**, *690*, 4349-4355.
[235] F. Wu, S. R. Foley, C. T. Burns and R. F. Jordan, *J. Am. Chem. Soc.* **2005**, *127*, 1841-1853.
[236] F. Wu and R. F. Jordan, *Organometallics* **2006**, *25*, 5631-5637.
[237] L. F. Groux, T. Weiss, D. N. Reddy, P. A. Chase, W. E. Piers, T. Ziegler, M. Parvez and J. Benet-Buchholz, *J. Am. Chem. Soc.* **2005**, *127*, 1854-1869.

[238] K. Nozaki, S. Kusumoto, S. Node, T. Kochi, L. W. Chung and K. Morokuma, *J. Am. Chem. Soc.* **2010**, *132*, 16030-16042.
[239] A. Michalak and T. Ziegler, *Organometallics* **2003**, *22*, 2660-2669.
[240] A. Michalak and T. Ziegler, *Organometallics* **2001**, *20*, 1521-1532.
[241] E. Y. X. Chen, *Chem. Rev.* **2009**, *109*, 5157-5214.
[242] H. von Schenck, S. Strömberg, K. Zetterberg, M. Ludwig, B. Åkermark and M. Svensson, *Organometallics* **2001**, *20*, 2813-2819.
[243] B. S. Williams, M. D. Leatherman, P. S. White and M. Brookhart, *J. Am. Chem. Soc.* **2005**, *127*, 5132-5146.
[244] M. S. Kang, A. Sen, L. Zakharov and A. L. Rheingold, *J. Am. Chem. Soc.* **2002**, *124*, 12080-12081.
[245] A. Sen and S. Borkar, *J. Organomet. Chem.* **2007**, *692*, 3291-3299.
[246] J. A. M. Simões and J. L. Beauchamp, *Chem. Rev.* **1990**, *90*, 629.
[247] S. R. Foley, R. A. Stockland, H. Shen and R. F. Jordan, *J. Am. Chem. Soc.* **2003**, *125*, 4350-4361.
[248] S. J. Luo and R. F. Jordan, *J. Am. Chem. Soc.* **2006**, *128*, 12072-12073.
[249] G. L. Tian, H. W. Boone and B. M. Novak, *Macromolecules* **2001**, *34*, 7656-7663.
[250] C. Elia, S. Elyashiv-Barad, A. Sen, R. López-Fernández, A. C. Albéniz and P. Espinet, *Organometallics* **2002**, *21*, 4249-4256.
[251] U. Klabunde, T. H. Tulip, D. C. Roe and S. D. Ittel, *J. Organomet. Chem.* **1987**, *334*, 141-156.
[252] A. C. Albéniz, P. Espinet and R. López-Fernández, *Organometallics* **2003**, *22*, 4206-4212.
[253] L. Visscher and K. G. Dyall, *Atomic Data and Nuclear Data Tables* **1997**, *67*, 207-224.
[254] J. W. Lauher and R. Hoffmann, *J. Am. Chem. Soc.* **1976**, *98*, 1729-1742.
[255] P. Margl, L. Q. Deng and T. Ziegler, *J. Am. Chem. Soc.* **1998**, *120*, 5517-5525.
[256] V. R. Jensen, K. Angermund, P. W. Jolly and K. J. Børve, *Organometallics* **2000**, *19*, 403-410.
[257] V. R. Jensen and W. Thiel, *Organometallics* **2001**, *20*, 4852-4862.
[258] R. Schmid and T. Ziegler, *Organometallics* **2000**, *19*, 2756-2765.
[259] W. Heyndrickx, G. Occhipinti, Y. Minenkov and V. R. Jensen, *J. Mol. Catal. A: Chem.* **2010**, *324*, 64-74.
[260] P. Kirkpatrick and C. Ellis, *Nature* **2004**, *432*, 823.
[261] R. S. Pearlman, *3D QSAR in Drug Design: Volume 1: Theory Methods and Applications*, Springer, New York, NY, USA, **1993**.
[262] D. E. Clark, *Evolutionary algorithms in molecular design*, Wiley-VCH, Weinheim, **2000**.
[263] H. Xu and D. K. Agrafiotis, *Current Topics in Medicinal Chemistry* **2002**, *2*, 1305-1320.
[264] G. Schneider and U. Fechner, *Nat. Rev. Drug Discov.* **2005**, *4*, 649-663.
[265] J. A. Hageman, J. A. Westerhuis, H. W. Fruhauf and G. Rothenberg, *Adv. Synth. Catal.* **2006**, *348*, 361-369.
[266] P. Comba, T. W. Hambley and B. Martin, *Molecular Modeling of Inorganic Compounds*, Wiley-VCH, Weinheim, **2009**.
[267] M. von Grotthuss, G. Koczyk, J. Pas, L. S. Wyrwicz and L. Rychlewski, *Comb. Chem. High T. Scr.* **2004**, *7*, 757-761.
[268] G. C. Vougioukalakis and R. H. Grubbs, *Chem. Rev. 110*, 1746-1787.
[269] P. Schwab, M. B. France, J. W. Ziller and R. H. Grubbs, *Angew. Chem. Int. Ed. Engl.* **1995**, *34*, 2039-2041.
[270] S. T. Nguyen, L. K. Johnson, R. H. Grubbs and J. W. Ziller, *J. Am. Chem. Soc.* **1992**, *114*, 3974-3975.
[271] M. Scholl, S. Ding, C. W. Lee and R. H. Grubbs, *Org. Lett.* **1999**, *1*, 953-956.
[272] G. Occhipinti, H. R. Bjørsvik and V. R. Jensen, *J. Am. Chem. Soc.* **2006**.
[273] T. M. Trnka, J. P. Morgan, M. S. Sanford, T. E. Wilhelm, M. Scholl, T. L. Choi, S. Ding, M. W. Day and R. H. Grubbs, *J. Am. Chem. Soc.* **2003**, *125*, 2546-2558.

[274] W. Janse van Rensburg, J. A. van den Berg and P. J. Steynberg, *Organometallics* **2007**, *26*, 1000-1013.